NBS MONOGRAPH 33

An Experimental Study of Phase Variations in Line-of-Sight Microwave Transmissions

U.S. DEPARTMENT OF COMMERCE

NATIONAL BUREAU OF STANDARDS

THE NATIONAL BUREAU OF STANDARDS

Functions and Activities

The functions of the National Bureau of Standards are set forth in the Act of Congress, March 3, 1901, as amended by Congress in Public Law 619, 1950. These include the development and maintenance of the national standards of measurement and the provision of means and methods for making measurements consistent with these standards; the determination of physical constants and properties of materials; the development of methods and instruments for testing materials, devices, and structures; advisory services to government agencies on scientific and technical problems; invention and development of devices to serve special needs of the Government; and the development of standard practices, codes, and specifications. The work includes basic and applied rsearch, development, engineering, instrumentation, testing, evaluation, calibration services, and various consultation and information services. Research projects are also performed for other government agencies when the work relates to and supplements the basic program of the Bureau or when the Bureau's unique competence is required. The scope of activities is suggested by the listing of divisions and sections on the inside of the back cover.

Publications

The results of the Bureau's research are published either in the Bureau's own series of publications or in the journals of professional and scientific societies. The Bureau itself publishes three periodicals available from the Government Printing Office: The Journal of Research, published in four separate sections, presents complete scientific and technical papers; the Technical News Bulletin presents summary and preliminary reports on work in progress; and Basic Radio Propagation Predictions provides data for determining the best frequencies to use for radio communications throughout the world. There are also five series of nonperiodical publications: Monographs, Applied Mathematics Series, Handbooks, Miscellaneous Publications, and Technical Notes.

A complete listing of the Bureau's publications can be found in National Bureau of Standards Circular 460, Publications of the National Bureau of Standards, 1901 to June 1947, ($1.25), and the Supplement to National Bureau of Standards Circular 460, July 1947 to June 1957, ($1.50), and Miscellaneous Publication 240, July 1957 to June 1960 (Includes Titles of Papers Published in Outside Journals 1950 to 1959) ($2.25); available from the Superintendent of Documents, Government Printing Office, Washington, D. C.

UNITED STATES DEPARTMENT OF COMMERCE • Luther H. Hodges, *Secretary*
NATIONAL BUREAU OF STANDARDS • A. V. Astin, *Director*

An Experimental Study of Phase Variations in Line-of-Sight Microwave Transmissions

K. A. Norton, J. W. Herbstreit, H. B. Janes, K. O. Hornberg, C. F. Peterson, A. F. Barghausen, W. E. Johnson, P. I. Wells, M. C. Thompson, Jr., M. J. Vetter, and A. W. Kirkpatrick

National Bureau of Standards Monograph 33

Issued November 1, 1961

For sale by the Superintendent of Documents, U.S. Government Printing Office,
Washington 25, D.C. - Price 55 cents

Contents

An Experimental Study of Phase Variations in Line-of-Sight Microwave Transmissions*

K. A. Norton, J. W. Herbstreit, H. B. Janes, K. O. Hornberg, C. F. Peterson, A. F. Barghausen, W. E. Johnson, P. I. Wells, M. C. Thompson, Jr., M. J. Vetter, and A. W. Kirkpatrick

During 1956 an experiment was conducted at Maui, Hawaii, to study the time variations in the phase of arrival of microwave signals propagated over a 15-mile line-of-sight path and the time variations in the phase difference of signals originating at a common antenna and received at two points on a horizontal baseline normal to the propagation path. These time variations are analyzed in terms of their serial correlation functions and power density spectra for different times of day, and for several baseline lengths ranging from 2.2 to 4,800 feet. The slope of the power spectra and the total variance of phase difference variations are shown to be dependent upon baseline length. In some instances there was evidence of a diurnal cycle in total variance of both phase and refractive index, with larger variances during the day time, but in other instances this diurnal effect was not detectable. The slope of the phase spectra appeared to be independent of time of day or meteorological conditions. The long-term variations in single-path phase were well correlated with variations in the mean value of refractive index measured at 5 points along the path.

1. Introduction

During the fall of 1956, the National Bureau of Standards performed a series of experimental measurements designed to study the statistics of time variations in the phase of microwave transmissions propagated over a line-of-sight path. The purpose of the experiment was twofold: (1) to provide information useful in determining the error or noise contributed by the turbulent troposphere to any radio system using phase comparison as a means of position location; and (2) to furnish statistics valuable in formulating and testing tropospheric propagation theories.

The measurements were made on the island of Maui, Hawaii, over a 15.46-mile path extending from the 10,000-ft summit of Haleakala to the airport at Puunene, at an elevation of 100 ft. A major consideration in the selection of this location was that, because of the relatively large variations in radio refractive index to be expected here, these data would form a valuable supplement to similar measurements made earlier over the Pikes Peak—Garden of the Gods path in Colorado [Herbstreit and Thompson, 1955].

The purpose of this report is to present an analysis of time variations in: (1) the phase (relative to a stable phase reference) of a 9,414 Mc/s signal transmitted over this path, referred to hereafter as single-path phase data; (2) the phase observed at one receiving antenna relative to that observed at an adjacent antenna, referred to as phase difference data; (3) atmospheric refractivity as recorded by a microwave refractometer located at the Haleakala terminal; (4) the wind velocity at both ends of the path, and (5) surface atmospheric refractivity measured at 5 stations located on or near the path.

The analysis of the phase data consists of determining the total variance, serial correlation function, and power spectrum for samples taken from approximately four days of almost continuous recording. The extent to which the total variance and power spectrum are functions of (1) baseline length, (2) long-term variability in atmospheric conditions (as evidenced by analysis of the meteorological data) and (3) length of data sample is discussed.

The refractometer data from Haleakala are analyzed in terms of variance, crossing rates, and maximum rates. (The latter two statistics are defined in the section on refractometer data.) The long-term variations in mean refractivity along the path are compared to the corresponding variations in electrical length of the path (single-path phase).

* The research described in this Monograph was sponsored by the Air Research and Development Command, Ballistic Missile Division, U.S. Air Force, under Contract AF -04-(647)-134.

2. Description of Propagation Path and Arrangement of Equipment

Figure 1 is a map showing the location of the propagation path and the meteorological instrument shelters. Figure 2 shows an expanded sketch of the antenna arrangement. The antennas at Puunene were arranged along a baseline that was approximately normal to the propagation path at antenna B. The 9,414 Mc/s antennas A, B, E, F, G, and H were 18–in., dipole-fed parabolic reflectors with half-power beam widths of approximately 6 deg in both the horizontal and vertical planes. The antenna marked C-D is actually a system of two 9,414 Mc/s antennas with an effective horizontal separation of 2.2 ft normal to the path and will be referred to hereafter simply as the "G.E. antenna".

A limited amount of single-path data at 1,046 Mc/s was obtained with a 10-ft dish at the locations marked "1KMc/s" on the maps, but this has not been analyzed for this report. Horizontal polarization was employed throughout the experiment.

Meteorological instrument shelters were located at both path terminals and at three intermediate points. The latter were located as near to the path as possible at altitudes of 3,000, 7,000, and 8,600 ft. Continuous recordings of atmospheric pressure, relative humidity, and temperature were made at each shelter.

Continuous recordings of short-term variations in refractive index, using microwave refractometers, were made at both path terminals. (Because of equipment troubles encountered, the refractometer data from Puunene are considered unreliable and are not included in this analysis.)

Figure 3 shows terrain profiles of the paths from Haleakala to the A and H locations at Puunene. The altitudes shown are of course greatly exaggerated relative to the distance scale and have been corrected for a 4/3 earth curvature. The 6–deg beamwidths of the 9,414 Mc/s dishes at each terminal drawn on the profile show that there was little chance of ground reflections interferring with the measurements. At locations A, B, C, D, E, and F there was some possibility of reflections from foliage in the foreground. To remedy this, an earthen wall approximately 8 ft high was erected about 350 ft in front of these antennas to block any such reflections.

3. Description of Data Output

The measurement techniques and circuitry employed in this experiment are similar to those described in other reports and hence will not be described in detail here [Herbstreit and Thompson, 1955; Thompson and Vetter, 1958].

In general, the radio measurements were recorded on Esterline-Angus charts moving at 3 in. per min with occasional special recording periods (on the order of 10 to 15 min in length) during which the same variables were also recorded on magnetic tape. This arrangement permitted study of power spectral frequencies up to 1 c/s on the charts and up to about 30 c/s on the magnetic tapes. The phase data were of two types. One consisted of recordings of the variations in single-path phase. These were made simultaneously at three of the six antennas, A, B, E, F, G, and H. Phase difference data were obtained from these by simply taking the difference between the phases recorded at two antennas. The combination of three antennas was changed twice during the experiment so that long baseline phase difference data were obtained for eight baseline lengths ranging from 42 to 4,847 ft. The other type of data was the direct recording of phase difference for a 2.2–ft baseline obtained from the G.E. antenna system.

Two output circuits were used for recording each phase variable on Esterline-Angus charts. One contained a high-pass filter to eliminate large, low-frequency "trends" and thereby permit amplification of the higher frequencies. This is referred to as the "band-pass" record because the recording meter itself limits the net response of the circuit above about 1 c/s. The other circuit had no high-pass filter and will be referred to as the "low-pass" record; i.e., the only filtering was that done by the low-pass characteristic of the meter. Band-pass and low-pass recordings of both single-path phase and G.E. phase difference were made simultaneously throughout the experiment. Figure 4 shows the frequency response characteristics of the low-pass and band-pass chart recording circuits. Samples of the low-pass, single-path recordings, along with the corresponding phase difference monitor record obtained during the scaling operation are shown in figures 5 and 6. Figure 7 shows examples of the band-pass and low-pass phase difference data obtained with the G.E. antenna.

The refractometer data were recorded on Esterline-Angus charts (at 3 in. per min.) at the Haleakala site. The data output of the airborne refractometer consisted of simultaneous low-pass Esterline-Angus and high-speed band-pass Sanborn chart recordings. Friez Aerovane wind measurement equipment was operated at both path terminals and yielded a continuous chart recording (at 3 in. per min.) of wind speed and direction. Meteorological data were obtained at the five instrument shelters by the use of microbarographs and

hygrothermographs. These instruments have a relatively longtime constant and a correspondingly slow chart speed, so no attempt was made to take readings from the continuous records closer than 4 per hr.

To record cloud activity on or near the path, a 16 mm motion picture camera was mounted at each path terminal and aimed toward the opposite terminal. A special timing device was used to operate the shutter at the rate of one exposure every 5 sec.

4. Analysis of Short-Baseline Phase Difference Data

The principal goal of the phase data analysis was to estimate the power spectrum[1] of single-path phase and phase difference fluctuations over as wide a power spectral frequency range as possible and under as many conditions as possible (e.g., different times of day, baseline lengths, lengths of sample, etc.) The phase difference data obtained with the 2.2–ft baseline G.E. antenna system was analyzed first and since this analysis differs in some important respects from the subsequent work done on the longer-baseline data, it will be discussed separately.

As was mentioned earlier, the phase variations were measured through both band-pass and low-pass filters and recorded simultaneously on two Esterline-Angus charts. The low-pass and band-pass recordings of the G.E. antenna data were calibrated at 25° and 2.5°–to–5° full-scale, respectively. From the chart samples shown in figure 7, it can be seen, however, that the variations on the low-pass record were small, making accurate analysis difficult. For this reason, the main effort was directed toward the band-pass Esterline-Angus record. Seven periods ranging in length from 18 to 32 min were chosen, the principal criteria used in their selection being that they were free of discontinuities and represented different times of the day.

The highest frequency which can properly be represented in the sample spectrum is $1/2\delta$ c/s, where δ is the sampling interval. Therefore, δ must be made sufficiently small to take into account the highest frequencies contained within the pass-band of the recording circuit. The values of δ used in scaling these seven periods are 0.341 and 0.5 sec. Since the lowest frequency within the pass-band has a period of about 1 min, it was decided that three samples 3 to 5 min in length taken from each period would be adequate. Table 1 contains the time, length of sample, and total variance of each sample.

Figures 8 to 14, inclusive, show power spectra of the G.E. antenna phase difference data for the seven periods along with estimates of the reading error noise spectra.[2] The ordinates are listed in table 2. The corresponding serial correlation functions are shown in figures 15 to 21. It will be seen that the reading error noise seriously contaminates the spectral estimates only at the high-frequency end in figures 8, 9, and 10. The reduction in reading error noise in the succeeding figures was a result of changing from semiautomatic to manual sampling and digitizing techniques. The frequency range of the spectra in figures 8, 9, and 10 was extended to lower frequencies simply by recomputing the spectra, using every third data point. These spectra are labeled 1a, 2a, 3a, etc., in the figures. They yield some information about the power at a frequency equal to one third of the lowest frequency shown in the spectra labeled 1, 2, 3, etc., but they are less reliable for two reasons. One is that the number of data points has been reduced by a factor of three, causing increased random fluctuation in the spectral estimates. The other is that the high-frequency ends of curves 1a, 2a, 3a, etc., are contaminated by "aliasing", or the artificial addition to the spectral density at these frequencies of power which was actually present at higher frequencies beyond the range of the analysis. This procedure of using every third data point was not practical after δ, had been increased to 0.5 (figs. 11 to 14), since any extension of the spectrum to lower frequencies would have gone out of the pass-band of the recording system.

Figure 22 shows an attempt to extend the range of the measured spectrum by the use of the low-pass Esterline-Angus record. Curve A, and curves B and C are spectra obtained by scaling the corresponding low-pass record with δ, equal to 10 sec and 1 sec, respectively. Even ignoring curve A, which looks deceptively horizontal because of aliasing at the high-frequency end, it still appears that the slope of the phase difference spectrum for a 2.2–ft baseline approaches zero as the spectral frequency decreases over the range from 10 to 0.001 c/s. In particular, the power density in the range 0.1 to 1.0 c/s, for which the most information has been obtained, varies approximately as $f^{-1.5}$, where f is the spectral frequency.

Figure 23 shows the total variance of the G.E. phase difference (band-pass) data samples plotted as a function of time of day. Although the amount of data available is too limited to draw any firm conclusions regarding diurnal variations, it is evident that the variance was considerably higher during the daylight hours than during the night. It should be remembered that these are variances of filtered data and are therefore systematically smaller than the estimate of variance that would be obtained by integrating the spectra, since the latter have

[1] The method of power spectrum analysis used is discussed in the appendix.

[2] The method of estimating the reading error noise spectrum is described in the appendix.

been corrected for recording circuit filter characteristics. However, there seems to be no systematic variation in the *slope* of the spectrum with time of day, so we may conclude that the variances of these filtered data are proportional to the variances of the data before filtering.

5. Analysis of Long-Baseline Phase Difference and Single-Path Phase Data

It was originally planned that the analysis of the long-baseline phase difference and single-path phase data would parallel the G.E. short-baseline data analysis. That is, the minimum data input would consist of samples chosen to coincide in time with the G.E. data samples, and the spectral frequency range would include that covered in the G.E. analysis. However, the discovery of two subtle and unanticipated characteristics of the data resulted in a revision of the analysis plan. As was pointed out previously, the long-baseline phase difference data actually consisted of pairs of simultaneous single-path phase recordings which were scaled by use of a semiautomatic device in the laboratory to obtain the phase difference. This device was designed and built at NBS by the Data Reduction Instrumentation Section. Its input is provided by two operators, who each retrace a chart record with a stylus. The angular displacement of each stylus is converted to a d-c voltage. The difference between the two voltages is recorded continuously on an Esterline-Angus monitoring meter and also sampled at a predetermined rate, digitized and punched on IBM cards. Figures 5 and 6 show samples of simultaneous single-path phase recordings along with the corresponding phase difference monitoring chart. Provision had been made in the design of the phase measuring equipment to manually shift the calibration of the recording charts a known number of degrees to prevent the trace from going off-scale. A corresponding provision was made for changing the calibration of the scaling device to allow for shifts in either or both charts. This system was entirely satisfactory for studying long-term variations in single-path phase. However, the variance of phase difference during periods on the order of 15 min in length was so small that the error in compensating for a shift in scale was appreciable, and showed up as a more or less abrupt discontinuity in the monitoring record. This difficulty limited the number of phase difference samples having a minimum acceptable length. It was decided that in order to provide as complete an analysis as possible, it should not be restricted to periods used in the short-baseline analysis but should include all sufficiently long periods during which all three single-path recordings were continuous.

The second difficulty which prevented direct comparison of long and short-baseline spectra was that one of the three phase-measuring systems yielded single-path phase spectra that were consistently different from those obtained from the other two systems. Since the difference showed up only in the frequency range above 1 c/s, it was decided that the analysis should be restricted to the low-pass recordings. As can be seen in the data samples in figures 5 and 6, the scale was compressed to record large low-frequency variations. As a consequence, although the frequency response of the low-pass record extends to 1 c/s, the power density above about 0.1 c/s was of the same order of magnitude as the reading error noise, and hence impossible to measure accurately. For this reason, the frequency range chosen extended from approximately 0.003 to 0.1 c/s.

It was considered desirable to maintain a uniform sample length so that a comparison of spectra would not be confounded by possible effects of variations in sample length. Fifteen minutes was chosen as a reasonable compromise between having statistically few longer samples, or many statistically short samples. Ten to thirteen such periods were selected for each of the three combinations of baseline lengths. (In the discussion which follows, these three major time periods will be identified by the letter designations of the three antenna locations in use at the time at Puunene; i.e., ABH, BGH, BEF.)

Six or seven samples of single-path phase record were selected from each of the periods ABH, BGH, and BEF. In general, these samples do not coincide in time with the phase difference samples. The prime consideration in their selection was that they be a part of a larger sample (one-half hour or longer), so that, although the spectra were computed for 15-min periods, it would be possible to study variance as a function of sample length. Tables 3 and 4 give the time, length of sample and total variance for phase difference and single-path samples, respectively, while tables 5 to 15, inclusive, list the corresponding densities computed for each sample. The serial correlation functions from which these spectra were computed are shown plotted in figures 24 to 34, inclusive.[3] When the individual spectra are plotted as curves, it is evident that no discernable characteristic (with the exception of total variance, which will be discussed later) varied systematically as a function of time of day, or at least any such variation is hidden by sampling fluctuations. For this reason, the spectral estimates for all samples at a given baseline length are shown in the subsequent figures simply as a cluster of points at each frequency. The range of these points is determined both

[3] Not shown are serial correlation functions of samples that were "detrended" in the way described in the appendix.

by sampling fluctuations and by more or less long-term changes in propagation conditions (nonstationarity). Some measure of the relative magnitude of these two effects can be obtained by considering the distribution of spectral densities to be expected if the samples had been taken from the same statistical population; i.e., if the time variations in phase difference constituted a stationary process. In that case, the spectral density estimates at each frequency would be distributed according to the chi-squared distribution with an effective number of degrees of freedom determined by the number (n) of data points, the number of frequencies (m) for which estimates are computed, and, to a very limited extent, by the slope of the spectral density. According to the method of approximation given by Blackman and Tukey [1958] these estimates have from 10 to 14 degrees of freedom, with an average value of 12. In this analysis, 10 was used arbitrarily as a slightly pessimistic estimate. The solid line in each of the figures 35 to 45 joins the median of the ordinates at each frequency. Using these sample medians to approximate the "true" median, the dashed lines labeled "95 percent stability limits" represent the bounds within which 95 percent of all such spectral estimates might be expected to fall if the process were indeed stationary. It is obvious that in some cases considerably more than 5 percent of all the points lie outside these limits, indicating that all of the spread cannot in these cases be ascribed to statistical fluctuation. In particular, it should be noted that the percentage of sample densities falling outside the stablity limits is greater in the case of longer-baseline and single-path data. As will be seen later, it is only in this case that any indication of a diurnal trend in total variance was detected. Such a trend could easily account for the increased variance of spectral estimates. (It should also be noted here that the slopes of the spectra become steeper with increasing baseline length, and although the effect of very steep slopes is to reduce the effective number of degrees of freedom and hence increase the variance of the spectral estimates, this effect is negligible for the range of slopes encountered here.)

The increase in slope with increasing baseline length is best seen in figures 46, 47, and 48, where the "median" spectra are shown for the BEF, BGH, and ABH recording periods, respectively. Caution should be exercised in comparing spectra obtained from different recording periods. The reason for this is illustrated in figure 49 which shows the median single-path spectra for each of the three periods and the median spectra for the 1,914-ft baseline data from the BGH and ABH periods. It can be seen that there is considerable change in the general level of the spectra (i.e., total variance) in going from one period to another.

This long-term variability in total variance can be seen in figure 50 in which the variance of each sample is plotted as a function of the time of day. On November 5 and 6, the ABH recording period, there seemed to be a clear-cut diurnal pattern, with higher variances during the day than during the night. However this pattern did not persist during the remainder of the recording periods and it must be concluded that if there is a tendency toward a diurnal variance cycle, it can apparently be obliterated by other longer-term changes in the propagation mechanism. Evidence of such long-term changes can be seen in the single-path phase variance which is noticeably larger during November 8 and 9 (the BEF period) than during the earlier periods.

Figures 51 and 52 show the single-path phase variance versus time compared to plots versus time of (1) long-term changes in mean single-path phase (i.e., changes in electrical path length) and (2) changes in a weighted[4] mean of the surface refractivity values measured at the meteorological stations along the path. It will be noted that the increased phase variance on November 8 and 9 coincided with a marked decrease in electrical path length and mean surface refractivity. Also shown in this figure are the wind velocities at the path terminals read from the continuous wind records. It should be pointed out that only during the November 8 and 9 period was the wind direction the same (roughly normal to the path) at both terminals with speeds as high as 15 mph.

Some examples of the time sequence pictures of cloud activity along the path are shown in figures 64 to 74 in the appendix. In general, these were chosen to coincide in time as nearly as possible with the data samples analyzed, and the appropriate data sample numbers are listed on the pictures. It is interesting to note that the marked diurnal pattern of November 5 and 6 coincides with the period of widest variation in cloudiness along the path. Only during these two afternoons was the Haleakala site completely enshrouded in clouds, while the intervening night was apparently clear.

Figure 53 shows the total variance of the phase variation samples plotted as a function of baseline length. This includes data taken from all three recording periods and hence the true dependence of phase variance on baseline length may be obscured by the long-term changes in variance discussed above. For example, the variances of the 1,914-ft data are in general higher for the BGH period than for the ABH period, and the fact that the single-path variances from the BEF period, are in general higher than those of the other two periods leads

[4] The weighting factors are proportional to the difference in altitude of adjacent meteorological stations so that each value of refractivity was weighted in proportion to the percentage of the path over which it might be expected to apply.

one to suspect that the 67 and 109-ft phase difference variances (also from the BEF period) may also be relatively high. However, comparisons of data taken within the same recording period are valid because the samples chosen were recorded simultaneously.

6. Analysis of Refractometer Data

The analysis of the microwave refractometer recordings made at the Haleakala path terminal consisted of determining the variance, crossing rate and maxima rate of sixteen 15-min samples selected from the 5 days of recording. Figure 54 summarizes the results of this analysis. Crossing rate is defined as the average number of times per min that the refractivity crossed its 15-min mean value in the positive direction. The maxima rate is the average number of times per minute that the trace passes through a maximum (i.e., with first derivative equal to zero, second derivative negative). There is some tendency toward higher values of all three of these statistics during the daylight hours than during the night, but aside from this there is no obvious correlation between, for example, the variances of phase and refractivity variations. This of course is not surprising in view of the fact that the latter reflect changes in the atmosphere at only one point of the path, while the former are determined by conditions over the entire path.

7. Appendix—Notes on the Data Analysis

7.1. Serial Correlation and Power Spectrum Computation

The power spectrum, or more precisely, the power spectral density, can be defined as the Fourier cosine transform of the autocorrelation function of a time series. This definition is consistent with the method used in obtaining the spectra shown in this report. However, it might be more satisfactory from the engineering standpoint to look at the power spectrum in the following way. Imagine that a d-c voltage proportional to the time-varying quantity being studied has been passed through a narrow-band filter with center frequency f, and that the variance (mean squared deviations from the mean) of the resulting filtered data has been measured. The ratio of this variance to the bandwidth of the filter is a measure of the spectral density, or variance per unit bandwidth, at the frequency f. If this is done for several values of f, the graph of these spectral densities plotted versus frequency is an estimate of the power spectrum of the variable.

The method of power spectrum estimation used throughout this report was developed by Blackman and Tukey [1958]. The input to the process is a time series consisting of n instantaneous values $p(t_i)$ read from a continuous recording at the rate of one reading every δ sec. The computation consists of first determining the autocovariance function given by:

$$R(\tau)=\frac{1}{n-k-1}\sum_{i=1}^{n-k}[p(t_i+\tau)-\bar{p}]\,[p(t_i)-\bar{p}],$$

where

$$\tau=k\delta\,(k=0,\,1,\,\ldots,\,m),$$

and

$$\bar{p}=\frac{1}{n}\sum_{i=1}^{n}p(t_i).$$

(In most of the work reported here $m=30$.)

The serial correlation function, which estimates the autocorrelation function of the process, is then given by

$$r(\tau)=\frac{R(\tau)}{R(0)}.$$

The next step is to compute the finite cosine series transform

$$U_h\left(\frac{h}{2m\delta}\right)=\delta\left[R(0)+2\sum_{k=1}^{m-1}R(k\delta)\cos\frac{\pi kh}{m}+R(m\delta)\cos\pi h\right],$$
$$h=0,\,1,\,2,\,\ldots,\,m.$$

$U_h\left(\frac{h}{2m\delta}\right)$ is itself a rough estimate of the power density at the frequency $\frac{h}{2m\delta}$ c/s. However, it is as though the imaginary narrow-band filter mentioned above had quite appreciable sidebands so that the estimate is influenced by variations at frequencies far removed from $\frac{h}{2m\delta}$. To get around this difficulty, a "refined" estimate of power density, $W(f)$, is computed by the following equations for $m+1$ frequency bands having center frequencies $f=\frac{h}{2m\delta}(h=0,\,1,\,2\ldots m)$:

$$W(0)=1.08\,U_0+0.92\,U_1$$
$$W\left(\frac{h}{2m\delta}\right)=0.46\,U_{h-1}+1.08\,U_h+0.46\,U_{h+1},$$
$$h=1,\,2,\,\ldots,\,m-1$$
$$W\left(\frac{h}{2\delta}\right)=0.92\,U_{m-1}+1.08\,U_m.$$

$W(f)$ is the quantity plotted in the spectrum graphs. $W(0)$ is not plotted because it should properly be shown at zero frequency and also because any estimate of the power near zero frequency based on a short data sample is of questionable practical value.

7.2. Estimating the Power Spectrum of Reading Error Noise

When discrete digital values of a variable are read from a continuous record, their variance is the sum of (1) the variance contributed by the continuous record and (2) the variance of random reading and rounding errors. In interpreting sample power spectra, it is important that some quantitative idea of the relative magnitude of these two variances be obtained. In this discussion, random variations introduced by reading error and those introduced by "rounding-off" the digitized data to, for example, three figures, will be lumped together and called simply reading error noise. If the errors in reading successive points are independent, the power spectrum of the reading error noise will be a "white noise" spectrum; i.e., the spectral density will be essentially constant over the range of frequencies observed. Also, assuming that the reading error is independent of the variable being read, the observed spectral density at a given frequency will be the sum of the "true" density and the reading error noise density. It is evident from this that, particularly if the "true" spectrum is very steep, the power densities at some frequencies may be of the same order of magnitude as the reading error noise and hence be obscured. An admittedly rough estimate of the reading error noise spectrum was obtained in the following way. Each chart record was scaled twice. Then the spectrum of the n differences between readings obtained in the two trials was computed. If the errors made in the two trials are independent, the total variance of the differences will be twice the variance of errors in either trial. Hence, the ordinates of the difference spectrum are divided by two to obtain the reading error noise spectrum. Figures 55 to 58, inclusive, show some examples of noise spectra compared to the corresponding data spectra. It can be seen that there is probably some contamination of the data spectra by noise at the high-frequency end. It was pointed out previously that 0.1 c/s was chosen as the upper frequency limit for spectrum analysis of the low-pass recordings because reading error noise would dominate the spectrum beyond that point. It should also be noted that the data spectra for the 67-ft phase difference are comparable in general level with the noise spectra. This is not surprising, however, in view of the relatively small variance of these data (as seen in the data sample in fig. 5). For this reason, no attempt was made to analyze phase differences with the 42-ft baseline (E-F) antenna combination. It should be borne in mind that these estimates tend to be pessimistic; i.e., on the average the noise spectral densities would probably be somewhat lower than those shown. This is because additional error is introduced by the small but practically unavoidable displacement on the time scale of the second set of readings relative to the first.

7.3. Eliminations of Trends

As used here, the term "trend" refers to variations occuring at spectral frequencies that are low compared to the reciprocal of the length of sample (i.e., the fundamental frequency). Whenever a trend contributes a large portion of the total variance, the sample spectrum will contain gross errors. This is because the sum of the spectral densities (including $W(0)$) multiplied by their respective bandwidths must equal the total variance, and variance that should properly be assigned to the "trend frequencies" is added to the variance at the higher frequencies.

In selecting the data samples, an effort was made to avoid trends by picking periods where the values of the variable at the endpoints were similar and where visual inspection indicated no obvious trends. This admittedly biases the data but as will be pointed out later, this bias is apparently very small, and in any case was considered unavoidable.

Trends were most difficult to avoid in the single-path and long-baseline phase difference data and the need for some sort of filtering or "detrending" was apparent. The trend removal method used consisted of computing the "rough" spectrum $U'_h(f)$ of the deviations of the individual data points from a running average and then applying a correction to allow for the frequency response of this "digital filter". If c is the number of points averaged and δ is the sampling interval in seconds, then it can be shown that the correction factor applied to $U'_h(f)$ to obtain the "rough" detrended spectrum $U_h(f)$ is given by:

$$U_h(f) = U'_h(f)\left[1-\left(\frac{\sin c\pi\delta f}{c\sin\pi\delta f}\right)^2\right]^{-1} .$$

The conversion of $U_h(f)$ to the refined estimate $W(f)$ is the same as was described previously. This process was found to be satisfactory for obtaining spectral estimates for values of $c\,\delta\,f$ above 1. Below this, the correction factor changes rapidly with frequency and it was found in repeated experiments that using the factor for the midpoint frequency of the band covered by U_1 was not satisfactory. For this reason, no values of $W\left(\frac{1}{2m\delta}\right)$ or $W\left(\frac{1}{2m\delta}\right)$ are given for the detrended spectra.

In the tables of spectral densities it will be noted that several sample spectra have alternating positive and negative densities. This is apparently caused by undetected trends. It

was found that detrending such samples changed the negative values to positive but did not change the other values appreciably (the latter are, of course, the only ones shown in the graphs).

7.4. Effect of Sample Length on Total Variances and Power Spectra

In general, the long-baseline and single-path phase variation samples analyzed were approximately 15 min long. It was mentioned previously that the sample length was held as nearly constant as possible to avoid confusing sample length dependence with other effects. An investigation of this dependence with regard to the total variance and power spectrum was made, using those samples taken from longer periods of continuous recording. Figure 59 shows some examples of the dependence of single-path and phase difference variances on sample length. The ordinate is the ratio of the average variance of a longer sample to the average variance of the 15-min periods contained within that sample. The largest increase in variance apparently occurs between 15 and 30 min with very little increase between 60 and 120 min. In none of the cases did the variances increase by as much as a factor of 3 over the average 15-min value. Figures 60 through 63 show the power spectra of longer samples compared to the spectra of the component shorter periods. These indicate that within the range of frequencies covered in this analysis, the slope and absolute level of the spectra remain essentially constant as the length of sample is increased from 15 to 60 or 120 min. Apparently, most of the increase in total variance with sample length shows up as an increase in $W(0)$ (not plotted) and $W\left(\frac{1}{2m\delta}\right)$ (plotted at 0.00306 c/s). Unfortunately, most of the short samples shown here were detrended and hence do not show the first two points. However, this point is illustrated in figures 60 and 62. The total variance of the 1-hr sample in figure 62 is 7,003 $(\text{deg})^2$ and the total variance of the one 15-min sample that was not detrended is 1,239 $(\text{deg})^2$. Most of this difference in variance can be accounted for in the difference between the power densities at 0.00306 c/s. Similarly, the total variances listed by the corresponding spectra in figure 60 indicate that only the first point in each is clearly a function of total variance.

It should be emphasized that the dependence of variance on sample length shown here is necessarily biased, since it is based on periods when the variance was small enough to permit relatively long recordings not interrupted by scale shifts or by the trace going off-scale. As a consequence the variances for the long periods are smaller than they would have been if they could have been selected at random from any part of the data.

The experiment discussed in this report was performed by the Radio Propagation Engineering Division, K. A. Norton, Chief. Key personnel and their respective areas of responsibility are as follows: J. W. Herbstreit, general supervision of the project; K. O. Hornberg, project manager; C. F. Peterson, transmitting equipment; A. F. Barghausen, receiving equipment; W. E. Johnson and P. I. Wells, recording equipment; M. C. Thompson, Jr., and M. J. Vetter, microwave refractometers and design of 9,414 Mc/s equipment; A. W. Kirkpatrick, meteorological measurements; H. B. Janes, data analysis and preparation of this report. E. L. Crow and M. M. Siddiqui contributed many valuable suggestions concerning the statistical analysis of the data.

References

Blackman, R. B., and J. W. Tukey, The measurement of power spectra (Dover Publications, Inc., New York, N. Y., 1959).

Herbstreit, J. W., and M. C. Thompson, Measurements of the phase of radio waves received over transmission paths with electrical lengths varying as a result of atmospheric turbulence, Proc. IRE 43, No. 10, 1391–1401 (Oct. 1955).

Thompson, M. C., and M. J. Vetter, Single path phase measuring system for three-centimeter radio waves, Rev. Sci. Instr. 29, 148–150 (1958).

TABLE 1. *Information relative to short-baseline phase difference data*

Baseline Length: 2.2 feet

Sample	Date and time *	Length of sample	Variance
	Nov. 5, 1956	*min*	*deg²*
1	1618	3.41	0.1349
2	1625	3.41	.1634
3	1632	3.41	.1083
4	1728	3.41	.0359
5	1735	3.41	.0525
6	1742	3.41	.0302
	Nov. 6, 1956		
7	0443	3.41	.0265
8	0450	3.41	.0421
9	0459	3.41	.0346
	Nov. 7, 1956		
10	0127	5.10	.0093
11	0135	5.15	.0137
12	0140	5.09	.0156
	Nov. 8, 1956		
13	0713	5.18	.1351
14	0721	5.17	.0975
15	0728	5.12	.0868
	Nov. 9, 1956		
16	0848	5.19	.0964
17	0856	5.16	.0581
18	0914	5.16	.1356
19	1502	5.17	.2896
20	1509	5.17	.1894
21	1516	5.17	.1625

* Time shown is for midpoint of sample.

TABLE 2. *Power spectral densities of short-baseline phase difference variations*

Baseline length: 2.2 feet

Units: (deg.)²/c/s

Frequency	Sample								
	1	2	3	4	5	6	7	8	9
c/s									
0.0489	1.093(0)	1.196(0)	8.701(−1)	3.180(−1)	4.630(−1)	3.728(−1)	2.679(−1)	2.961(−1)	2.884(−1)
.0978	4.434(−1)	6.857(−1)	3.619	2.004	2.389	1.528	1.154	2.289	1.535
.147	3.062	4.808	2.616	1.345	1.513	9.344(−2)	8.399(−2)	1.748	8.395(−2)
.196	3.221	2.773	2.318	6.696(−2)	1.121	7.076	6.487	8.738(−2)	6.431
.244	2.505	2.379	2.407	5.479	9.896(−2)	6.721	4.158	5.260	6.592
.293	2.015	1.742	1.753	4.167	6.637	4.637	3.648	4.914	4.983
.342	1.760	1.436	1.038	3.426	5.621	2.217	2.869	3.933	4.045
.391	1.369	1.514	6.763(−2)	3.634	4.938	1.603	2.039	4.156	3.697
.440	1.022	1.505	6.686	2.971	3.345	1.159	1.482	3.494	2.755
.489	8.482(−2)	1.121	6.932	1.729	2.532	1.226	1.048	2.640	2.153
.538	6.605	8.469(−2)	6.840	1.417	2.683	1.185	1.087	2.029	2.159
.587	4.354	6.628	5.878	1.566	2.456	8.847(−3)	1.389	1.678	2.290
.636	4.235	7.420	5.041	1.490	2.681	8.074	1.589	1.567	1.944
.684	5.775	7.376	3.287	1.081	2.762	7.635	1.121	1.744	1.461
.733	5.620	6.838	2.782	8.071(−3)	1.834	6.309	5.841(−3)	2.055	1.090
.782	3.949	5.969	3.198	6.791	1.340	6.058	5.111	1.550	9.101(−3)
.831	3.559	5.928	3.141	8.064	1.141	4.490	6.572	8.366(−3)	8.676
.880	3.893	6.847	3.485	8.156	1.096	3.934	6.689	6.688	7.407
.929	4.451	6.890	3.355	7.176	1.084	5.061	5.368	7.965	7.046
.978	4.556	5.547	2.289	6.834	9.342(−3)	5.574	4.438	6.212	6.555
1.03	3.433	3.874	2.751	6.062	8.085	4.090	4.460	5.124	5.756
1.08	3.145	3.287	3.498	5.819	9.269	3.044	3.352	6.774	6.417
1.12	3.986	4.040	3.657	5.284	1.006(−2)	3.019	3.404	7.542	6.605
1.17	3.182	5.375	2.623	4.274	8.510(−3)	3.957	3.675	7.668	6.189
1.22	2.606	5.661	1.863	3.755	7.479	3.755	3.316	7.275	7.615
1.27	2.997	4.031	1.756	3.419	8.761	3.178	4.016	5.665	7.561
1.32	3.692	4.758	2.516	3.897	8.858	3.599	4.240	5.714	5.321
1.37	3.455	6.076	3.345	4.431	8.873	4.231	3.514	5.357	4.339
1.42	3.642	4.591	4.441	4.487	5.215	5.183	3.718	5.901	5.177
1.47	4.242	3.868	5.086	4.307	4.826	6.246	4.201	6.724	7.161

Note: Number in parentheses indicates power of 10 multiplying adjacent and following entries.

TABLE 2. *Power spectral densities of short-baseline phase difference variations*—Continued

Baseline length: 2.2 feet

Units: (deg.)²/c/s

Frequency	Sample											
	10	11	12	13	14	15	16	17	18	19	20	21
c/s												
0.0333	4.902(−1)	6.062(−1)	4.124(−1)	3.274(0)	3.285(0)	2.406(0)	2.064(0)	1.414(0)	2.711(0)	4.498(0)	3.220(0)	3.814(0)
.0667	1.256	1.975	1.462	1.267	9.964(−1)	6.429(−1)	5.954(−1)	5.228(−1)	1.341	2.197	1.533	1.808
.100	5.337(−2)	8.095(−2)	8.494(−2)	6.663(−1)	5.623	3.820	3.749	3.058	7.586(−1)	1.174	1.014	1.010
.133	2.854	3.260	6.957	4.383	2.649	3.155	3.062	1.915	5.904	8.865(−1)	7.053(−1)	6.529(−1)
.167	2.103	2.165	5.083	3.214	1.953	2.667	2.044	1.472	4.862	1.196(0)	5.389	5.036
.200	1.655	1.864	4.711	3.248	2.116	1.768	1.369	1.720	2.897	1.117	4.334	3.559
.233	1.130	1.390	4.156	3.714	1.617	1.471	1.338	1.284	2.500	8.058(−1)	3.106	2.898
.267	7.632(−3)	1.296	2.709	2.788	1.027	1.504	1.591	8.789(−2)	2.189	4.921	3.148	2.269
.300	7.151	9.022(−3)	1.530	1.680	9.815(−2)	1.008	1.409	7.028	1.894	3.247	3.422	1.364
.333	6.954	5.343	8.966(−3)	1.055	7.945	7.569(−2)	1.166	5.303	1.516	2.376	2.401	1.158
.367	5.503	6.991	7.890	9.843(−2)	5.926	6.638	8.906(−2)	4.359	1.133	2.276	1.702	1.163
.400	4.001	7.562	6.969	8.379	6.354	4.777	6.800	3.683	8.415(−2)	2.189	1.482	8.282(−2)
.433	3.090	5.843	7.502	6.227	6.090	3.948	5.981	4.048	6.530	2.048	1.761	8.418
.467	1.681	4.641	6.641	5.834	5.000	3.479	5.061	4.189	5.796	2.200	1.604	1.027(−1)
.500	1.849	3.392	5.199	5.698	3.416	3.245	3.715	3.244	5.629	1.784	9.943(−2)	9.942(−2)
.533	2.576	3.929	5.035	4.411	2.880	2.864	5.255	2.547	5.264	1.292	6.574	7.339
.567	2.498	4.603	5.408	5.370	3.274	2.438	7.275	1.924	4.822	8.833(−2)	6.440	5.227
.600	1.805	4.904	3.344	6.311	3.125	2.545	8.441	1.435	3.038	5.793	7.423	3.534
.633	1.800	4.628	2.372	5.139	2.495	3.881	7.185	1.519	2.331	4.719	5.863	3.136
.667	1.651	4.284	2.577	3.765	2.453	4.602	4.705	2.147	2.443	5.438	5.914	3.332
.700	1.258	5.624	2.342	3.733	2.297	4.155	3.796	1.975	3.453	6.257	5.558	3.352
.733	1.002	7.585	1.801	3.198	1.852	3.077	3.052	1.182	3.399	6.619	3.324	3.181
.767	1.181	7.872	1.801	2.679	1.907	3.103	3.419	8.360(−3)	2.555	6.010	3.027	3.727
.800	9.540(−4)	5.349	1.653	3.131	2.763	3.357	6.167	9.916	2.179	5.869	3.647	3.261
.833	6.536	3.921	1.376	2.970	3.285	3.268	7.155	9.191	1.924	5.478	4.115	3.616
.867	7.946	5.404	1.373	3.522	2.849	2.669	6.205	1.055(−2)	1.639	5.346	3.205	3.383
.900	8.610	4.562	1.421	3.468	2.789	2.006	6.595	1.171	1.768	8.021	2.799	2.167
.933	6.264	2.651	1.099	3.582	3.035	2.006	5.221	8.885(−3)	1.499	7.807	3.870	2.023
.967	7.979	1.750	1.586	3.438	2.273	1.535	3.473	8.781	1.914	6.227	5.636	2.823
1.00	1.072(−3)	1.171	2.234	3.060	1.491	1.181	3.085	9.230	2.182	5.988	7.051	3.153

Note: Number in parentheses indicates power of 10 multiplying adjacent and following entries.

TABLE 3. *Information relative to long-baseline phase difference data*

Sample	Baseline length	Date and time *	Length of sample	Variance	Sample	Baseline length	Date and time *	Length of sample	Variance
	ft	Nov. 8, 1956	*min*	*deg²*		*ft*	Nov. 7, 1956	*min*	*deg²*
104		1400	16.6	111.607	87		1520	14.5	3457.81
105		1530	14.8	56.220	88		1845	15.8	2149.32
106		1715	17.5	90.587	89		1925	17.1	10629.8
107	67(B–E)	2000	18.9	77.934	90	1,914(B–H)	2150	19.4	1358.56
108		2025	15.4	112.195	91		2240	18.9	11079.9
109		2050	18.4	41.698	92		2330	13.3	2661.22
110		2330	18.6	47.909			Nov. 8, 1956		
		Nov. 9, 1956			93		0310	16.8	1371.56
111		0100	20.1	70.266	94		0340	14.5	893.528
112		0125	16.2	91.490	95	1,914(B–H)	0620	20.9	3961.77
113	67(B–E)	0140	20.6	170.847	96		0730	17.7	2674.64
114		0300	18.3	90.413			Nov. 5, 1956		
115		1515	18.5	126.493	48		1325	18.2	14248.0
116		1740	17.4	93.029	49		1650	16.8	4136.34
		Nov. 8, 1956			50		1745	16.7	1856.60
117		1400	16.7	206.618	51	1,914(B–H)	2000	16.9	737.643
118		1530	15.5	111.858	52		2015	13.7	676.319
119		1715	19.7	131.761	53		2100	14.4	446.079
120	109(B–F)	2000	20.1	187.960	54		2130	19.2	261.034
121		2025	15.5	195.691			Nov. 6, 1956		
122		2050	19.3	100.643	55		0320	14.5	319.419
123		2330	19.3	107.061	56		0340	18.5	653.355
		Nov. 9, 1956			57		0445	18.2	1394.56
124		0100	15.5	185.145	58	1,914(B–H)	0505	16.4	535.305
125		0125	17.3	155.268	59		0550	16.4	636.727
126	109(B–F)	0140	18.2	492.441	60		0740	18.2	1032.71
127		0300	17.9	180.678			Nov. 5, 1956		
128		1515	20.2	237.058	22		1325	17.3	19515.7
129		1740	18.4	149.991	23		1650	18.0	8964.13
		Nov. 7, 1956			24		1745	16.4	3621.69
67		1520	15.1	3578.52	25	3,003(A–B)	2000	17.1	1530.17
68		1845	19.5	1212.17	26		2015	15.0	1296.21
69		1925	17.6	2498.34	27		2100	14.2	1925.22
70	733(G–H)	2150	18.5	415.578	28		2130	18.5	739.131
71		2240	23.4	2543.56			Nov. 6, 1956		
72		2330	13.3	1401.91	29		0320	16.0	237.649
		Nov. 8, 1956			30		0340	17.5	215.370
73		0310	17.9	924.856	31		0445	18.4	12055.0
74		0340	16.4	169.361	32	3,003(A–B)	0505	18.7	1550.35
75	733(G–H)	0620	16.4	1659.30	33		0550	16.4	2102.60
76		0730	16.4	676.375	34		0740	21.0	4038.13
		Nov. 7, 1956					Nov. 5, 1956		
77		1520	13.8	2174.00	35		1325	17.8	9986.66
78		1845	16.0	1200.27	36		1650	15.2	9300.79
79		1925	17.1	5459.92	37		1745	16.5	3290.69
80	1,181(B–G)	2150	18.5	901.855	38	4,847(A–H)	2000	17.8	1649.19
81		2240	16.4	5251.55	39		2015	15.3	2006.26
82		2330	12.4	1486.09	40		2100	14.7	2115.66
		Nov. 8, 1956			41		2130	15.2	916.589
83		0310	19.1	865.233			Nov. 6, 1956		
84		0340	16.7	456.800	42		0320	14.6	83.626
85	1,181(B–G)	0620	18.4	979.755	43		0340	21.3	1432.45
86		0730	16.4	1245.73	44	4,847(A–H)	0445	20.8	1140.86
					45		0505	16.7	4172.50
					46		0550	20.2	8351.24
					47		0740	20.6	4234.91

* Time shown is for midpoint of sample.

Table 4. *Information relative to single-path phase data*

Sample	Recording period	Date and time *	Length of sample	Variance
		Nov. 8, 1956	*min*	*deg²*
130		1400	16.9	22677.4
131		1530	17.2	7726.53
132	BEF	1715	14.7	8168.50
133		2000	18.1	4922.38
134		2250	19.2	7458.60
		Nov. 9, 1956		
135	BEF	0120	22.0	21243.0
136		1710	16.9	3050.60
		Nov. 7, 1956		
97		1600	19.1	2723.70
98	BGH	1840	21.8	9043.15
99		2025	22.2	7067.35
		Nov. 8, 1956		
100		0000	18.5	3771.88
101		0255	16.6	1304.76
102	BGH	0620	16.2	9658.20
103		0820	17.3	5000.85
		Nov. 5, 1956		
61	ABH	1305	19.7	12185.8
		Nov. 6, 1956		
62	ABH	0340	15.0	703.075
		Nov. 5, 1956		
63	ABH	1625	16.8	5252.00
64		1945	20.3	1268.44
		Nov. 6, 1956		
65	ABH	0000	20.1	2382.58
66		0720	16.4	8072.40

* Time shown is for midpoint of sample.

TABLE 5. *Power spectral densities of long-baseline phase difference variations*

Baseline length: 67 feet (B–E)

Units: (deg.)²/c/s

Frequency	Sample												
	104	105	106	107	108	109	110	111	112	113	114	115	116
c/s													
0.00306	7.677(3)	3.994(3)	8.049(3)	6.302(3)	8.665(3)	1.575(3)	2.887(3)	6.151(3)	5.607(3)	1.644(4)	4.234(3)	1.225(4)	9.830(3)
.00611	6.416	2.685	1.346	4.014	4.698	1.595	1.354	2.674	3.155	6.486(3)	4.098	5.123(3)	5.164
.00917	3.078	1.025	1.028	2.246	2.157	1.924	1.032	1.169	2.111	3.167	3.307	2.138	1.791
.0122	1.631	5.661(2)	9.505(2)	1.475	1.490	1.177	6.422(2)	1.590	1.693	2.862	2.274	1.083	9.514(2)
.0153	1.415	4.105	1.157(3)	8.697(2)	1.119	5.353(2)	6.429	1.250	1.352	1.869	1.601	1.040	1.267(3)
.0183	1.525	4.732	1.457	6.057	1.233	4.685	8.326	6.222(2)	6.853(2)	1.310	9.746(2)	1.461	1.062
.0214	1.153	8.654	8.639(2)	8.616	1.621	5.101	8.068	4.242	7.841	1.020	1.018(3)	1.529	5.923(2)
.0244	5.851(2)	8.785	2.786	7.360	1.406	4.280	5.275	3.904	8.515	7.592(2)	8.585(2)	7.207(2)	2.205
.0275	4.051	6.740	3.011	3.647	1.258	2.544	4.739	4.112	9.225	8.170	7.975	5.017	3.152
.0306	5.152	3.130	2.575	2.213	8.969(2)	3.796	5.566	3.298	1.328(3)	1.053(3)	8.348	9.641	4.399
.0336	4.144	1.593	1.821	1.774	6.940	4.512	4.933	3.981	9.355(2)	9.142(2)	9.068	7.474	3.074
.0367	3.639	1.723	1.807	1.648	4.417	4.042	2.820	4.051	3.094	6.825	6.029	2.548	2.498
.0397	6.495	1.456	2.673	1.629	6.060	2.090	2.576	3.478	2.515	5.638	5.035	2.952	2.775
.0428	8.081	1.608	3.533	2.464	5.219	1.754	3.343	3.349	2.186	4.380	3.441	3.593	3.339
.0458	9.722	1.859	5.068	2.600	4.308	2.139	1.888	3.612	2.091	2.268	2.905	3.219	2.880
.0489	7.272	2.959	4.329	2.015	6.817	2.973	1.253	3.110	2.142	2.376	4.117	2.584	2.255
.0519	4.800	4.350	2.959	2.192	6.619	2.745	1.697	1.836	3.879	4.048	3.469	2.626	2.170
.0550	4.336	4.157	3.851	2.983	4.008	2.275	1.857	1.381	5.312	5.611	3.231	2.345	1.435
.0581	3.312	2.683	5.446	2.613	2.143	2.213	1.886	1.218	3.808	5.885	3.779	2.279	1.238
.0611	4.342	2.134	4.919	2.221	2.217	2.160	1.455	1.575	1.814	5.235	4.215	4.352	1.642
.0642	5.036	3.304	3.815	2.665	2.040	1.573	9.128(1)	1.198	2.343	3.660	2.526	6.058	1.351
.0672	2.800	3.167	2.293	1.684	1.962	1.032	1.918(2)	1.042	2.673	2.531	1.468	5.159	1.005
.0703	1.918	2.310	2.100	2.161	2.703	1.808	2.417	1.087	3.668	3.774	2.935	2.971	8.301(1)
.0733	3.394	2.664	2.126	3.559	2.483	1.788	1.466	1.602	2.517	4.240	3.483	3.214	6.664
.0764	5.004	3.024	1.741	2.931	2.104	1.035	6.661(1)	1.611	2.977	4.834	2.747	3.162	5.466
.0795	4.048	3.418	1.802	1.799	2.027	6.330(1)	7.304	1.849	6.752	4.210	2.371	2.611	3.357
.0825	4.205	2.864	2.547	1.518	2.181	8.066	1.344(2)	2.510	6.126	2.320	2.145	1.595	4.369
.0856	4.429	1.867	2.312	1.886	2.901	1.051(2)	1.451	2.028	3.655	3.796	2.003	1.356	5.572
.0886	3.551	1.256	2.040	2.062	3.042	1.037	1.727	1.714	3.790	4.979	1.415	1.617	8.746
.0917	3.425	7.627(1)	2.970	2.658	2.569	1.044	1.997	2.029	3.500	4.226	9.773(1)	1.399	1.141(2)

Note: Number in parentheses indicates power of 10 multiplying adjacent and following entries.

TABLE 6. *Power spectral densities of long-baseline phase difference variations*

Baseline length: 109 feet (B–F)

Units: (deg.)²/c/s

Frequency	Sample												
	117	118	119	120	121	122	123	124	125	126	127	128	129
c/s													
0.00306	1.490(4)	8.607(3)	9.080(3)	1.560(4)	5.929(3)	4.706(3)	6.419(3)	1.655(4)	6.555(3)	5.606(4)	9.328(3)	2.134(4)	1.440(4)
.00611	1.042	4.243	2.893	6.272(3)	7.563	3.476	4.360	7.766(3)	5.098	1.630	1.039(4)	1.154	5.825(3)
.00917	5.880(3)	2.251	2.211	2.527	6.174	3.643	2.904	3.180	4.297	5.680(3)	6.391(3)	4.975(3)	3.151
.0122	5.302	1.178	1.504	3.135	4.435	2.873	1.438	4.393	3.429	6.119	3.888	2.944	2.342
.0153	3.682	7.896(2)	1.408	2.549	3.187	1.588	1.385	3.293	2.598	4.721	3.706	2.666	1.405
.0183	2.374	1.129(3)	1.576	2.298	3.865	9.582(2)	1.462	2.024	1.652	3.867	2.755	2.715	9.341(2)
.0214	1.548	1.558	1.216	2.787	3.838	1.102(3)	1.309	1.675	1.557	2.815	2.011	2.591	1.033(3)
.0244	1.358	1.728	6.780(2)	2.376	3.302	1.262	9.063(2)	8.826(2)	2.210	2.189	2.261	1.924	1.116
.0275	7.130(2)	1.323	9.864	1.750	3.211	1.195	7.320	8.172	2.649	2.017	2.392	1.207	1.095
.0306	5.557	7.222(2)	7.299	1.411	2.687	1.293	8.346	8.445	2.755	2.073	1.908	1.988	8.084(2)
.0336	8.082	7.104	6.488	1.140	1.847	9.915(2)	1.191(3)	1.016(3)	2.161	2.112	1.473	1.834	6.431
.0367	8.994	6.251	8.569	8.551(2)	1.041	7.884	9.370(2)	8.705(2)	1.215	1.554	9.983(2)	1.098	6.415
.0397	1.582(3)	4.892	1.053(3)	7.626	8.743(2)	5.043	8.374	9.807	9.063(2)	9.176(2)	8.799	1.070	3.229
.0428	1.730	6.184	1.201	4.900	6.449	3.198	9.015	1.218(3)	4.633	8.129	5.705	8.338(2)	1.813
.0458	1.484	7.140	1.142	5.133	1.091(3)	4.635	4.520	6.744(2)	4.080	9.161	3.415	6.312	2.677
.0489	9.978(2)	4.391	8.537(2)	7.130	1.463	8.059	2.682	2.307	3.454	1.059(3)	5.677	4.865	4.179
.0519	4.782	2.563	6.255	6.113	1.448	5.589	2.341	2.051	8.217	1.057	6.790	5.275	5.950
.0550	5.494	2.405	5.154	4.192	1.087	3.404	2.841	1.903	1.268(3)	1.167	5.115	4.701	4.723
.0581	6.308	2.142	5.045	3.500	5.781(2)	4.270	3.673	4.114	9.966(2)	1.044	4.306	3.523	4.307
.0611	7.619	2.081	6.175	4.135	7.207	4.807	2.840	7.416	4.809	8.505(2)	5.122	3.529	2.860
.0642	8.417	3.473	5.846	5.852	8.916	3.330	2.657	5.209	6.588	6.395	4.376	4.000	1.544
.0672	6.440	4.194	4.932	6.435	8.388	1.755	3.000	3.703	6.009	6.973	2.726	4.565	1.513
.0703	5.266	4.278	5.969	1.036(3)	7.319	2.319	3.573	3.296	5.731	1.466(3)	2.423	4.212	1.806
.0733	5.504	3.397	6.271	1.058	7.979	2.770	5.277	2.434	4.610	1.190	3.083	3.826	2.399
.0764	5.647	3.327	5.723	6.108(2)	7.073	1.545	5.477	2.487	4.362	5.895(2)	4.535	4.103	1.706
.0795	4.535	2.743	5.469	3.855	5.604	1.126	3.144	2.449	4.126	4.119	5.347	3.834	1.442
.0825	3.286	2.416	4.146	3.069	6.126	2.254	1.507	2.160	4.155	3.303	3.668	2.757	1.060
.0856	5.512	3.125	1.886	2.536	7.597	2.377	2.175	1.911	6.095	5.316	2.352	2.784	1.047
.0886	7.997	3.720	1.103	2.972	9.064	1.583	2.976	1.313	5.296	5.679	1.994	3.420	1.601
.0917	8.033	3.152	1.366	2.882	7.146	1.265	2.437	1.246	3.798	4.218	1.105	3.352	1.669

Note: Number in parentheses indicates power of 10 multiplying adjacent and following entries.

TABLE 7. *Power spectral densities of long-baseline phase difference variations*

Baseline length: 733 feet (G–H)

Units: (deg.)²/c/s

Frequency	Sample									
	67	68	69	70	71	72	73	74	75	76
c/s										
0.00306	4.428(5)	7.687(4)	3.775(5)	2.186(4)	2.407(5)	1.594(5)	9.892(4)	1.847(4)	2.421(5)	4.555(4)
.00611	3.321	8.478	1.658	2.122	1.541	3.707(4)	6.553	5.270(3)	4.786(4)	6.409
.00917	1.050	7.697	2.682(4)	1.428	1.052	2.677	4.131	3.410	1.037	3.972
.0122	2.907(4)	6.037	1.875	1.605	5.058(4)	1.573	1.722	2.724	1.045	1.573
.0153	2.495	2.702	1.541	1.632	3.033	1.090	7.293(3)	1.588	7.597(3)	6.039(3)
.0183	1.340	5.164(3)	8.418(3)	8.803(3)	2.512	9.891(3)	5.802	8.631(2)	8.433	4.478
.0214	7.743(3)	3.319	5.641	7.007	1.535	8.262	2.624	1.113(3)	5.175	3.635
.0244	5.790	2.975	4.365	4.190	1.910	4.197	9.970(2)	1.199	2.085	3.115
.0275	3.333	3.170	2.055	2.535	1.508	9.013	4.932	8.423(2)	2.687	3.741
.0306	3.459	2.580	9.488(2)	2.815	6.975(3)	1.037(4)	3.733	6.015	1.916	3.443
.0336	2.461	1.846	7.734	1.951	5.350	5.491(3)	4.949	4.245	9.723(2)	2.034
.0367	1.340	1.733	5.256	1.646	4.661	3.115	4.567	4.821	6.869	1.747
.0397	1.369	1.035	3.699	1.360	2.329	2.264	3.930	4.514	6.941	1.428
.0428	1.239	3.968(2)	3.528	6.978(2)	1.727	1.296	4.208	3.418	4.156	1.540
.0458	1.217	7.406	3.196	4.145	1.812	1.750	3.217	3.241	6.081	1.114
.0489	1.105	9.884	1.407	1.047(3)	1.661	1.614	2.558	2.490	7.337	6.841(2)
.0519	1.033	6.826	7.706(1)	1.170	1.942	1.382	2.537	1.049	6.088	1.569(3)
.0550	1.068	2.056	4.668	5.474(2)	1.612	6.477(2)	1.989	5.723(1)	2.945	1.741
.0581	7.056(2)	2.772	5.790	3.979	1.217	7.957	1.017	1.256(2)	3.455	8.665(2)
.0611	5.414	3.437	8.936	3.728	9.967(2)	5.769	7.338(1)	1.509	1.968	4.419
.0642	5.944	3.752	1.329(2)	2.865	6.112	2.824	9.922	1.580	1.264	5.616
.0672	4.409	3.109	9.214(1)	9.327(1)	3.612	3.083	1.207(2)	1.001	1.585	6.659
.0703	2.949	2.614	6.098	2.498(2)	2.043	6.472	1.568	6.793(1)	2.554	5.295
.0733	2.747	2.415	8.444	2.399	2.744	6.253	2.603	7.761	1.420	3.830
.0764	2.114	4.580	1.094(2)	1.191	4.315	4.426	1.974	8.316	2.195	2.065
.0795	1.938	4.227	5.063(1)	1.417	5.590	2.453	9.215(1)	5.955	2.562	2.068
.0825	3.958	3.753	8.506	1.782	4.623	2.983	6.510	7.728	2.240	1.527
.0856	5.651	3.386	6.158	1.106	4.331	1.920	6.019	6.234	8.314(1)	7.739(1)
.0886	5.295	3.322	2.818	6.120(1)	3.489	1.520	3.265	3.922	9.490	9.109
.0917	4.784	2.664	1.022	−1.685(−1)	2.075	5.760(1)	2.551	3.413	6.657	1.789(2)

Note: Number in parentheses indicates power of 10 multiplying adjacent and following entries.

TABLE 8. *Power spectral densities of long-baseline phase difference variations*

Baseline length: 1,181 feet (B–G)

Units: (deg.)²/c/s

Frequency	Sample									
	77	78	79	80	81	82	83	84	85	86
c/s										
0.00306	2.586(5)	7.399(4)	----------	7.556(4)	5.627(5)	1.942(5)	1.130(5)	5.822(4)	1.193(5)	8.339(4)
.00611	2.560	1.001(5)	----------	5.275	2.742	7.214(4)	2.123(4)	4.992(3)	4.685(4)	1.182(5)
.00917	7.960(4)	8.250(4)	7.802(4)	2.090	1.940	2.315	1.382	4.143	1.981	8.580(4)
.0122	1.476	5.317	3.910	1.890	9.961(4)	1.858	7.141(3)	4.025	1.324	4.139
.0153	8.818(3)	2.921	1.584	1.936	4.188	9.873(3)	4.606	2.792	1.066	1.329
.0183	3.731	1.067	6.852(3)	1.943	1.462	1.171(4)	5.008	2.787	9.713(3)	3.515(3)
.0214	1.484	3.884(3)	4.377	1.917	1.216	1.157	4.178	3.053	5.204	2.843
.0244	3.050	2.177	3.661	9.743(3)	1.500	7.147(3)	3.050	1.874	2.555	4.564
.0275	2.358	1.843	2.212	6.231	9.923(3)	4.534	1.406	1.501	2.176	4.949
.0306	1.676	1.542	8.410(2)	6.582	4.611	3.348	8.547(2)	9.762(2)	1.162	3.818
.0336	1.212	1.746	7.581	3.375	5.421	1.625	8.318	3.537	1.054	1.649
.0367	9.385(2)	7.505(2)	7.088	1.890	5.782	2.239	5.954	2.551	9.279(2)	2.012
.0397	2.341	4.723	5.461	1.751	3.713	2.400	4.679	5.900	5.465	2.003
.0428	4.420	2.427	5.887	1.447	2.797	1.650	4.108	5.053	2.535	1.644
.0458	4.044	5.127	7.924	6.382(2)	2.163	1.442	1.340	2.626	5.410	9.826(2)
.0489	3.362	3.752	5.452	6.092	2.241	1.385	3.419(1)	1.343	5.376	7.198
.0519	8.119(1)	1.685	5.352	6.037	2.115	1.439	5.318	1.832	3.966	7.800
.0550	2.404(2)	1.173	4.075	5.025	1.556	1.177	1.209(2)	1.851	2.767	5.788
.0581	5.777(1)	2.511	4.769	3.346	6.498(2)	8.234(2)	1.594	1.676	2.084	3.897
.0611	1.289(2)	1.184	3.445	3.455	3.368	4.047	1.573	1.471	8.207(1)	3.941
.0642	1.198	1.273	2.126	4.030	4.964	3.575	1.505	1.490	5.930	1.955
.0672	2.143	1.483	9.686(1)	5.344	2.909	2.866	1.503	1.324	6.953	1.469
.0703	−1.769(1)	1.989	1.466(2)	5.362	3.682(1)	1.729	1.236	1.391	1.136(2)	1.165
.0733	7.665	1.120	1.339	4.770	1.054(2)	1.305	1.295	1.376	1.091	1.633
.0764	−1.910	1.442	1.569	3.348	2.057	2.125	5.729(1)	7.901(1)	1.346	1.123
.0795	9.654	4.955(1)	6.255(1)	4.446	1.164	3.245	3.022	4.446	6.914(1)	1.133
.0825	7.254	8.482	9.991	4.156	1.333	3.398	7.032	7.483	5.121	2.135(1)
.0856	1.707(2)	3.938	1.729(2)	4.047	2.396	2.720	5.047	8.386	1.499	1.067(2)
.0886	9.420(1)	8.250	2.657	2.948	2.009	1.728	3.819	1.633(2)	3.549	1.723
.0917	2.306(2)	6.480	2.300	2.504	7.773(1)	8.823(1)	3.099	2.274	2.472	2.381

Note: Number in parentheses indicates power of 10 multiplying adjacent and following entries.

TABLE 9. *Power spectral densities of long-baseline phase difference variations*

Baseline length 1,914 feet (B–H)
(Samples taken from BGH recording period)
Units: (deg.)²/c/s

Frequency	Sample									
	87	88	89	90	91	92	93	94	95	96
c/s										
0.00306	5.009(5)	2.044(5)		1.307(5)	1.473(6)	3.158(5)	1.918(5)	1.222(5)	5.584(5)	2.223(5)
.00611	2.717	1.807		7.479(4)	6.064(5)	1.540	3.745(4)	1.240(4)	1.862	2.568
.00917	7.008(4)	1.106	5.969(4)	2.239	2.489	7.355(4)	1.500	7.980(3)	6.280(4)	1.716
.0122	1.805	3.678(4)	4.644	3.667	1.283	3.899	9.436(3)	6.763	2.834	6.542(4)
.0153	5.776(3)	1.973	2.137	4.543	4.283(4)	2.820	5.954	3.557	1.113	1.579
.0183	3.206	9.887(3)	1.100	2.669	1.831	1.210	3.376	2.313	8.403(3)	7.339(3)
.0214	2.180	4.933	5.909(3)	1.818	2.564	5.424(3)	3.829	3.957	6.512	6.722
.0244	2.196	2.120	3.614	1.168	3.124	5.085	2.800	2.653	2.662	5.599
.0275	1.034	1.502	2.050	5.551(3)	1.528	7.104	9.927(2)	8.725(2)	1.714	3.388
.0306	4.874(2)	1.350	1.266	3.625	3.517(3)	5.037	4.449	4.904	9.504(2)	2.544
.0336	3.695	1.470	1.340	1.031	3.063	1.652	4.134	3.631	8.075	1.629
.0367	3.489	1.094	1.691	6.187(2)	3.820	1.746	2.506	2.601	6.100	1.477
.0397	1.512	6.273(2)	1.581	1.063(3)	1.920	2.440	3.730	1.599	9.365	5.608(2)
.0428	8.765(1)	3.618	1.505	1.240	7.165(2)	1.146	3.934	2.521	5.343	1.859
.0458	3.618	3.451	1.474	7.332(2)	1.589	3.091(2)	3.463	3.430	3.302	7.742(1)
.0489	2.182(2)	2.731	1.174	1.094(3)	5.726	7.566	2.315	2.345	3.258	5.083(2)
.0519	1.988	2.420	1.048	1.107	1.041(3)	1.281(3)	2.282	1.661	3.934	7.747
.0550	1.973	8.030(1)	1.071	1.009	1.402	8.793(2)	1.051	1.576	2.574	7.897
.0581	1.355	7.478	8.720(2)	7.287(2)	1.129	4.430	8.806(1)	1.052	2.379	2.898
.0611	5.517(1)	6.481	6.907	3.752	1.347	1.660	8.341	4.651(1)	4.374(1)	3.066
.0642	2.937	2.870	5.011	1.662	1.127	2.356	1.101(2)	3.388	1.490(2)	3.170
.0672	1.905(2)	−1.616	2.833	2.257	1.049	1.956	7.214(1)	5.424	2.706	3.741
.0703	1.005	2.456	1.973	2.524	2.472(2)	3.258	1.002(2)	8.237	3.315	6.115(1)
.0733	1.227(1)	9.518(0)	2.462	2.901	1.112(1)	4.453	1.207	4.806	1.737	1.001(2)
.0764	−2.658	1.678(1)	4.529	1.894	−6.989	4.229	8.702(1)	5.465	2.478	5.807(1)
.0795	4.293(0)	1.071	6.467	2.024	8.290	2.481	3.536	7.883	2.018	2.045(2)
.0825	1.515(1)	6.416	6.029	1.627	3.477	1.858	4.629	6.828	1.931	8.953(1)
.0856	3.580	2.153	6.277	3.297	1.334(2)	8.444(1)	7.802	9.886(0)	7.907(1)	1.776(2)
.0886	1.559(0)	4.123	5.160	4.867	−1.433(1)	2.054(2)	8.375	6.727	1.030(2)	4.487(1)
.0917	1.516(1)	1.236	4.261	6.104	1.189(2)	2.460	3.500	−8.054	2.012(1)	7.475

Note: Number in parentheses indicates power of 10 multiplying adjacent and following entries.

TABLE 10. *Power spectral densities of long-baseline phase difference variations*

Baseline length: 1,914 (B–H)

(Samples taken from ABH recording period)

Units: (deg.)²/c/s

Frequency	Sample												
	48	49	50	51	52	53	54	55	56	57	58	59	60
c/s													
0.00306	1.958(6)	5.364(5)	2.695(5)	9.973(4)	6.049(4)	4.969(4)	2.484(4)	4.915(4)	1.053(5)	1.987(5)	6.545(4)		1.179(5)
.00611	7.967(5)	2.533	1.649	2.029	5.261	3.556	1.763	8.019(3)	1.618(4)	4.423(4)	5.024		7.700(4)
.00917	2.790	9.958(4)	3.219(4)	1.073	3.881	1.965	1.064	8.726(2)	8.838(2)	1.947	1.687	8.863(3)	4.031
.0122	1.837	4.803	1.361	4.929(3)	1.704	6.985(3)	4.462(3)	2.423	5.004	1.123	3.055(3)	4.343	1.182
.0153	9.711(4)	2.294	7.759(3)	1.854	7.130(3)	1.932	2.850	4.157	2.248	3.224(3)	1.266	1.933	6.032(3)
.0183	3.447	1.901	3.788	2.435	4.229	2.188	3.829	1.995	9.412(1)	5.855(2)	9.045(2)	8.211(2)	4.565
.0214	1.681	1.846	3.654	3.005	2.212	1.941	2.696	1.112	2.365(2)	7.226	9.170	8.079	3.407
.0244	6.146(3)	8.825(3)	3.254	1.777	2.253	8.719(2)	1.220	1.373	9.104(1)	6.187	8.796	6.781	2.159
.0275	6.198	7.482	1.190	8.327(2)	1.760	5.991	4.844(2)	1.120	1.336(2)	5.885	6.499	2.984	1.303
.0306	7.557	5.174	4.407(2)	3.678	9.471(2)	3.183	4.009	6.072(1)	−2.618(1)	3.167	5.752	1.780	6.481(2)
.0336	6.415	8.108	3.248	2.940	6.115	2.845	5.359	4.137	4.379	2.204	3.029	1.323	7.935
.0367	3.695	7.605	3.031	2.729	2.520	1.433	5.375	2.648(0)	−4.440(0)	−1.037(1)	2.678	1.983	5.775
.0397	4.964	3.827	3.226	2.446	4.156	1.575	3.292	2.077(1)	3.951(1)	6.084	2.524	3.311	5.366
.0428	5.262	2.565	3.304	1.523	7.739	2.872	3.241	7.844(0)	−9.227(0)	−7.931(0)	2.422	2.306	2.542
.0458	3.886	2.310	1.542	1.942	5.986	2.315	2.860	1.037(1)	5.918(1)	2.654(1)	1.135	1.078	3.702
.0489	1.906	1.363	1.675	1.174	2.525	5.887(1)	2.087	−1.137(0)	−2.278	−1.722	1.034	1.360	3.492
.0519	2.443	6.560(2)	1.249	6.592(1)	1.515	7.363	1.331	1.086(1)	1.394	3.401	6.917(1)	1.451	2.873
.0550	2.805	4.262	2.556	3.161	3.684(1)	1.094(2)	1.285	−2.818(0)	−1.834	−3.420	1.226(2)	1.244	1.386
.0581	2.249	5.074	2.299	8.454	2.774	1.361	1.036	5.181	2.276	1.476	1.330	1.122	1.381
.0611	5.269(2)	6.058	1.745	4.865	3.411	6.869(1)	8.965(1)	−4.010	−1.294	−1.007	9.799(1)	1.123	1.372
.0642	9.072	6.881	1.182	2.243	1.510(2)	6.600	4.774	8.979(−1)	1.399	1.933	5.231	1.091	1.925
.0672	1.135(3)	4.052	1.419	9.981(0)	2.579	6.911	3.689	−2.782(0)	−2.265	−2.806	6.116	9.800(1)	1.256
.0703	1.428	3.004	9.341(1)	3.325(1)	2.354	6.175	2.867	8.982	1.453	2.356	6.434	6.896	1.484
.0733	5.516(2)	1.260	6.984	−1.657(0)	1.155	6.589	6.671	1.801	−4.214(0)	6.748(0)	7.014	7.042	5.496(1)
.0764	9.083	1.945	5.277	1.671(1)	1.356	8.263	5.086	5.303	1.567(1)	2.497(1)	4.743	5.975	9.830
.0795	6.276	2.355	1.033(2)	−4.415(0)	1.062	6.103	2.772	5.826(−1)	−2.214	−4.833(0)	4.403	5.000	9.529
.0825	8.659	3.180	6.454(1)	3.888	3.262(1)	7.174	1.226	6.473(0)	5.733(0)	1.885(1)	2.478	3.781	1.508(2)
.0856	4.465	4.977(1)	6.268	−1.659	−2.103(0)	4.612	2.808	−4.037	−1.889(1)	−2.007	4.733	2.704	9.242(1)
.0886	7.824	1.722(2)	1.947	3.602(1)	3.357(1)	3.812	3.775	5.481	1.360	−1.396(0)	3.672	1.336	1.313(2)
.0917	7.735	1.253	3.490	3.254	2.691	1.095	5.926	3.187	−8.534(0)	−2.760(1)	3.004	2.265	1.150

Note: Number in parentheses indicates power of 10 multiplying adjacent and following entries.

TABLE 11. *Power spectral densities of long-baseline phase difference variations*

Baseline length: 3,003 feet (A–B)

Units: (deg.)²/c/s

Frequency	Sample 22	23	24	25	26	27	28	29	30	31	32	33	34
c/s													
0.00306	3.169(6)	----------	5.756(5)	1.992(5)	1.742(5)	3.030(5)	1.121(5)	----------	----------	1.515(5)	----------	----------	----------
.00611	1.538	----------	2.033	1.095	6.986(4)	6.095(4)	4.523(4)	----------	----------	3.584(4)	----------	----------	----------
.00917	1.341(5)	1.393(5)	3.801(4)	3.138(4)	1.742	8.847(3)	8.422(3)	1.080(3)	5.937(2)	6.150(3)	7.426(3)	9.615(3)	2.193(4)
.0122	4.914(4)	9.489(3)	1.460	1.413	1.237	9.374	5.928	3.728(2)	5.466	3.676	3.371	7.627	1.605
.0153	3.676	6.443	3.772(3)	1.212	1.254	4.671	1.726	1.240	4.043	2.066	1.188	2.796	1.536
.0183	2.778	5.643	1.236	1.041	8.997(3)	2.135	2.138	1.163	2.129	1.163	6.331(2)	1.950	9.173(3)
.0214	2.627	5.056	6.797(2)	5.501(3)	3.820	2.454	2.513	2.272	8.438(1)	1.804	9.671	1.672	5.087
.0244	1.932	5.439	2.871	2.740	1.167	1.434	1.475	1.494	1.211(2)	1.648	1.202(3)	7.749(2)	4.184
.0275	7.794(3)	1.957	1.020(3)	2.109	1.348	1.136	8.874(2)	8.848(1)	1.305	6.085(2)	8.672(2)	4.895	2.961
.0306	1.049(4)	2.667	3.527(2)	1.524	6.995(2)	7.327(2)	6.329	1.000(2)	7.472(1)	1.501	4.178	4.049	1.413
.0336	7.443(3)	4.542	4.581	1.497	7.609	7.364	4.386	5.521(1)	2.721	3.592	1.783	1.689	7.219(2)
.0367	5.095	3.571	2.074	1.599	7.732	2.652	3.030	1.852	1.614	3.803	1.830	9.285(1)	5.668
.0397	4.052	1.008	6.092	1.242	5.153	4.334	1.956	2.111	2.524	1.971	1.690	1.564(2)	4.909
.0428	4.020	1.086	7.825(1)	1.007	2.654	1.646	3.476	4.535	4.934	1.930(1)	9.562(1)	1.252	4.267
.0458	3.691	−4.672(1)	1.044(2)	9.121(2)	1.625	3.753	3.051	3.989	4.384	4.805	7.652	1.102	2.401
.0489	2.386	2.903(2)	−8.251(1)	9.241	4.304(1)	2.629	9.090(1)	3.662	2.865	7.334	7.528	1.376	1.574
.0519	8.163(2)	3.984	8.088	7.023	7.352	4.162	4.034	2.135	2.677	1.473(2)	6.081	9.549(1)	1.335
.0550	1.641(3)	9.469	−1.469(2)	4.413	5.461	1.296	6.591	2.127	3.343	9.449(1)	8.868	1.138(2)	1.756
.0581	9.137(2)	1.698	4.619(1)	3.335	2.638	1.137	6.336	1.828	3.333	4.822	9.720	1.800	1.897
.0611	3.505	1.777	−7.339	3.847	4.932	3.205(1)	6.023	1.185	3.472	2.371	6.884	1.582	1.907
.0642	4.858(1)	−6.120(1)	1.237(2)	4.220	1.037(2)	1.749(2)	4.140	1.247	2.682	3.074	3.340	1.257	1.780
.0672	1.142(2)	4.278(2)	−2.259(1)	5.425	7.800(1)	4.040(1)	3.475	1.456	1.364	−4.567(0)	3.906	1.325	2.200
.0703	1.793	2.210	1.240(2)	4.597	7.176	7.580	2.758	1.300	1.045	2.029(1)	3.976	9.930(1)	1.865
.0733	2.799	2.885	−9.306(0)	3.285	4.773	−2.369	4.598	1.381	1.407	1.520	5.213	8.655	1.178
.0764	−7.395(1)	−6.368(1)	7.649(1)	2.954	7.303	9.875	3.470	1.254	1.548	4.592	6.635	3.308	5.742(1)
.0795	2.105(2)	2.963(2)	−4.337	2.601	1.575	2.566	3.415	1.361	2.396	3.336	4.979	1.523	8.767
.0825	1.916	1.094	8.899	2.107	3.512(0)	9.189	5.160	1.273	2.239	3.702	5.131	8.406(0)	5.742
.0856	1.374	3.078	−5.155	1.902	5.002	1.626(0)	4.325	1.410	1.852	1.001	3.664	1.896(1)	3.865
.0886	2.128	1.489	5.814	2.144	8.361(1)	8.390(1)	1.611	8.382(0)	1.217	2.733	4.416	2.300	2.230
.0917	9.549	5.435	−7.168	2.148	1.127(2)	−2.508(0)	9.653(0)	4.822	1.052	1.551	4.399	4.060	3.722

Note: Number in parentheses indicates power of 10 multiplying adjacent and following entries.

TABLE 12. *Power spectral densities of long-baseline phase difference variations*

Baseline length: 4,847 feet (A–H)

Units: (deg.)²/c/s

Frequency	Sample 35	36	37	38	39	40	41	42	43	44	45	46	47
c/s													
0.00306	1.316(6)	1.436(6)	5.026(5)	2.113(5)	2.751(5)	3.378(5)	1.411(5)	7.995(3)	----------	1.702(5)	----------	----------	6.448(5)
.00611	5.416(5)	7.625(5)	2.129	1.009	1.223	8.275(4)	7.296(4)	6.587	----------	3.937(4)	----------	----------	4.623(4)
.00917	2.257	1.071	4.850(4)	4.062(4)	3.914(4)	9.235(3)	1.072	3.428	2.780(3)	1.068	1.449(4)	1.666(4)	1.725
.0122	1.566	6.410(4)	2.087	1.885	1.984	4.630	3.755(3)	1.227	1.284	5.323(3)	3.933(3)	7.057(3)	8.697(3)
.0153	5.577(4)	3.151	1.135	1.031	9.669(3)	3.828	2.694	7.311(2)	5.671(2)	1.306	2.883	3.462	5.225
.0183	3.182	1.013	5.016(3)	6.235(3)	4.806	2.334	2.597	3.891	4.902	5.681(2)	2.400	1.503	3.508
.0214	3.822	3.701(3)	1.843	3.094	2.330	2.065	1.249	2.512	4.125	7.348	1.108	6.734(2)	3.025
.0244	2.424	3.682	9.290(2)	2.768	1.359	8.265(2)	1.033	1.932	1.986	7.016	6.216(2)	2.836	2.237
.0275	1.499	1.776	7.831	2.966	1.641	7.434	6.202(2)	1.811	4.112(1)	5.805	9.098	3.548	1.099
.0306	1.570	2.885	1.545	1.952	1.418	4.441	5.241	1.786	7.301	2.599	7.705	3.715	4.178(2)
.0336	1.391	1.237	5.145	8.824(2)	9.463(2)	5.697	3.577	1.348	8.807	3.070	5.557	3.259	9.051
.0367	5.779(3)	1.420	1.378	7.739	6.615	4.190	3.120	1.130	8.444	2.420	5.470	2.883	6.328
.0397	4.224	7.768(2)	2.591	1.072(3)	3.626	5.761	8.297(1)	1.164	6.289	1.954	2.906	1.811	5.806
.0428	3.658	1.339(3)	−1.779	9.880(2)	2.949	1.113	1.476(2)	1.103	5.898	2.165(1)	1 762	1.222	1.350
.0458	1.794	6.560(2)	2.820(1)	7.518	4.781	3.777	1.332	1.025	4.316	3.731	1.179	1.078	1.184
.0489	2.217(2)	1.364(3)	−7.193(1)	6.244	4.025	8.937(1)	1.583	9.741(1)	3.195	2.798	8.722(1)	1.077	−6.272(1)
.0519	1.979(3)	4.793(2)	1.528(2)	5.839	3.333	3.404(2)	1.020	1.214(2)	3.810	8.309	4.979	1.367	2.814
.0550	2.089	5.297	−6.200(0)	5.251	3.581	1.692	1.160	1.105	6.251	7.537	5.175	1.179	−3.115
.0581	1.950	6.840(1)	9.174(1)	4.254	2.318	1.710	−1.775(0)	9.610(1)	4.056	8.219	5.048	9.460(1)	1.258(2)
.0611	1.457	4.315(2)	−9.900	2.777	8.068(1)	2.105(1)	2.084(1)	1.044(2)	1.994	1.569	5.409	1.084(2)	1.030(1)
.0642	1.981	−1.940	3.294	3.277	3.185	1.856(2)	3.991	1.003	1.291	2.757	4.162	6.722(1)	3.547
.0672	2.237	2.904	−7.446	3.872	5.459	9.739(1)	9.106	1.024	2.231	−1.555	4.207	5.282	−5.230
.0703	2.017	1.181	6.592	3.047	3.183	1.561(2)	1.274(−1)	1.005	2.177	1.307	3.017	6.852	5.111
.0733	7.604(2)	5.122	−6.789	2.150	−5.953(0)	−2.042(1)	1.690(0)	1.007	2.905	2.467	2.708	4.766	−4.471
.0764	9.775	4.910(1)	4.010	2.063	1.023(1)	1.102(2)	−1.332(1)	7.884(1)	2.530	4.170	3.664(0)	1.989	3.000
.0795	2.877	2.888(2)	−8.043	2.190	3.909	6.266(1)	4.663	6.192	2 441	−6.590(0)	2.376(1)	1.543	1.451
.0825	2.802	2.194	3.760	2.768	7.698	1.393(2)	3.251	5.919	8.831(0)	1.227(1)	5.313	1.742	1.287(2)
.0856	1.809	4.888	−7.346	3.581	9.637	−5.005(1)	4.146	7.329	6.363	7.472(0)	5.602	1.718	4.245(1)
.0886	4.400	5.996(1)	2.921(0)	3.251	9.075	4.042	−1.610	9.186	7.806	4.957(1)	4.334	3.901	6.446
.0917	6.274(1)	4.915(2)	−1.178(2)	2.421	6.736	−6.512	9.811(0)	9.237	1.844(1)	4.873	4.682	6.821	3.115(−1)

Note: Number in parentheses indicates power of 10 multiplying adjacent and following entries.

TABLE 13. *Power spectral densities of single-path phase samples taken from BEF recording period*

Units: (deg.)²/c/s

Frequency	Sample						
	130	131	132	133	134	135	136
c/s							
0.00306	3.084(6)	9.150(5)	1.024(6)	5.895(5)	1.078(6)	3.341(6)	3.546(5)
.00611	1.586	7.110	4.791(5)	3.287	5.350(5)	5.280(5)	2.586
.00917	4.349(5)	2.970	2.452	1.576	1.109	4.441(4)	1.156
.0122	1.959	6.025(4)	7.675(4)	5.270(4)	3.820(4)	2.171	2.577(4)
.0153	1.356	1.824	3.270	3.450	1.894	1.334	1.374
.0183	4.296(4)	2.135	2.138	2.625	9.285(3)	6.710(3)	1.169
.0214	2.387	2.170	1.691	1.550	7.205	8.950	8.535(3)
.0244	2.620	1.444	1.124	5.995(3)	9.620	8.910	4.396
.0275	2.267	9.295(3)	8.520(3)	3.568	5.465	8.750	2.715
.0306	2.070	2.394	1.674	2.710	3.998	2.838	1.262
.0336	1.020	2.260	2.117	2.844	3.405	4.536	1.185
.0367	4.603(3)	5.060	2.534	1.726	3.718	2.187	7.740(2)
.0397	4.288	5.655	4.024	2.044	2.316	2.520	6.565
.0428	3.493	2.465	1.040	1.014	1.876	8.800(2)	4.050
.0458	2.022	1.836	1.918	8.880(2)	1.402	2.064(3)	4.584
.0489	2.588	1.996	3.016	4.750	1.191	4.474(2)	3.010
.0519	2.314	2.126	2.476	1.126(3)	4.194(2)	1.181(3)	2.284
.0550	2.990	1.204	6.035(2)	5.410(2)	9.585	7.355(2)	9.640(1)
.0581	2.734	9.945(2)	1.054(3)	6.215	8.105	1.662(3)	2.459(2)
.0611	2.622	5.885	5.645(2)	4.564	9.525	4.881(1)	1.436
.0642	1.831	6.940	1.072(3)	5.155	3.897	4.902(2)	3.411
.0672	1.294	3.690	1.301(2)	5.610	4.885	-3.867(1)	1.414
.0703	1.073	3.593	5.275	1.202(3)	-4.214(1)	1.002(3)	1.591
.0733	1.237	1.040	2.288	6.335(2)	2.876(2)	-4.924(1)	8.955(1)
.0764	6.100(2)	2.010	9.100	3.822	4.730	3.892(2)	2.632(2)
.0795	3.196	-3.494(1)	7.325	3.066	7.665	8.020(1)	1.156
.0825	1.260	3.490	9.915	5.475	4.221	9.105(2)	1.811
.0856	9.965	4.098	2.211	3.094	7.325	-1.040	7.390(1)
.0886	9.175	3.030(2)	6.535	3.757	4.159	2.844	1.035(2)
.0917	8.890	4.126(1)	1.476	1.615	5.550	-3.466	-2.062(1)

Note: Number in parentheses indicates power of 10 multiplying adjacent and following entries.

TABLE 14. *Power spectral densities of single-path phase samples taken from BGH recording period*

Units: (deg.)²/c/s

Frequency	Sample						
	97	98	99	100	101	102	103
c/s							
0.00306	----------	1.386(6)	1.110(6)	5.145(5)	----------	----------	6.070(5)
.00611	----------	1.844(5)	3.238(5)	1.432	----------	----------	3.854
.00917	2.126(4)	2.829(4)	4.974(4)	4.676(4)	4.641(3)	2.526(4)	1.484
.0122	8.560(3)	1.797	1.338	4.211	1.146	1.158	8.740(4)
.0153	7.755	5.650(3)	5.095(3)	2.391	6.725(2)	8.765(3)	4.686
.0183	6.535	2.362	1.882	1.156	3.431	6.655	2.613
.0214	2.493	2.166	2.656	8.515(3)	3.840	1.920	1.890
.0244	1.180	1.296	1.461	6.155	6.120	1.104	1.322
.0275	1.178	1.631	1.895	4.308	4.992	1.032	6.245(3)
.0306	1.143	9.970(2)	6.890(2)	2.485	3.568	3.534(2)	2.828
.0336	4.967(2)	8.835	1.032(3)	2.638	1.913	4.112	2.256
.0367	2.992	2.080	4.528(2)	3.058	1.357	6.640	1.904
.0397	1.352	9.475(1)	8.445	3.455	1.028	5.465	1.326
.0428	3.238	-3.935	3.348	2.611	7.935(1)	5.245	2.216
.0458	5.630	2.548(2)	6.960	1.830	2.074	4.391	2.964
.0489	3.754	2.652	2.100	1.418	3.121	2.910	1.916
.0519	1.245	2.978	4.738	1.224	3.592	1.778	9.525(2)
.0550	1.022	4.498(1)	1.404	9.420(2)	7.225	1.632	1.113(3)
.0581	7.075(1)	1.920(2)	4.520	1.159(3)	4.792	9.835(1)	9.040(2)
.0611	1.248(2)	8.480(1)	1.936	9.680(2)	2.704	8.990	9.925
.0642	6.115(1)	1.317(2)	4.145	8.235	1.442	7.185	1.156(3)
.0672	4.480	3.670(1)	1.144	6.985	3.844	9.170	1.106
.0703	2.704	1.129(2)	3.470	8.350	3.586	7.215	8.305(2)
.0733	5.525	1.812(1)	1.424	8.950	3.948	6.420	7.020
.0764	3.368	1.076(2)	3.528	8.940	2.545	2.616	6.225
.0795	7.025	4.264(1)	9.505(1)	6.840	1.971	6.670	6.300
.0825	4.136	1.424(2)	3.031(2)	7.005	1.654	5.565	4.303
.0856	4.204	4.668(1)	1.216	6.255	1.822	2.774	4.791
.0886	-1.370	9.075	3.200	7.710	8.265(0)	1.216	4.842
.0917	-5.520(0)	7.230(0)	1.010	7.585	1.242(1)	3.252	7.130

Note: Number in parentheses indicates power of 10 multiplying adjacent and following entries.

TABLE 15. *Power spectral densities of single-path phase samples taken from ABH recording period*

Units: (deg.)²/c/s

Frequency	Sample					
	61	62	63	64	65	66
c/s						
0.00306	1.834(6)	----------	7.645(5)	----------	3.602(5)	----------
.00611	3.950(5)	----------	2.740	----------	2.685(4)	----------
.00917	7.050(4)	6.815(2)	4.199(4)	6.850(3)	5.850(3)	6.000(3)
.0122	2.094	3.498	1.534	2.915	3.049	3.672
.0153	1.952	2.204	2.854	9.135(2)	1.422	4.634
.0183	1.670	7.590(1)	3.078	7.265	8.430(2)	4.484
.0214	8.400(3)	6.000	1.886	1.104(3)	6.000	3.236
.0244	4.580	7.580	6.600(3)	8.605(2)	2.606	1.297
.0275	3.098	7.830	2.985	4.138	3.064	7.985(2)
.0306	1.832	6.375	3.270	2.465	2.196	1.050(3)
.0336	2.337	2.125	3.460	1.194	3.080	1.032
.0367	2.700	1.154	2.253	1.132	1.424	6.185(2)
.0397	3.194	1.746	7.975(2)	1.426	1.342	3.910
.0428	2.150	2.896	2.636	1.354	7.230(1)	1.984
.0458	1.064	2.217	3.378	7.285(1)	1.559(2)	8.985(1)
.0489	4.462(2)	7.650(0)	2.824	6.635	8.280(1)	8.245
.0519	6.190	3.530	1.439	5.450	7.685	6.035
.0550	6.955	4.220	3.246(1)	5.570	3.314	1.034(2)
.0581	4.917	5.905	1.766	2.934	7.435	1.451
.0611	1.864	1.274(1)	6.600	2.452	2.153	1.273
.0642	6.455(1)	1.246	1.457(2)	1.861	5.315	5.290(1)
.0672	−7.540	1.028	3.373(1)	3.848	3.301	1.324
.0703	1.562(2)	1.033	−1.891(0)	3.677	7.325	2.671
.0733	1.356	9.270(0)	−1.540(1)	3.273	3.601	1.296
.0764	−4.736(1)	6.640	4.278	2.110	6.150	−5.625(−1)
.0795	−5.320	4.476	1.029	2.860	4.546	1.370(1)
.0825	−5.470(0)	2.892	1.059	2.379	7.345	2.864
.0856	−1.648(2)	4.764	−2.034	4.587	3.266	2.522
.0886	−1.720	4.417	1.522	5.200	4.460	2.106
.0917	−1.560	3.578	6.075(−1)	4.369	1.222	1.920

Note: Number in parentheses indicates power of 10 multiplying adjacent and following entries.

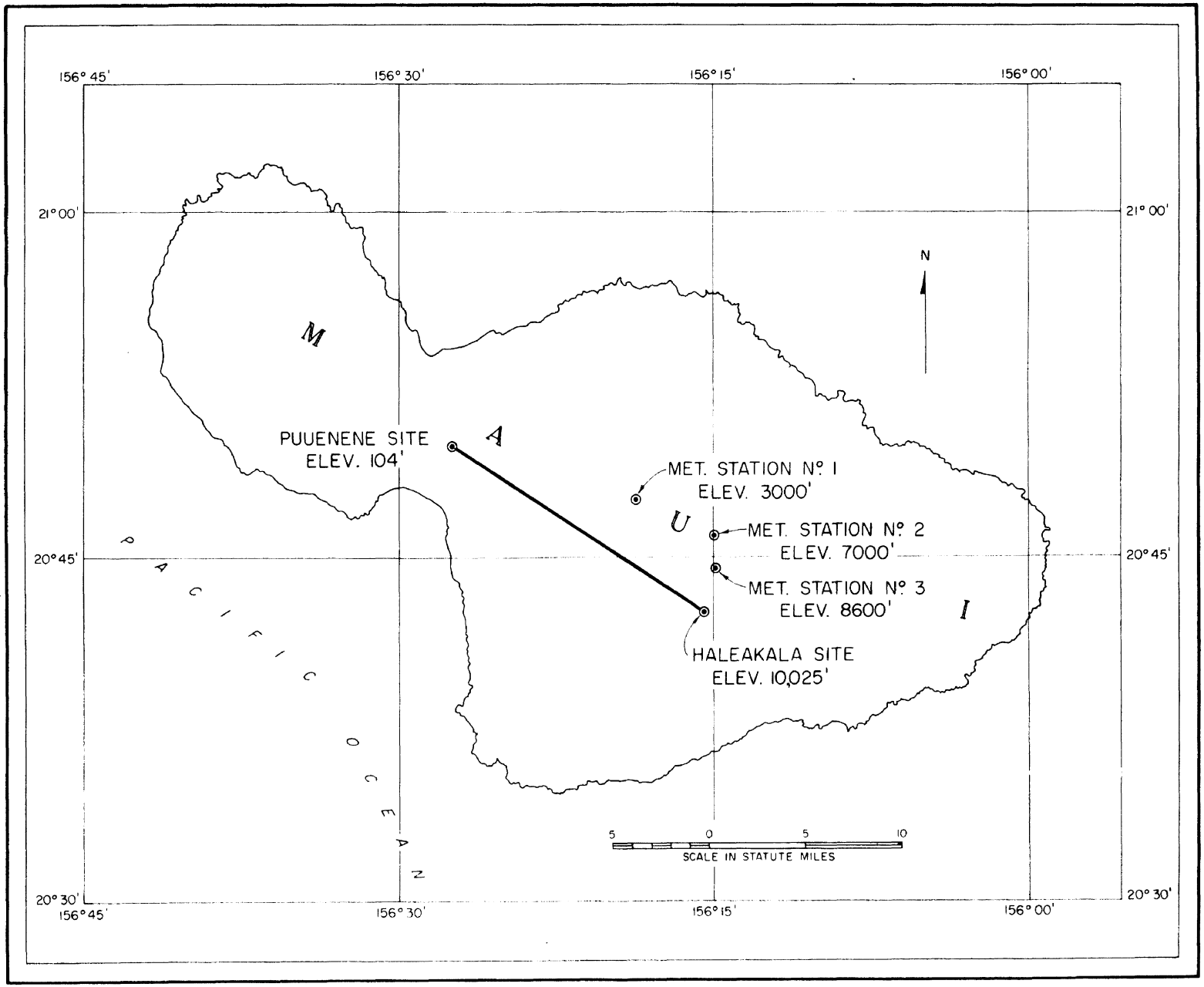

FIGURE 1. *Location of propagation paths used in Maui experiment.*

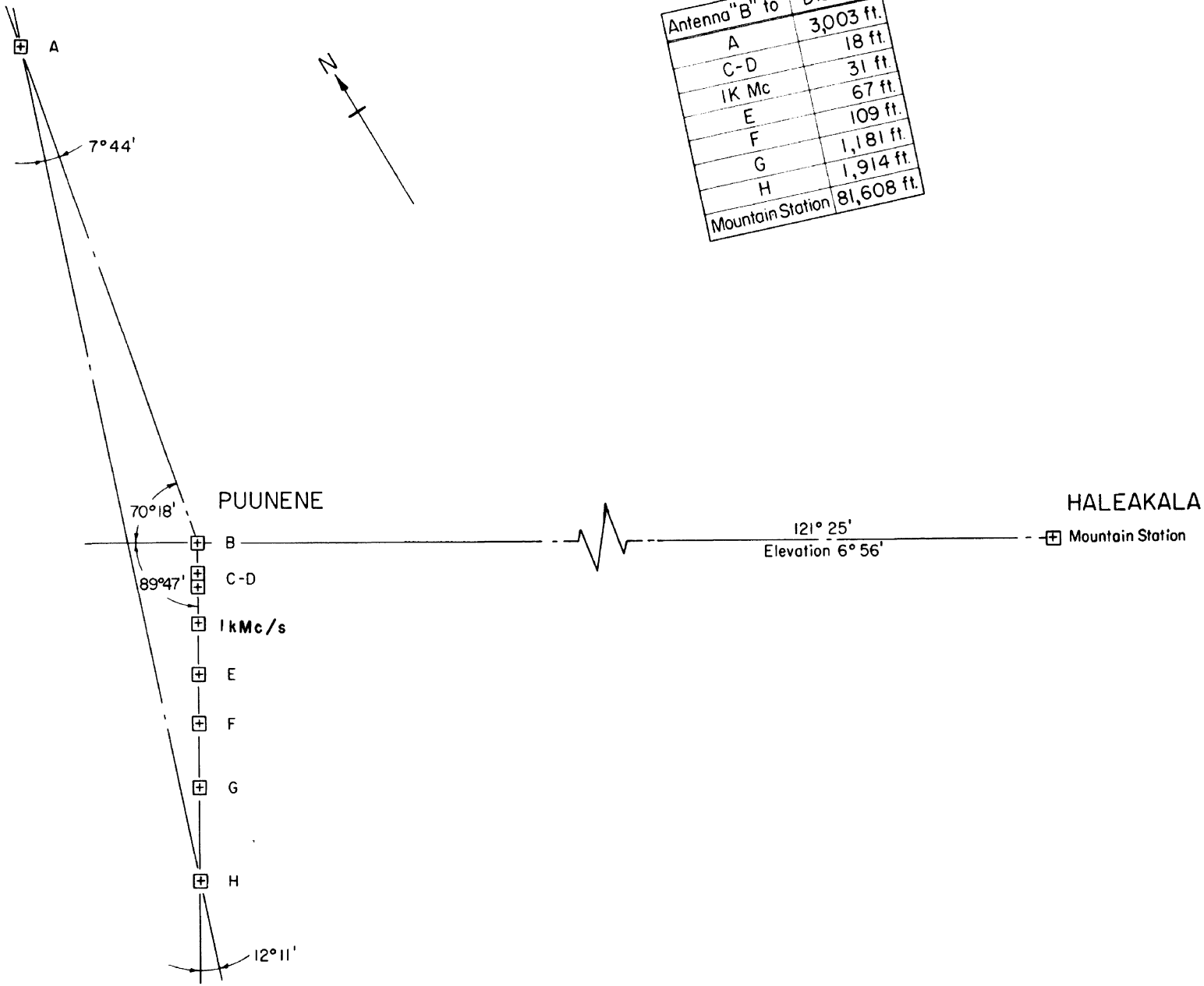

Antenna "B" to	Distance
A	3,003 ft.
C-D	18 ft.
1K Mc	31 ft.
E	67 ft.
F	109 ft.
G	1,181 ft.
H	1,914 ft.
Mountain Station	81,608 ft.

FIGURE 2. *Arrangement of antennas on the Haleakala-Puunene path.*

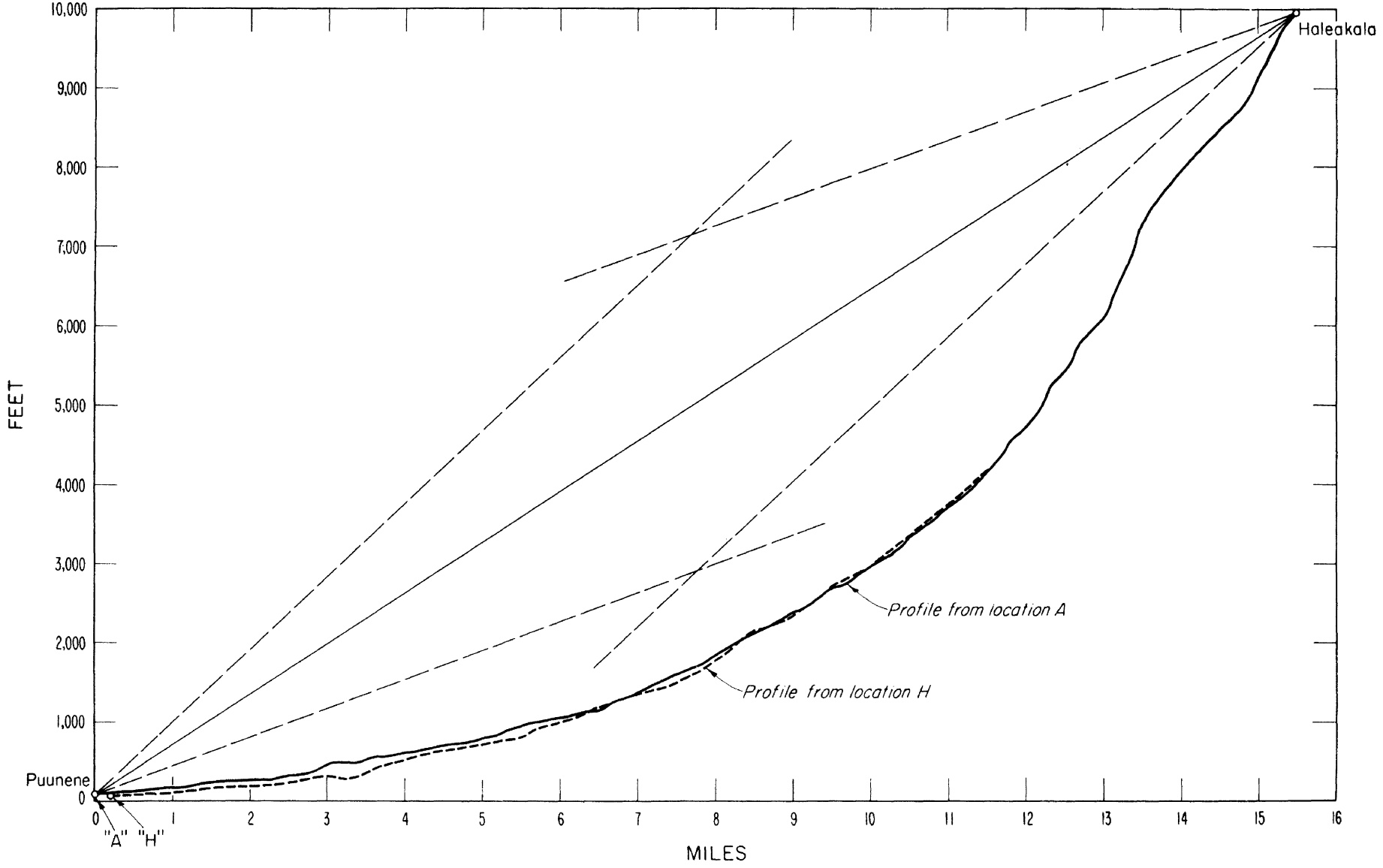

FIGURE 3. *Profile of Haleakala-Puunene path showing half-power beam-widths of 9,414 Mc/s antennas.*

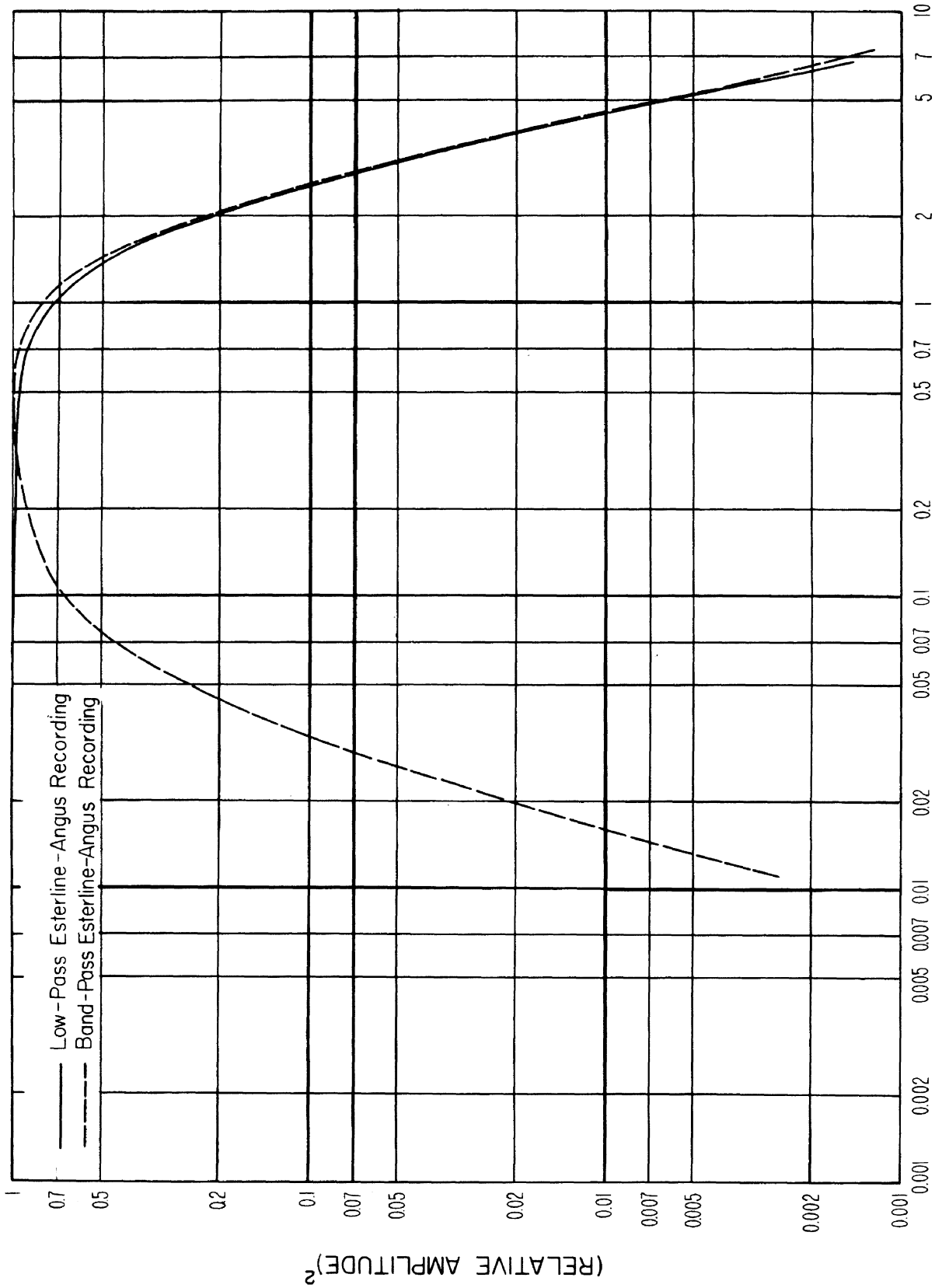

FIGURE 4. *Frequency response characteristics of phase measuring equipment.*

Haleakala-Puunene Path

November 8, 1956

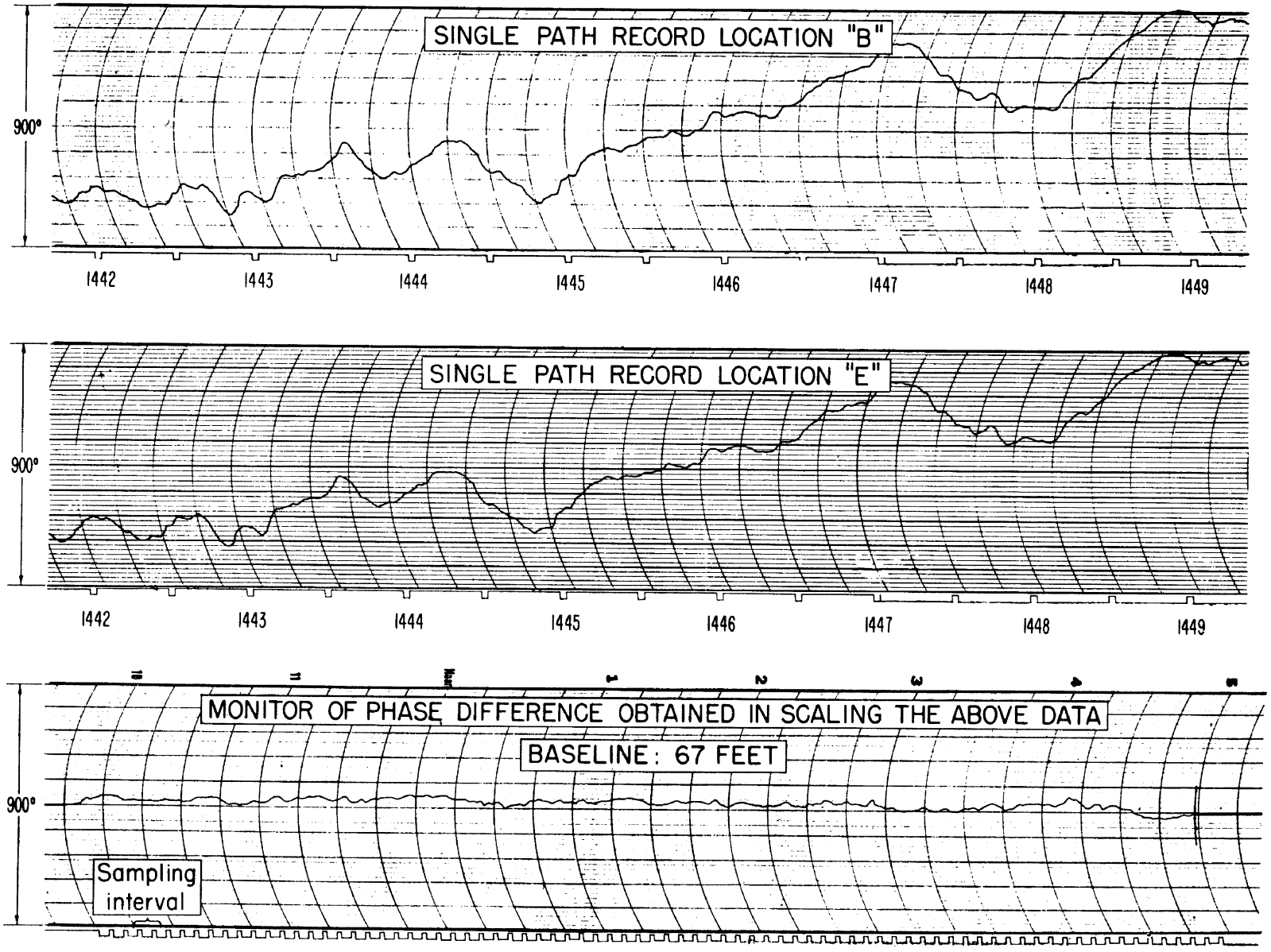

FIGURE 5. *Sample of 9,414 Mc/s single-path phase data (low-pass) with corresponding phase difference monitor.*

Haleakala - Puunene Path

November 5, 1956

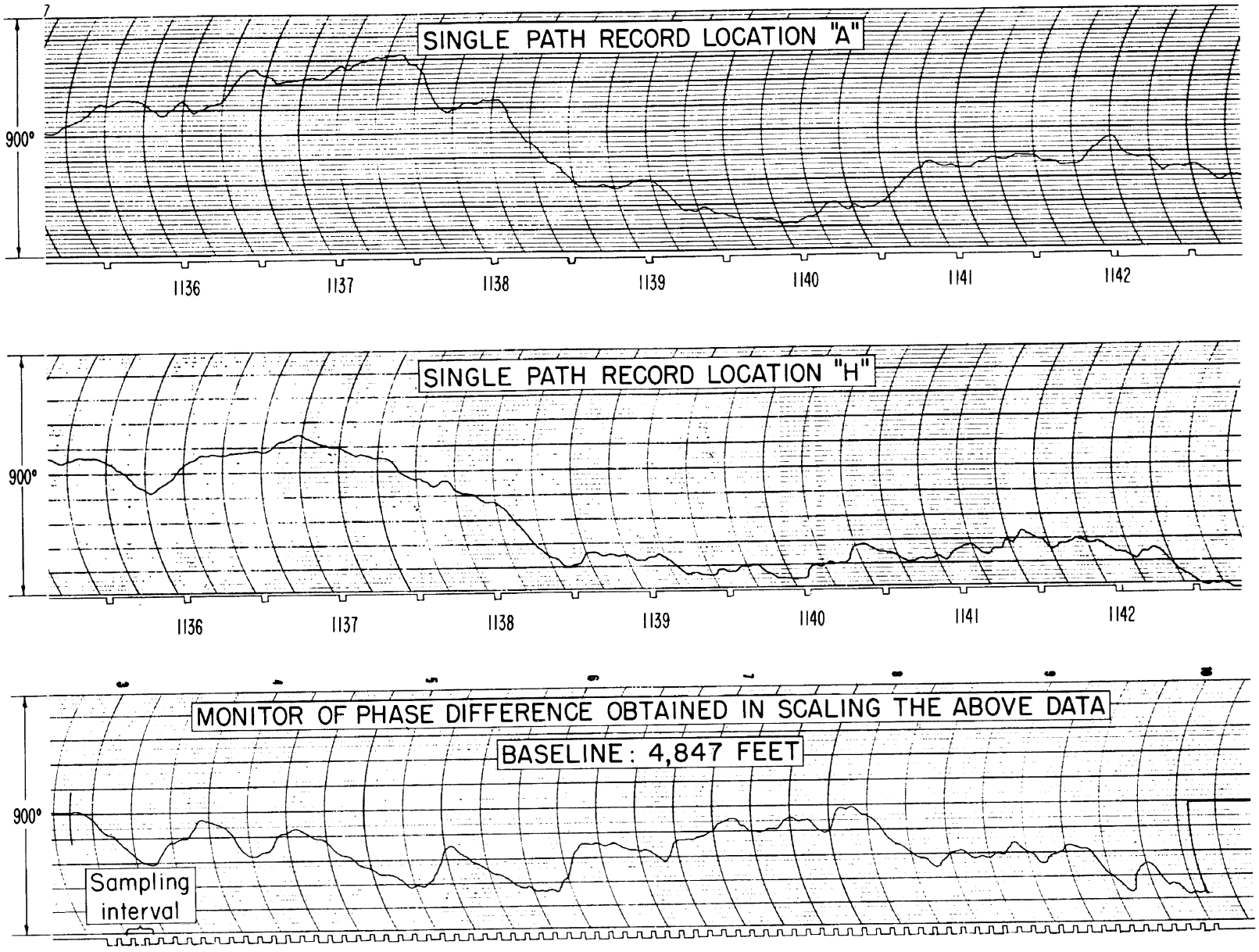

FIGURE 6. *Sample of 9,414 Mc/s single-path phase data (low-pass) with corresponding phase difference monitor.*

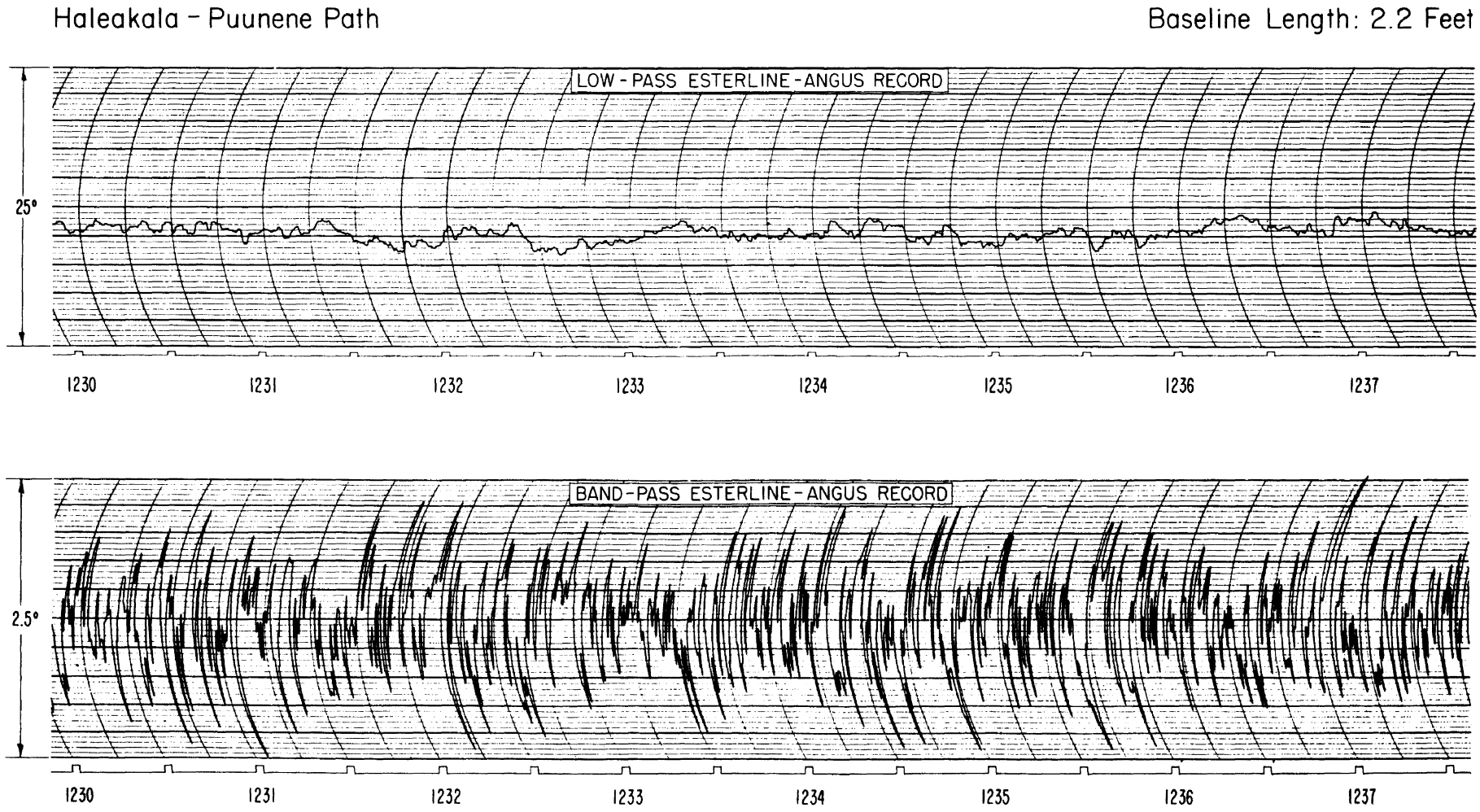

FIGURE 7. *Sample of 9,414 Mc/s phase difference data using G. E. antenna system.*

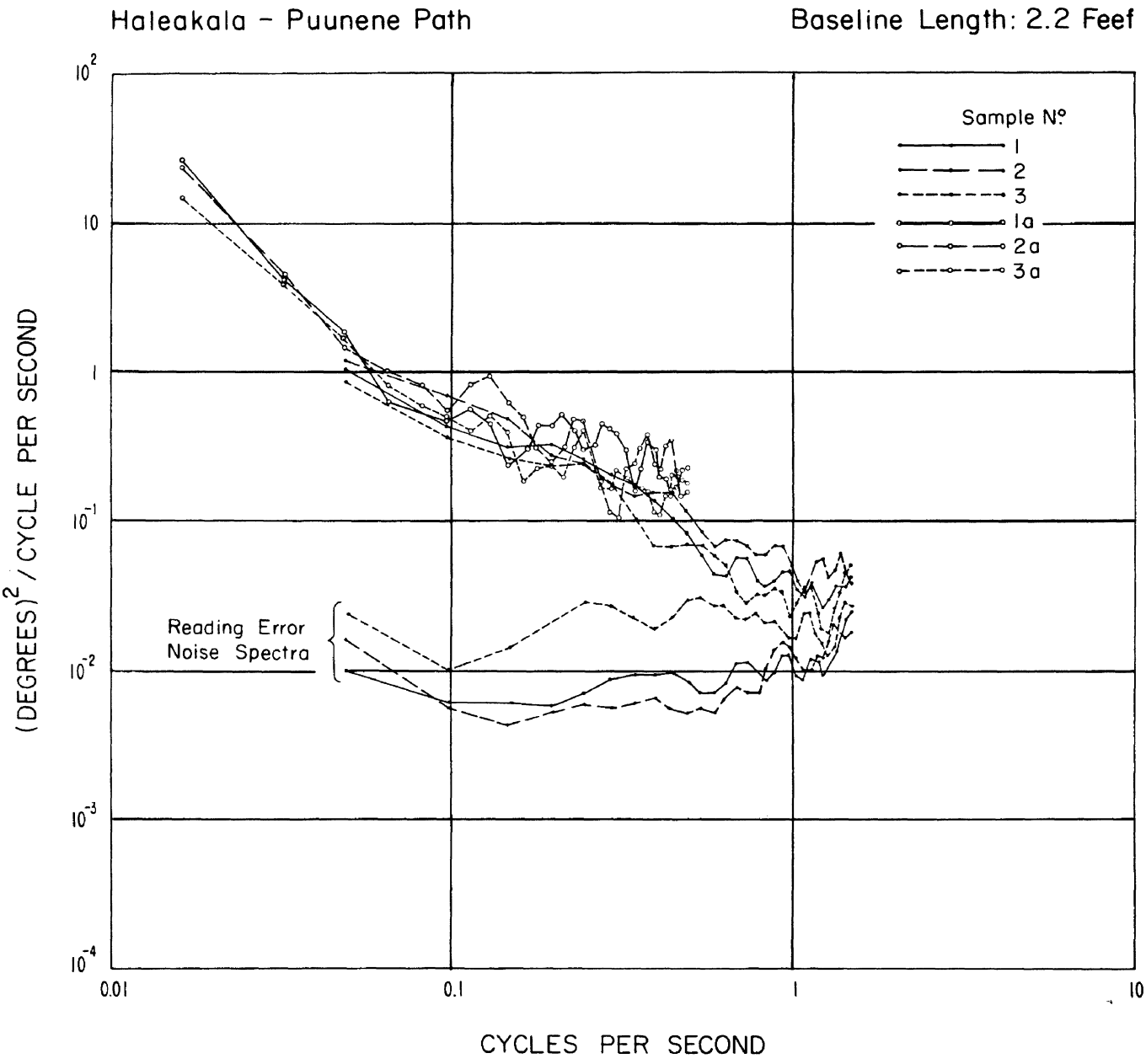

FIGURE 8. *Power spectra of 9,414 Mc/s phase difference variations.*

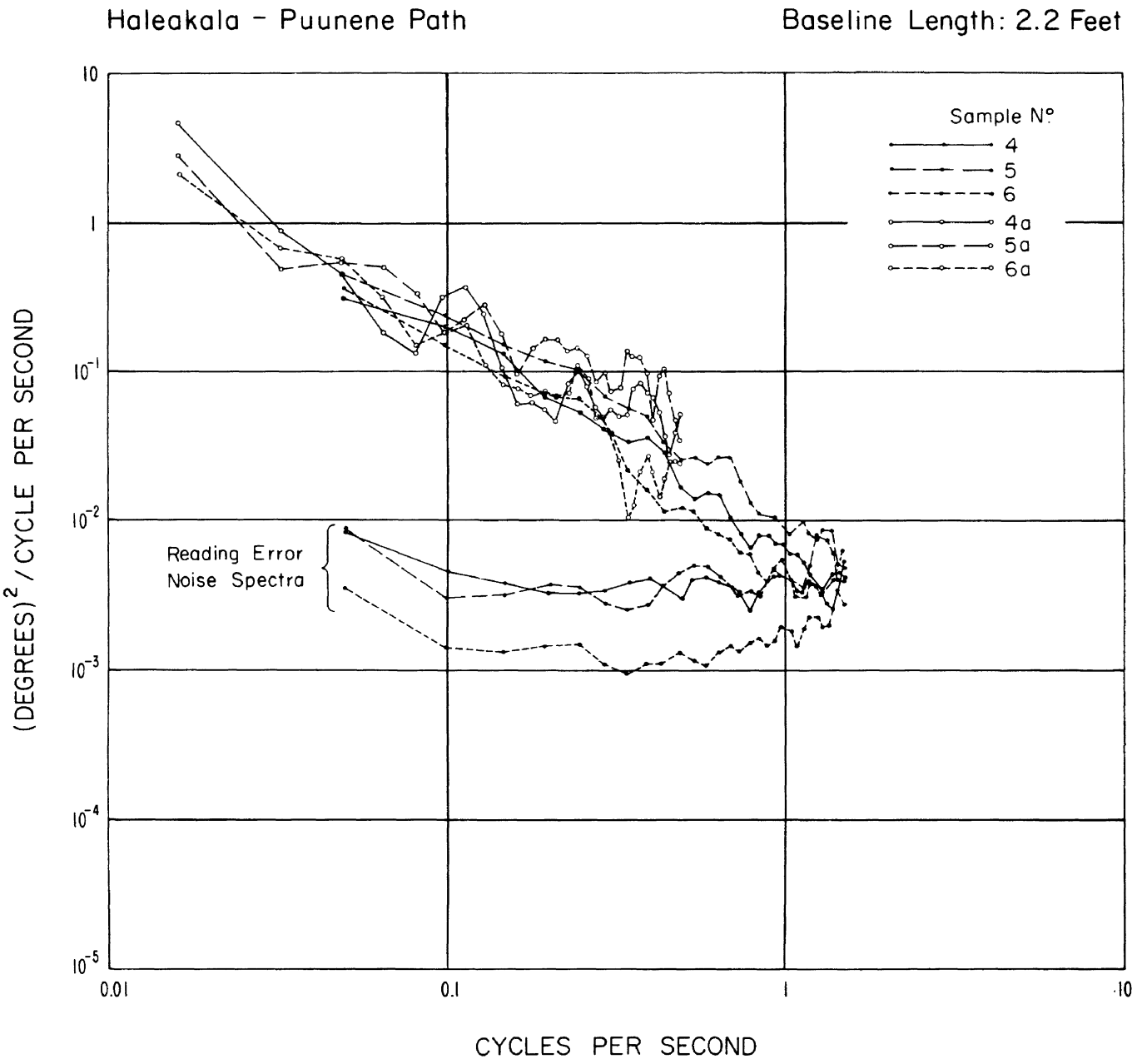

FIGURE 9. *Power spectra of 9,414 Mc/s phase difference variations.*

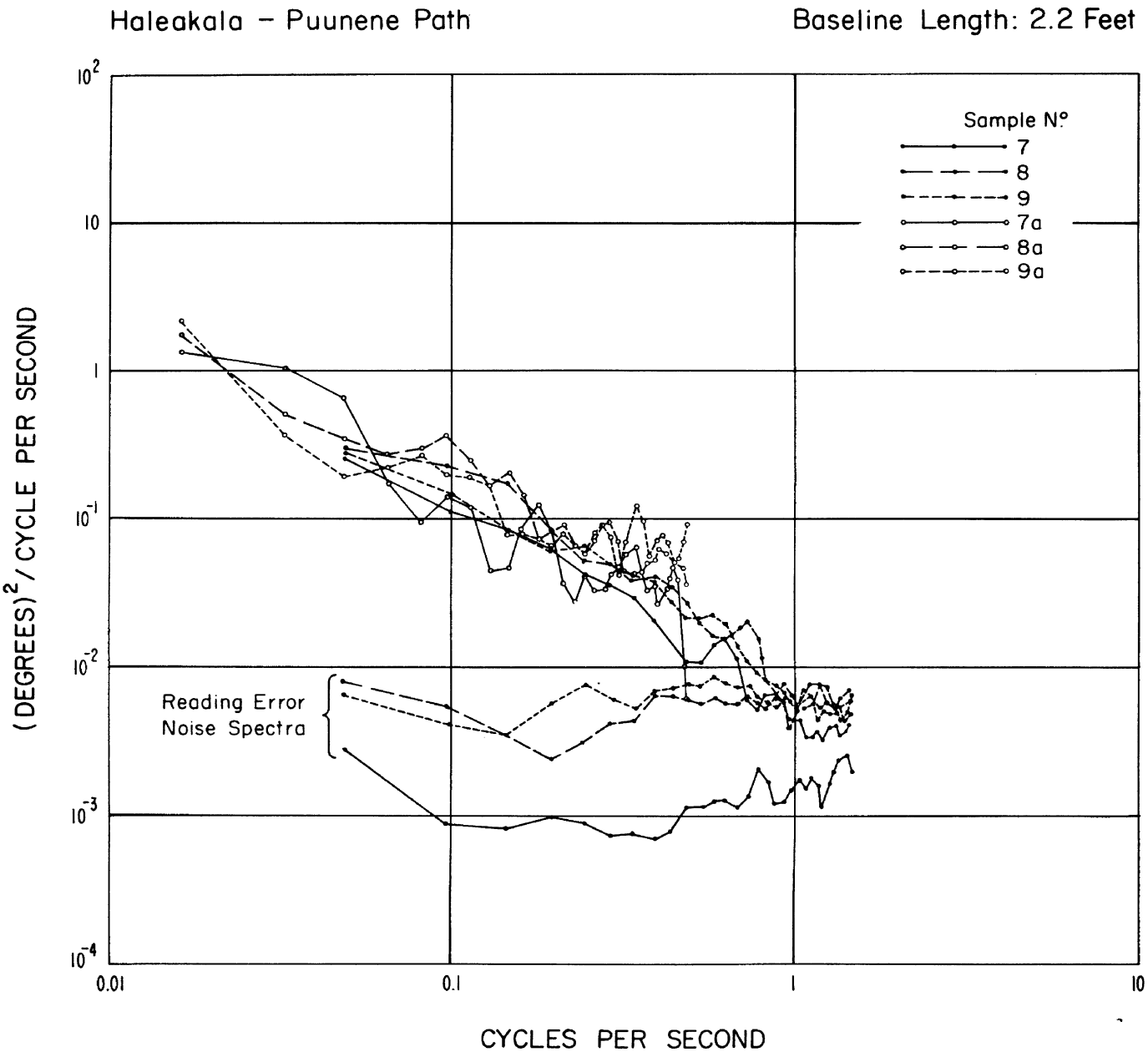

FIGURE 10. *Power spectra of 9,414 Mc/s phase difference variations.*

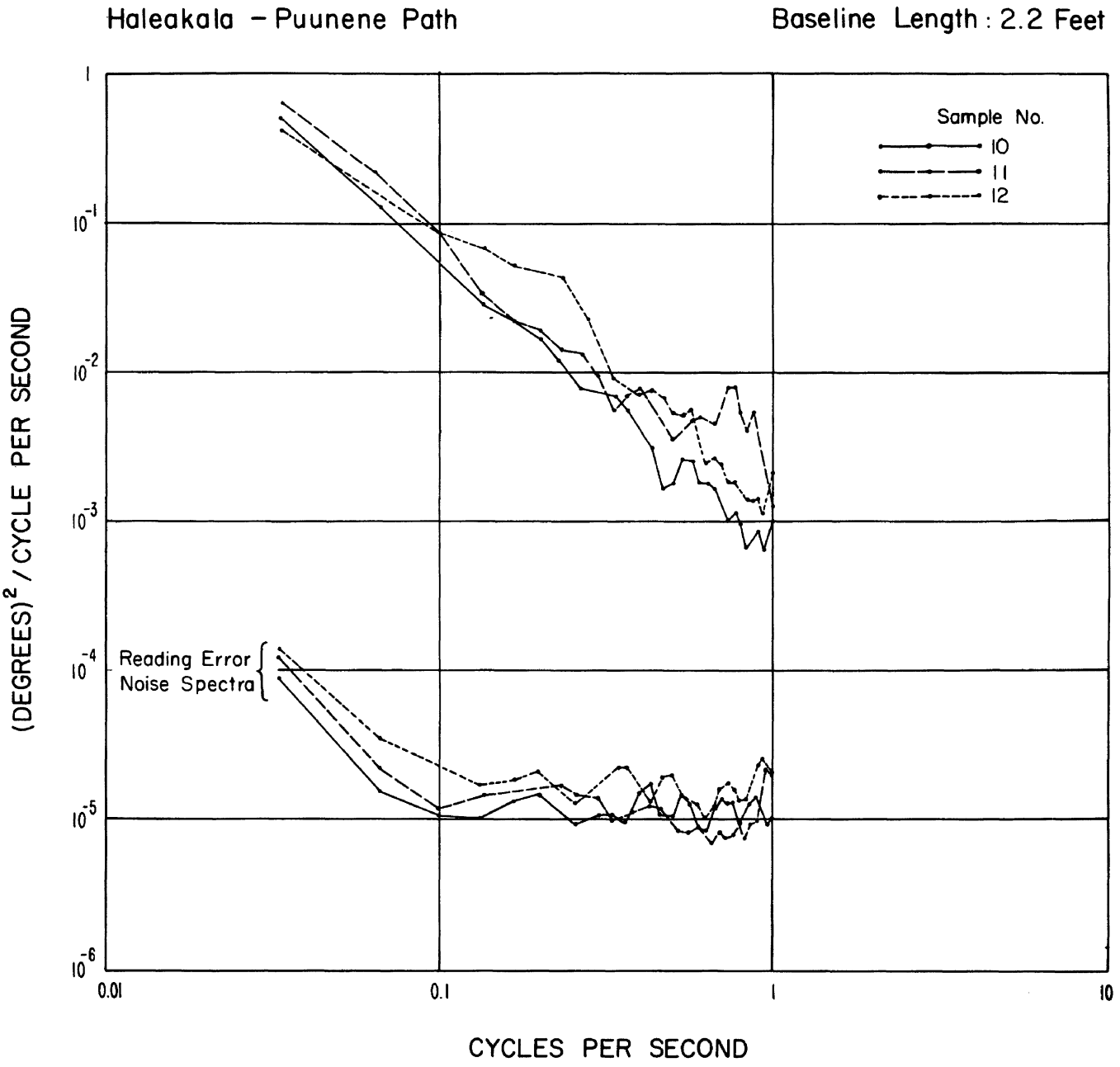

FIGURE 11. *Power spectra of 9,414 Mc/s phase difference variations.*

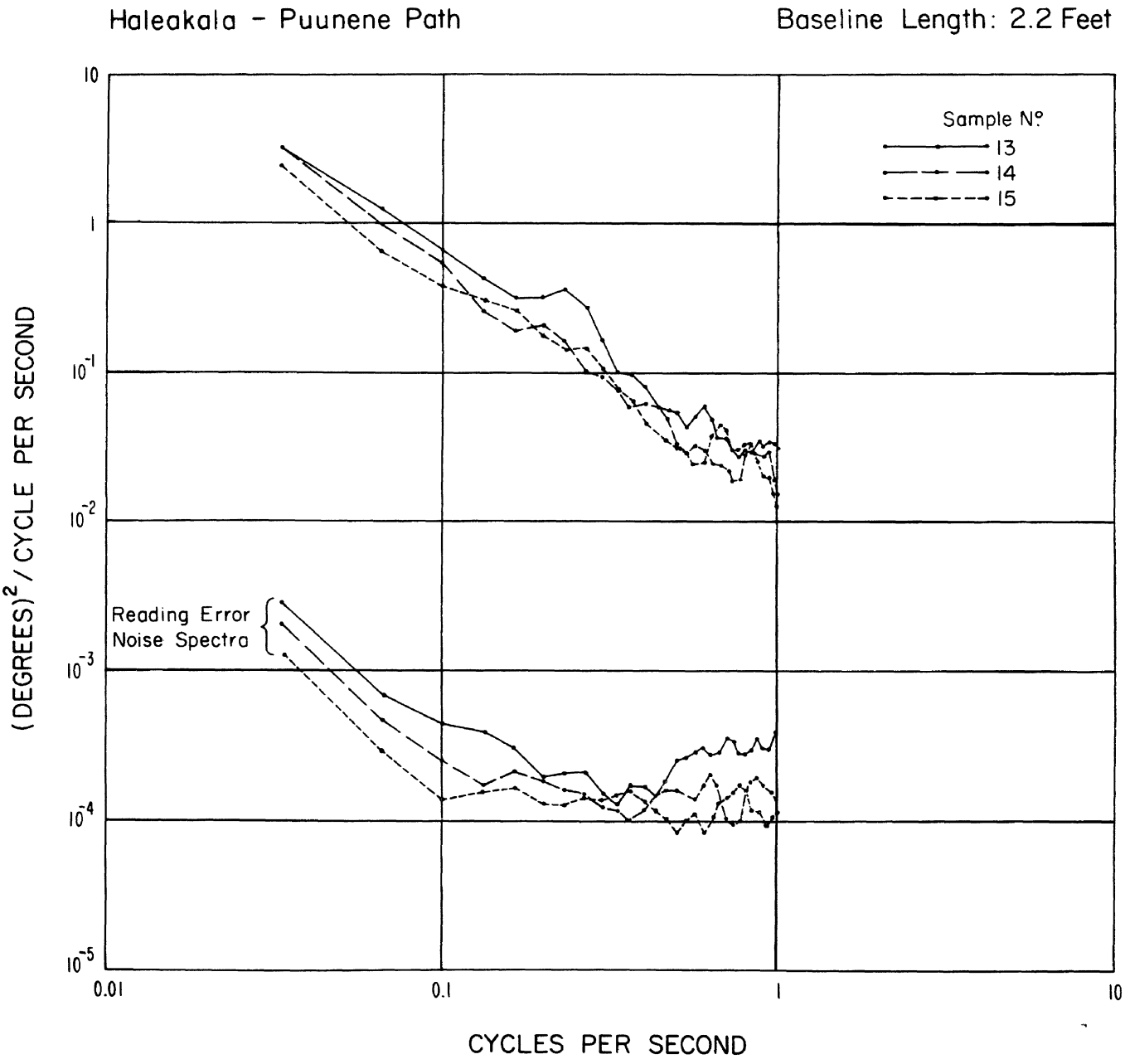

FIGURE 12. *Power spectra of 9414 Mc/s phase difference variations.*

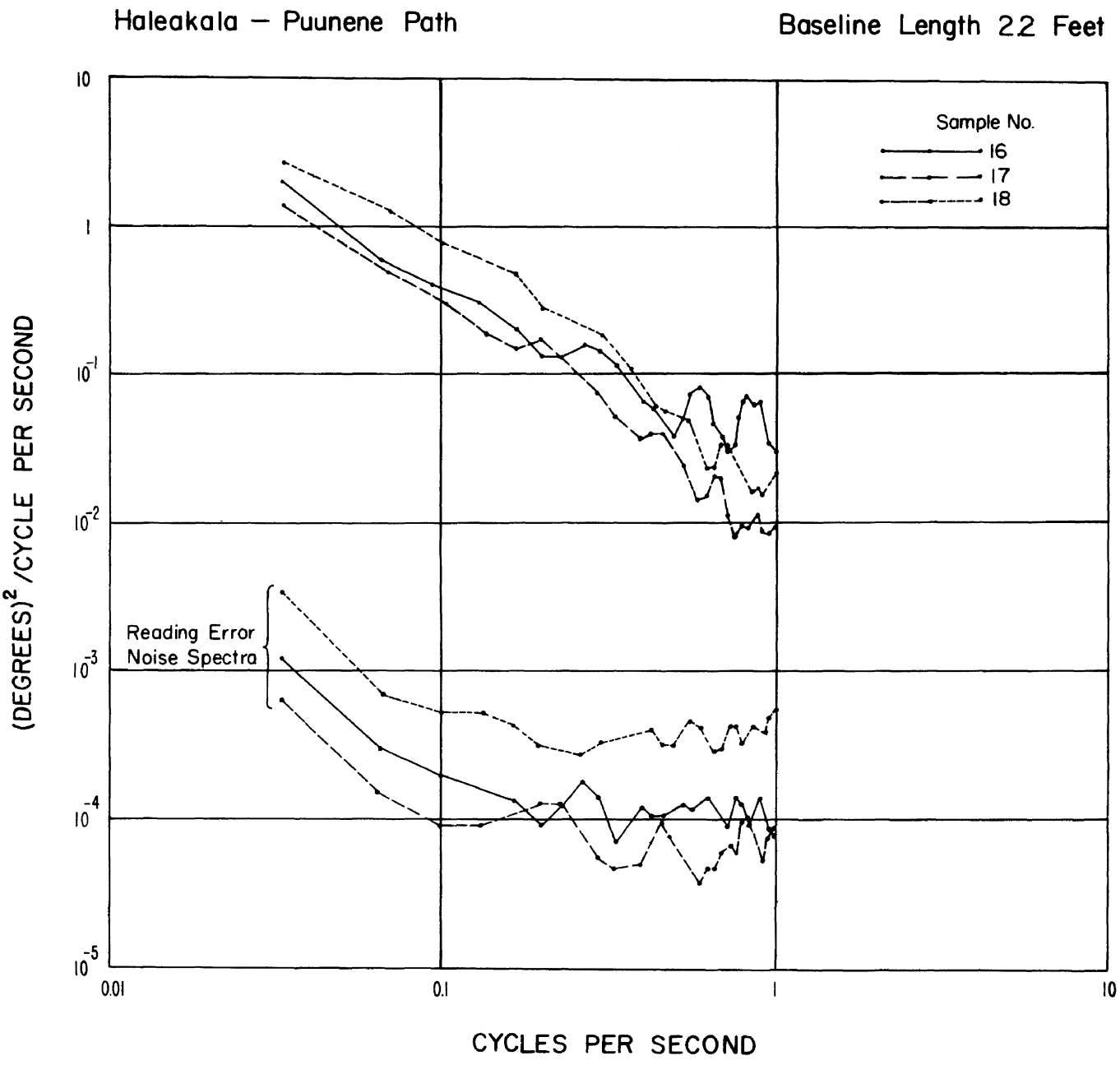

FIGURE 13. *Power spectra of 9,414 Mc/s phase difference variations.*

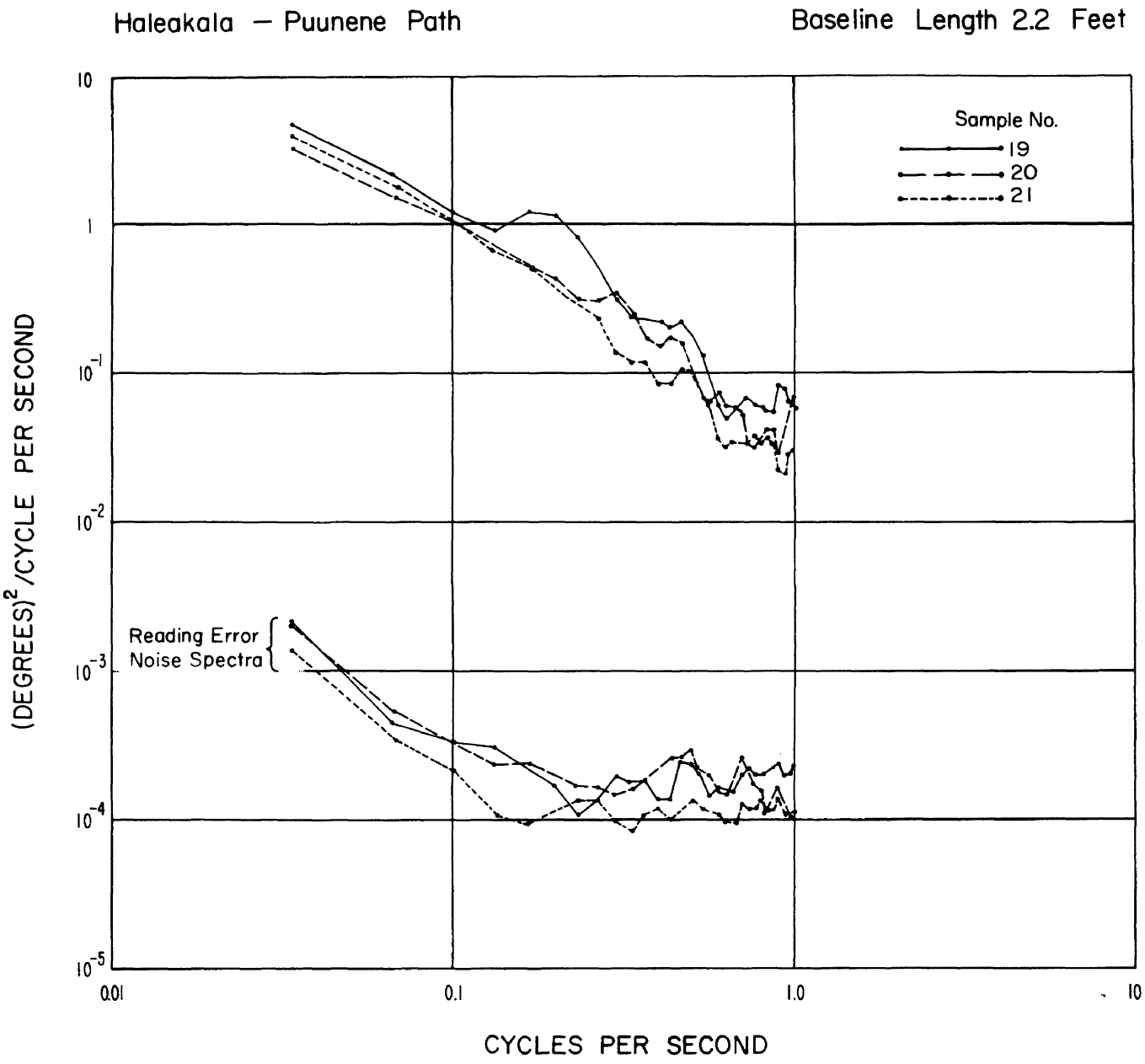

FIGURE 14. *Power spectra of 9,414 Mc/s phase difference variations.*

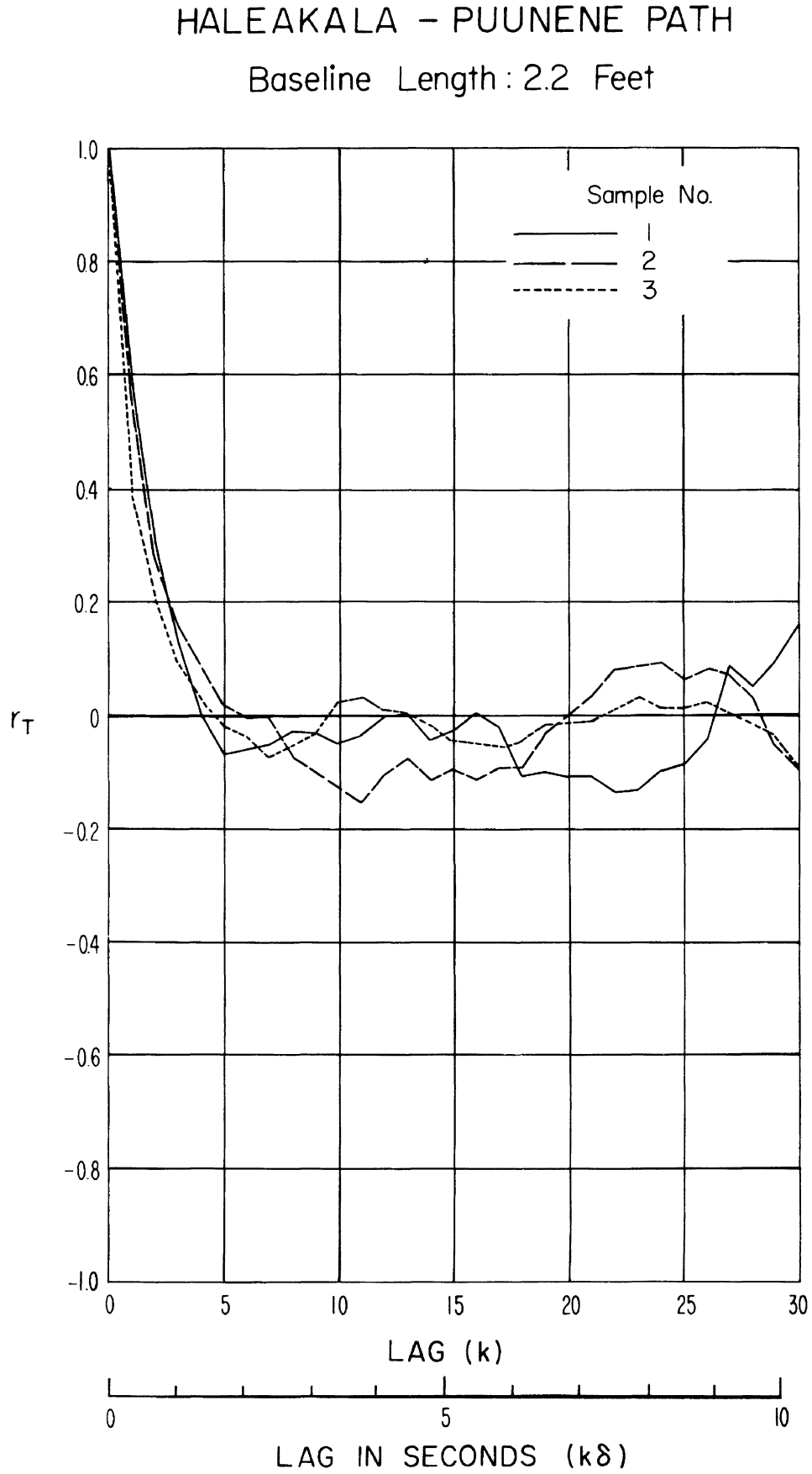

FIGURE 15. *Serial correlation functions of 9,414 Mc/s phase difference variations.*

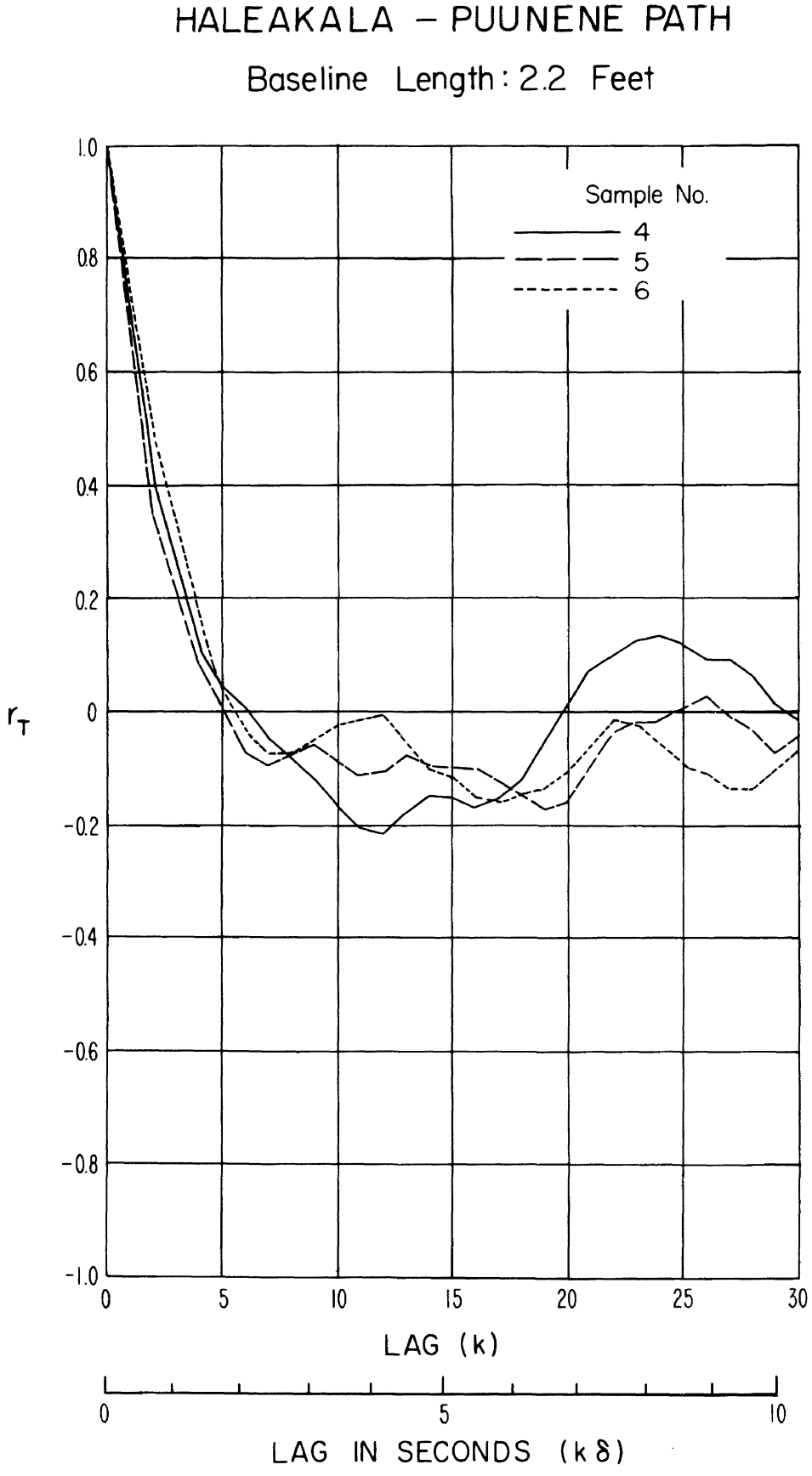

FIGURE 16. *Serial correlation functions of 9,414 Mc/s phase difference variations.*

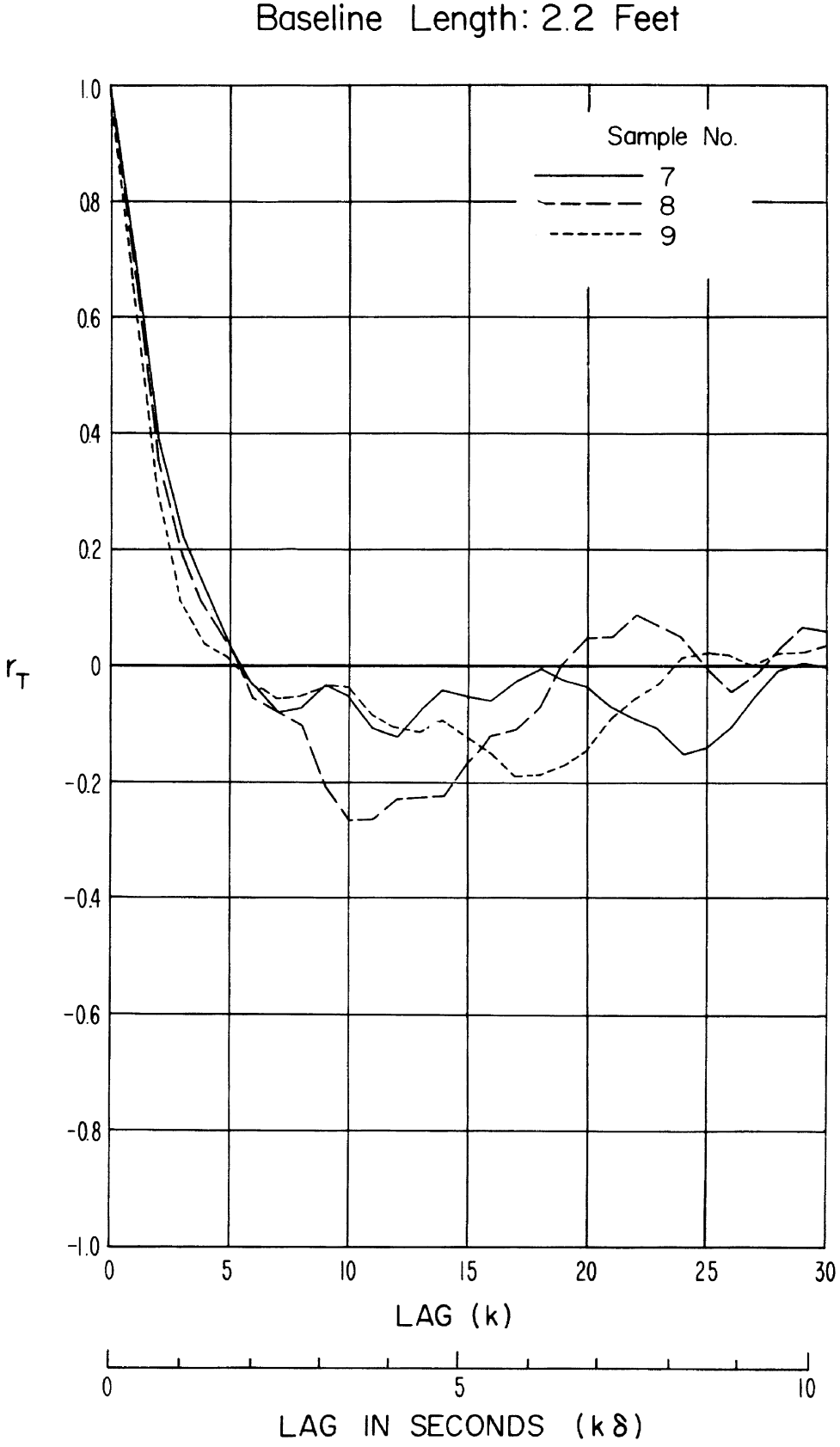

FIGURE 17. *Serial correlation functions of 9,414 Mc/s phase difference variations.*

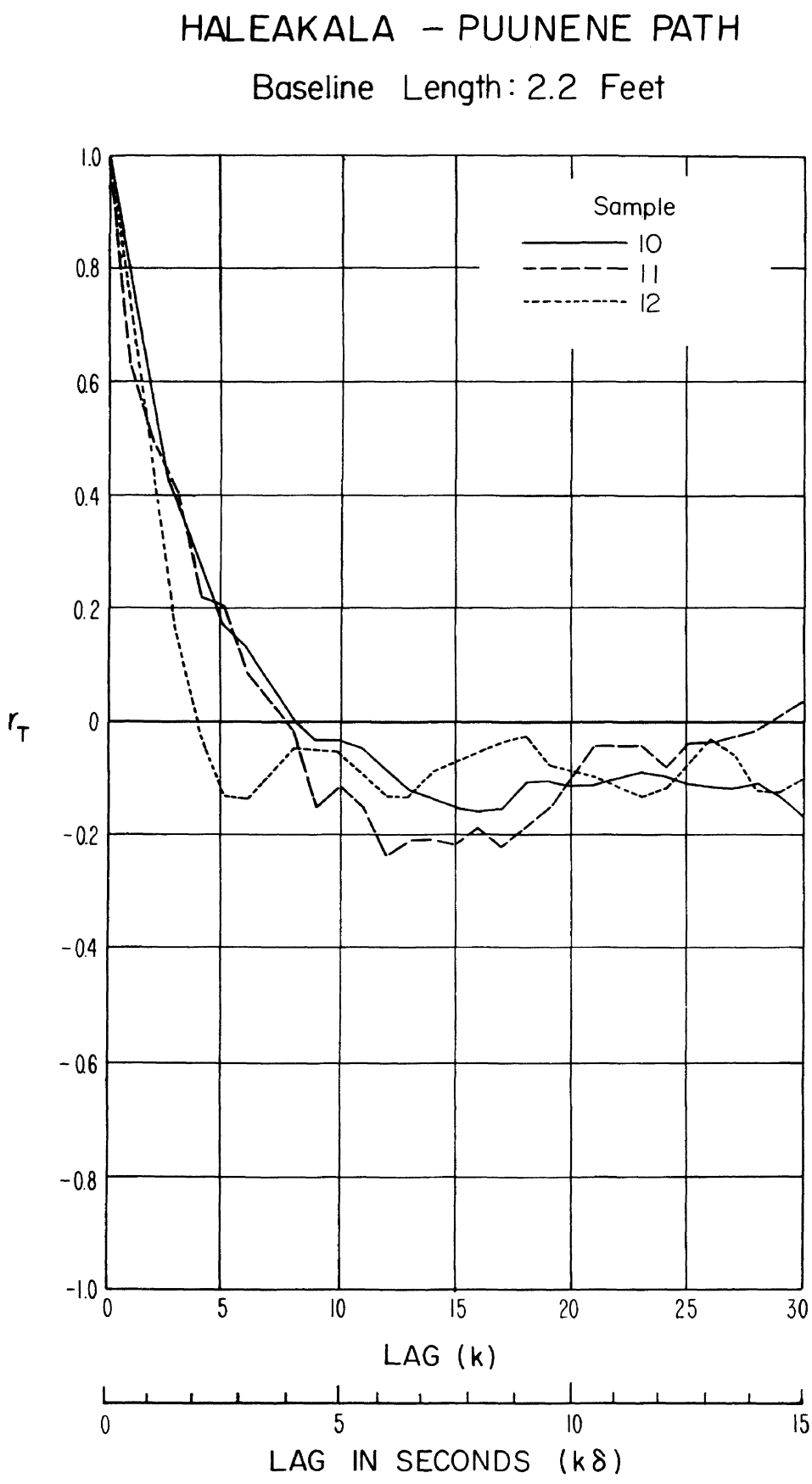

FIGURE 18. *Serial correlation functions of 9,414 Mc/s phase difference variations.*

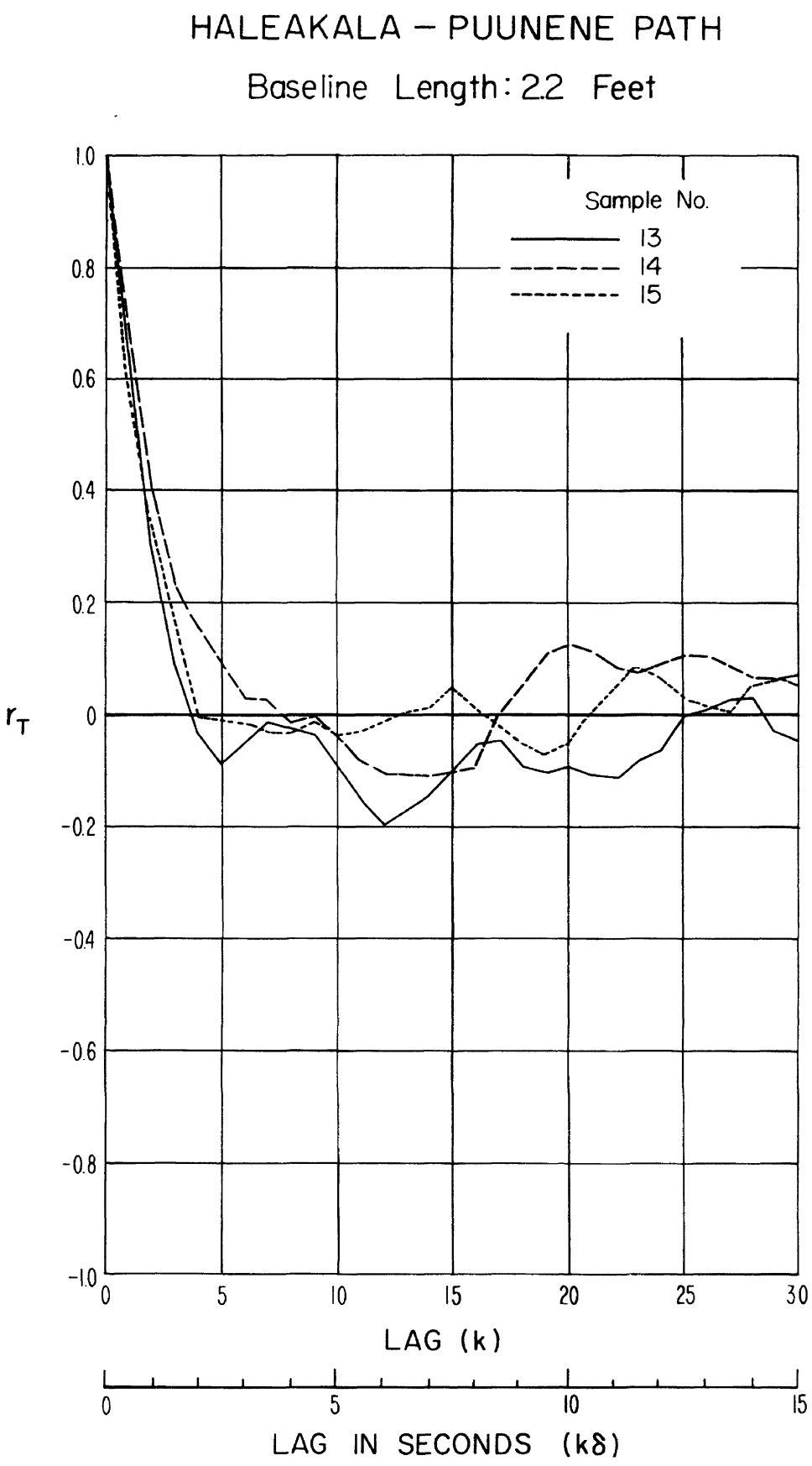

FIGURE 19. *Serial correlation functions of 9,414 Mc/s phase difference variations.*

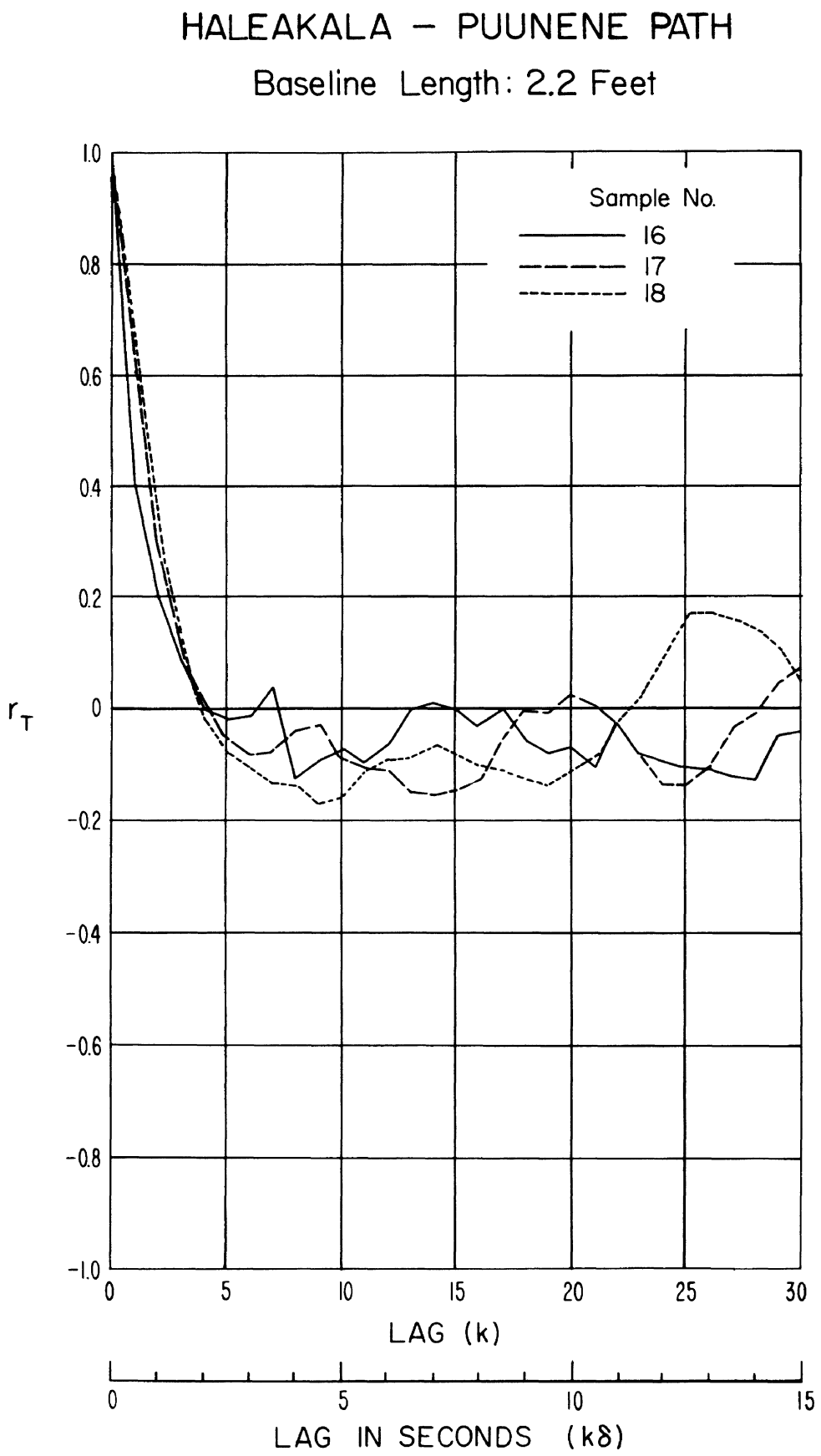

FIGURE 20. *Serial correlation functions of 9,414 Mc/s phase difference variations.*

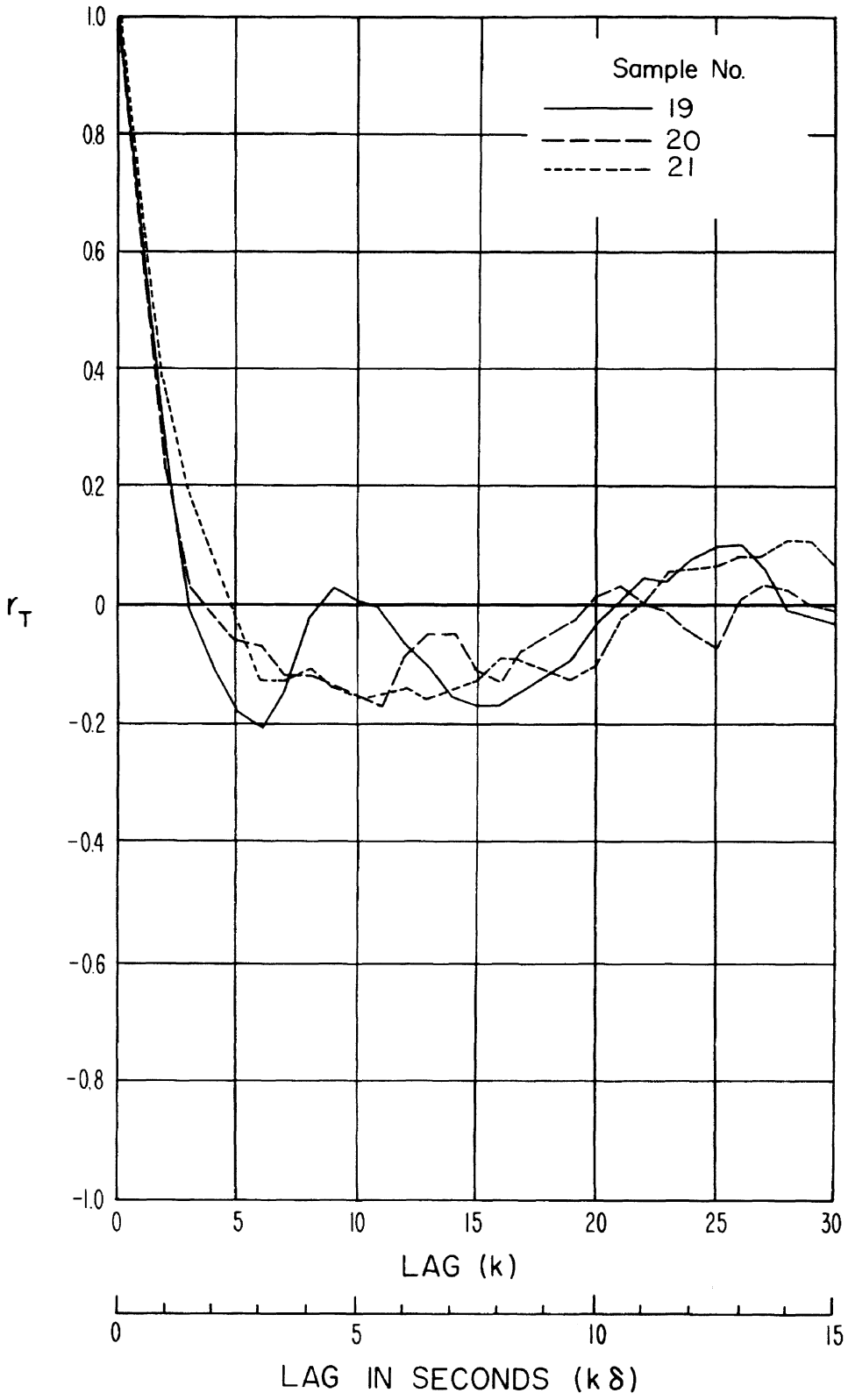

FIGURE 21. *Serial correlation functions of 9,414 Mc/s phase difference variations.*

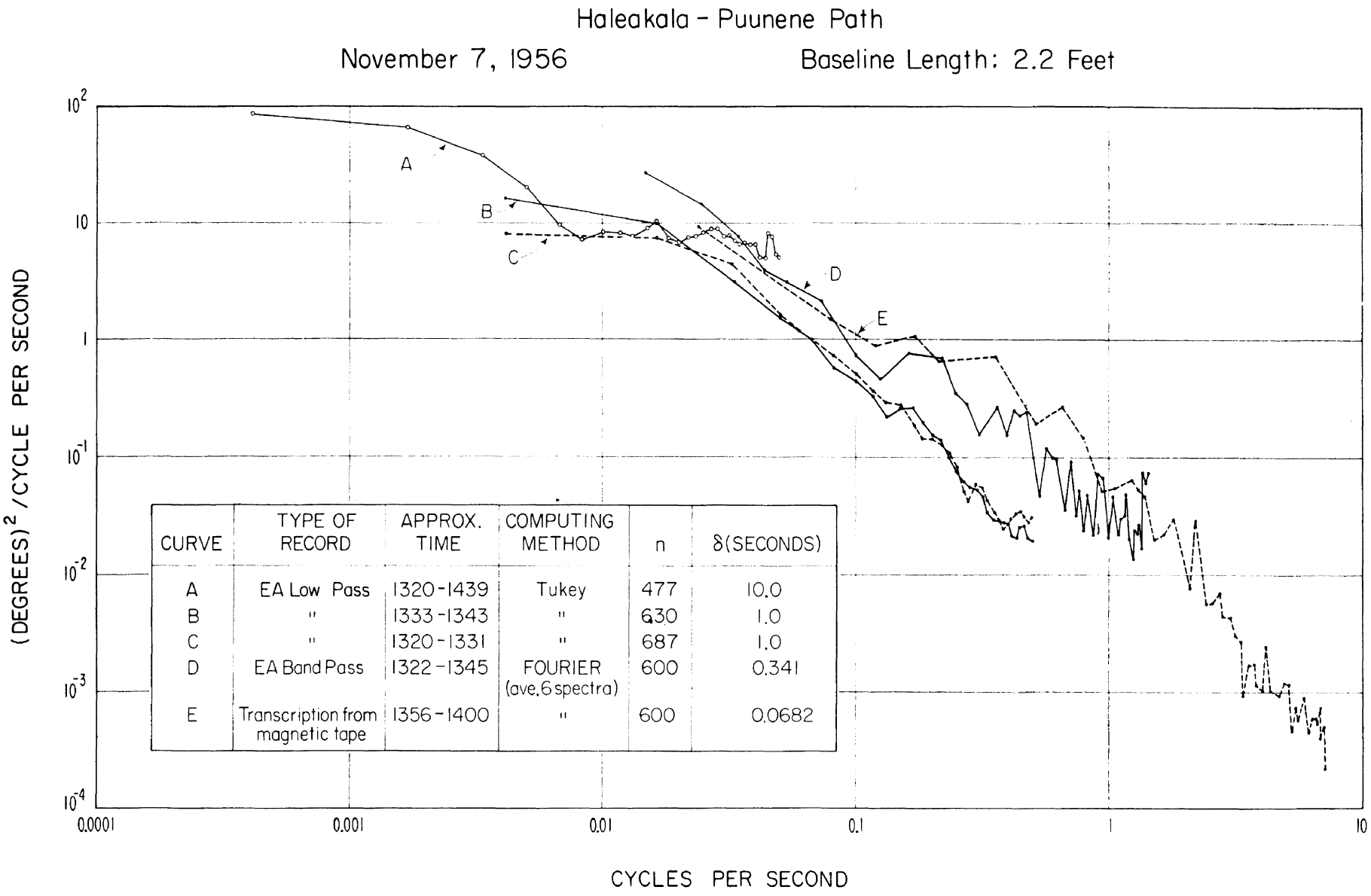

FIGURE 22. *Power spectrum of 9,414 Mc/s phase difference variations.*

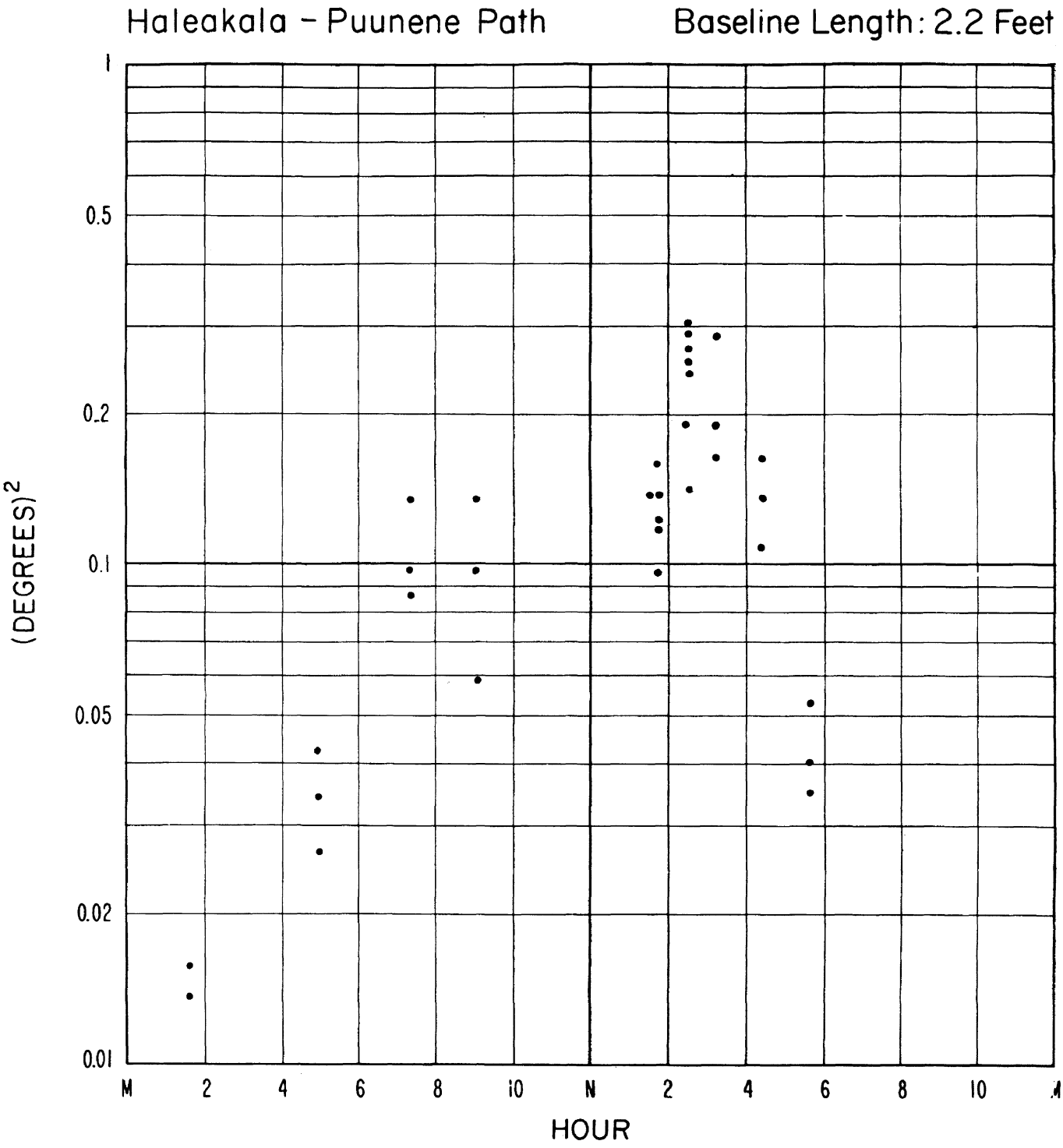

FIGURE 23. *Variance of phase difference versus time of day.*

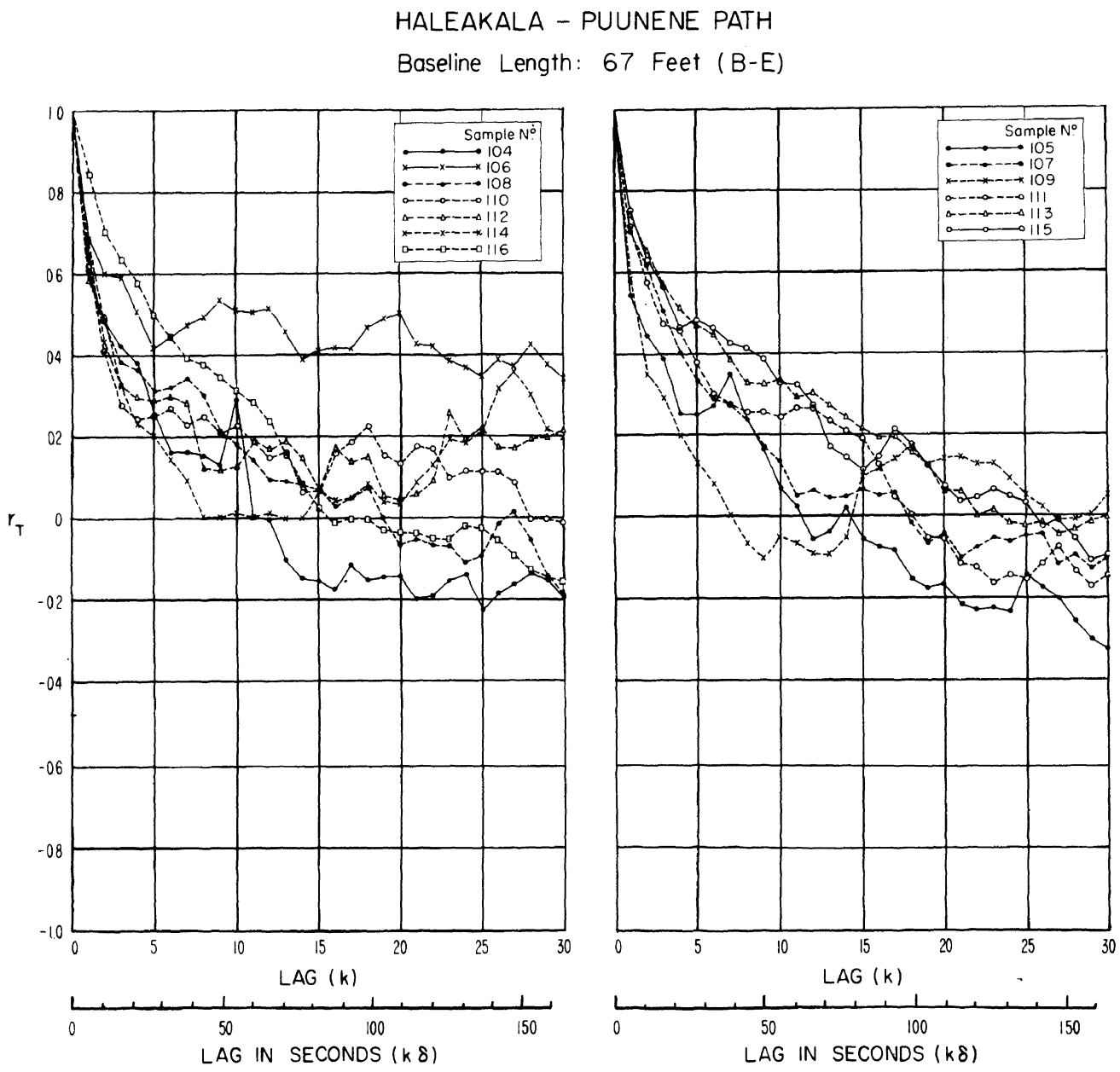

FIGURE 24. *Serial correlation functions of 9,414 Mc/s phase difference variations.*

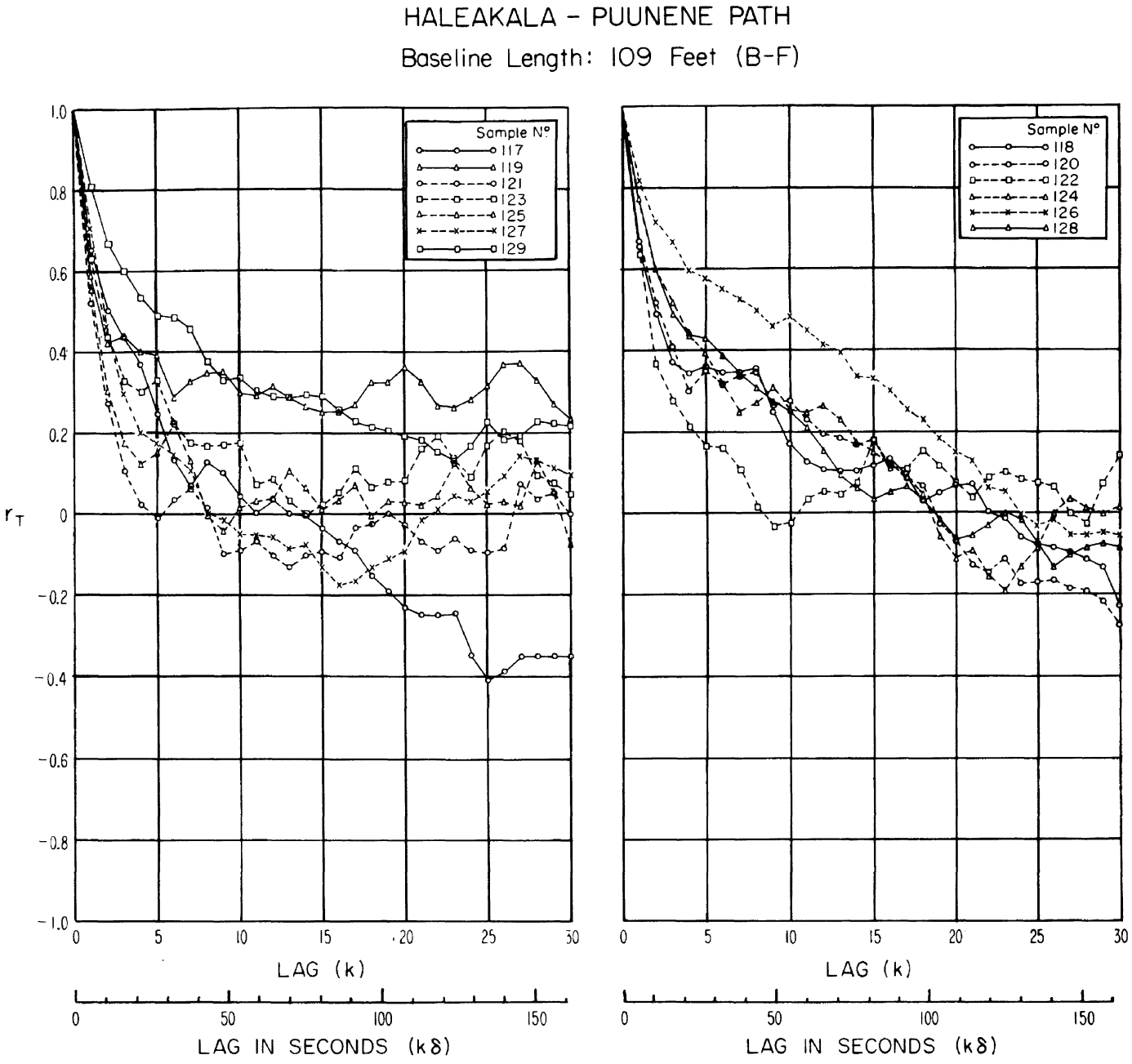

FIGURE 25. *Serial correlation functions of 9,414 Mc/s phase difference variations.*

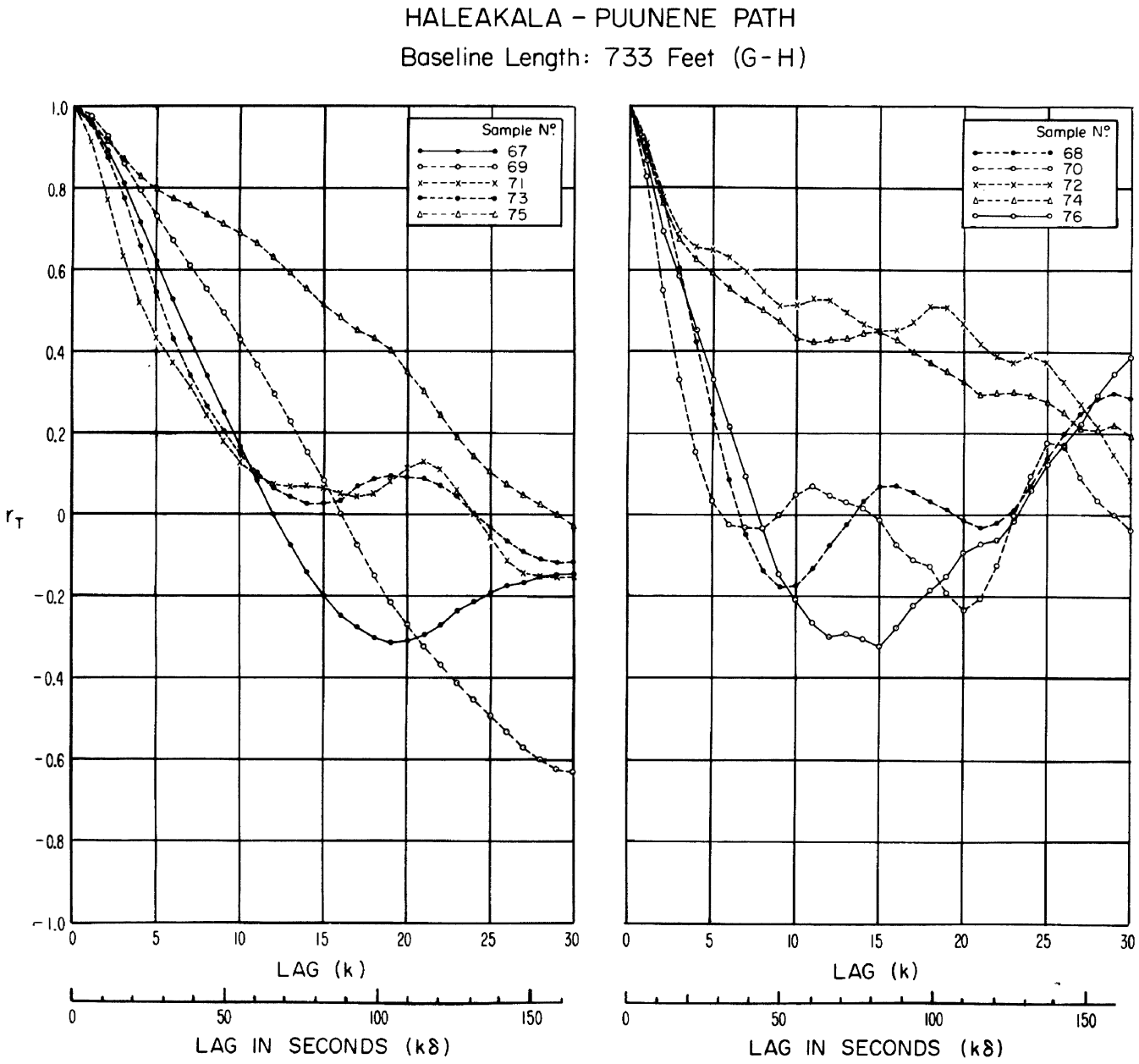

FIGURE 26. *Serial correlation functions of 9,414 Mc/s phase difference variations.*

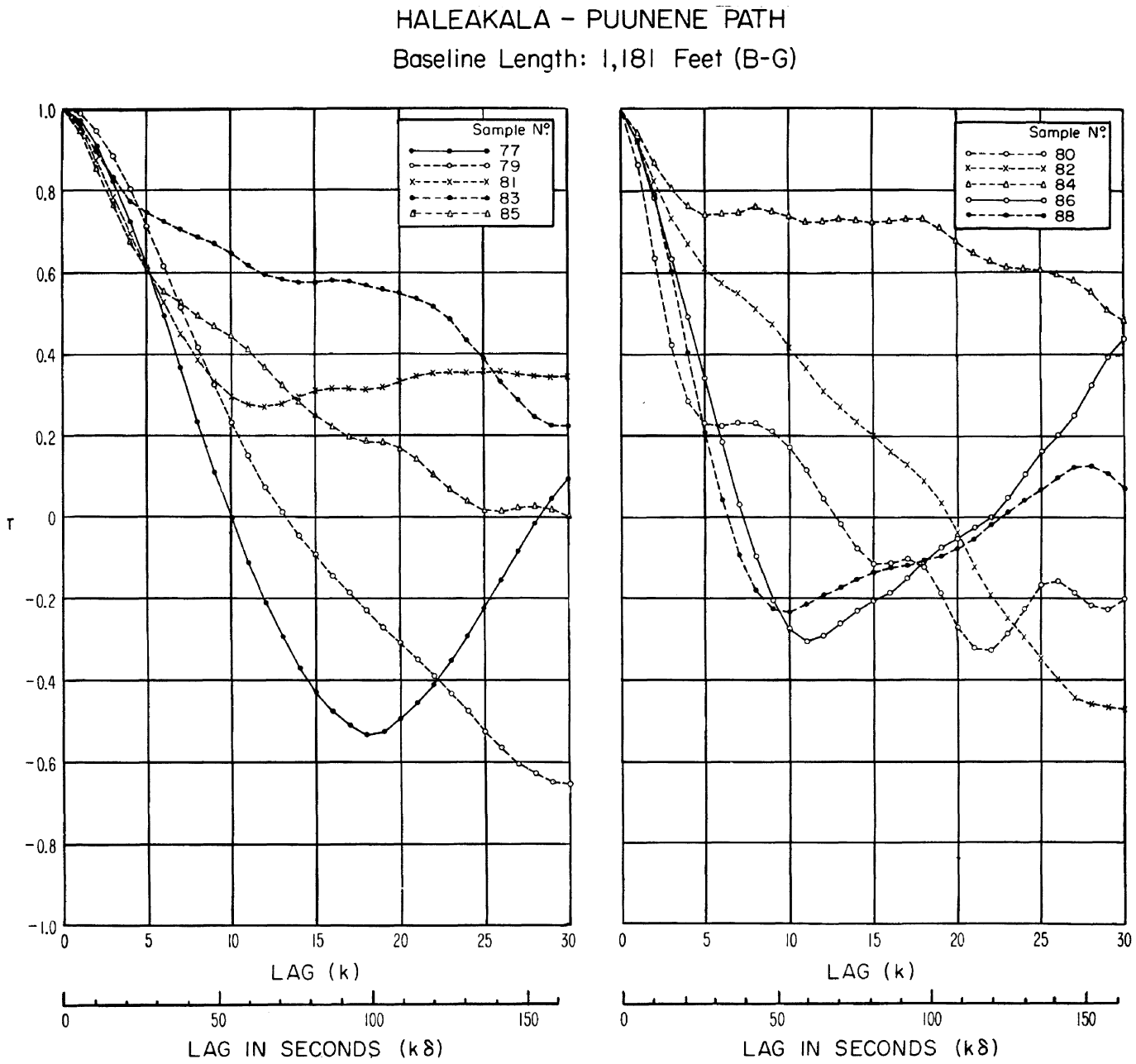

FIGURE 27. *Serial correlation functions of 9,414 Mc/s phase difference variations.*

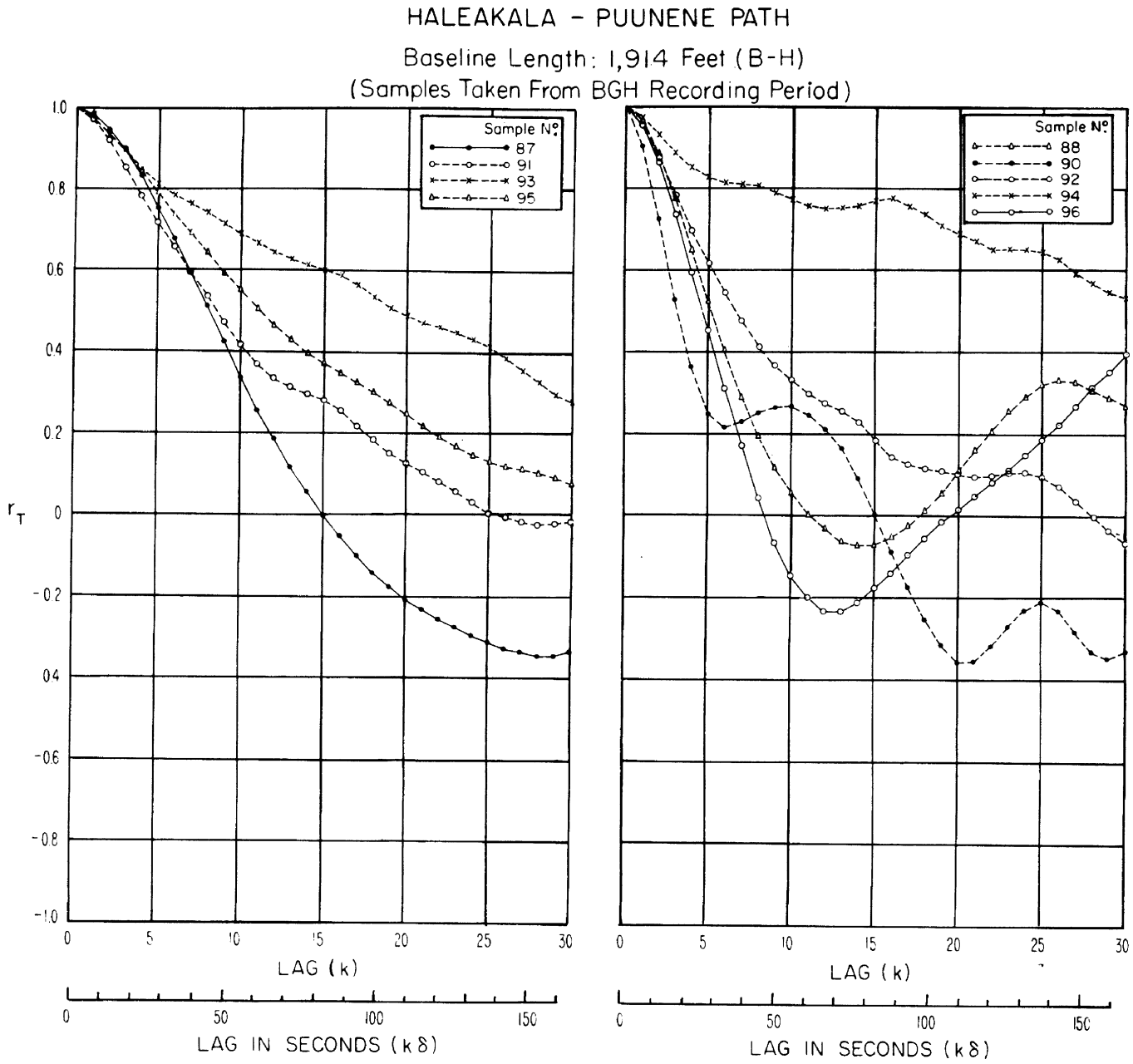

FIGURE 28. *Serial correlation functions of 9,414 Mc/s phase difference variations.*

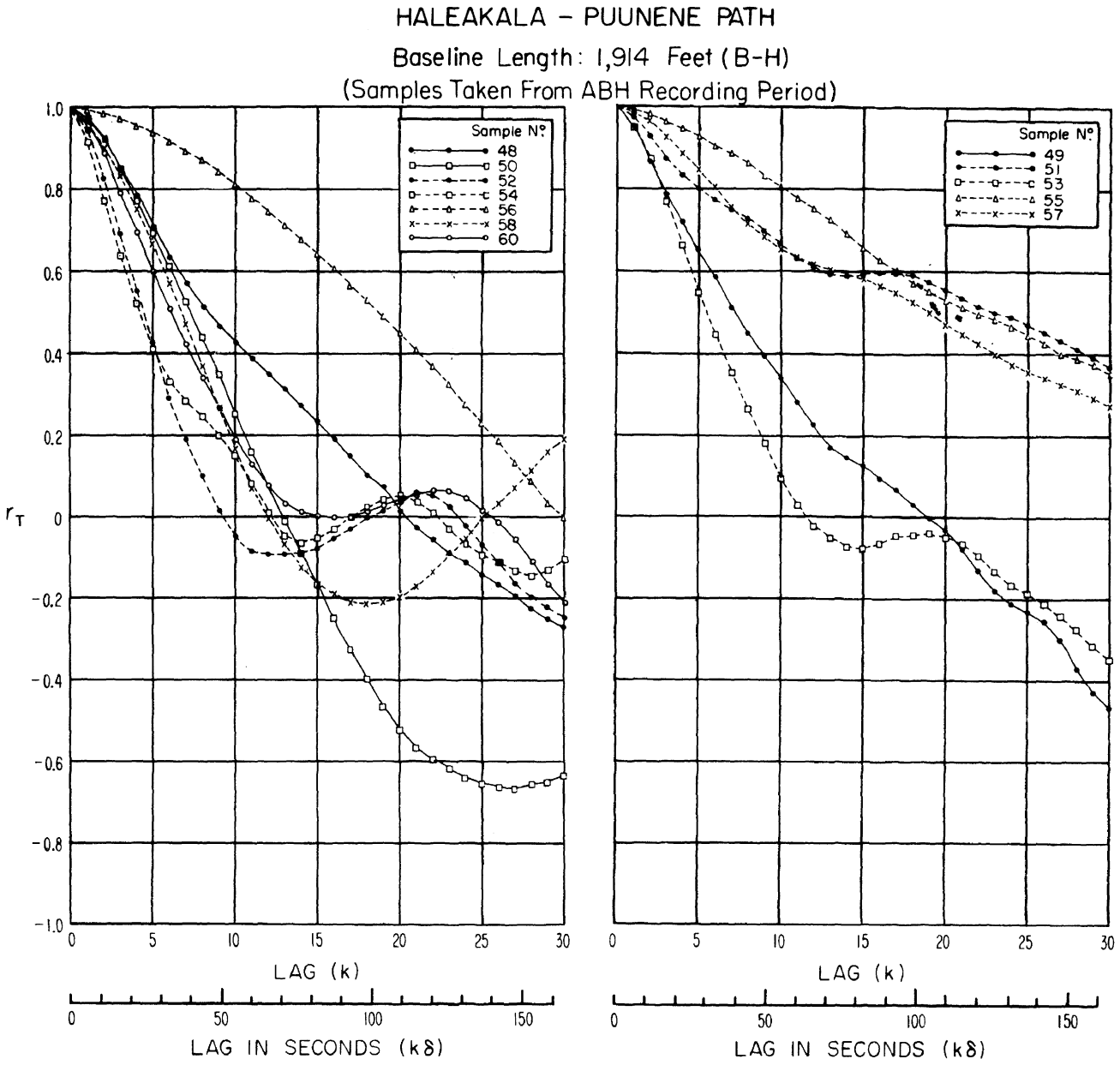

FIGURE 29. *Serial correlation functions of 9,414 Mc/s phase difference variations.*

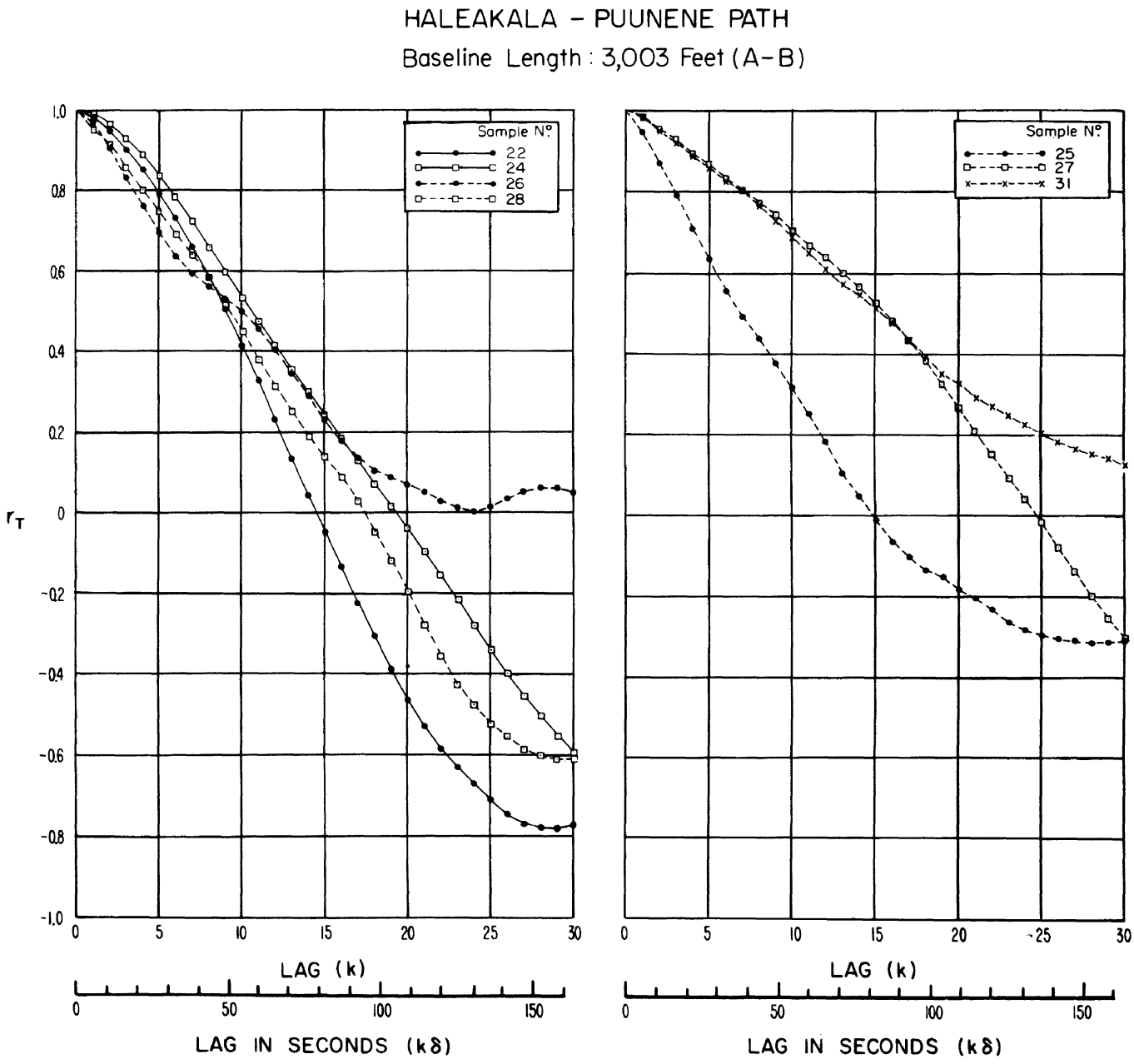

FIGURE 30. *Serial correlation functions of 9,414 Mc/s phase difference variations.*

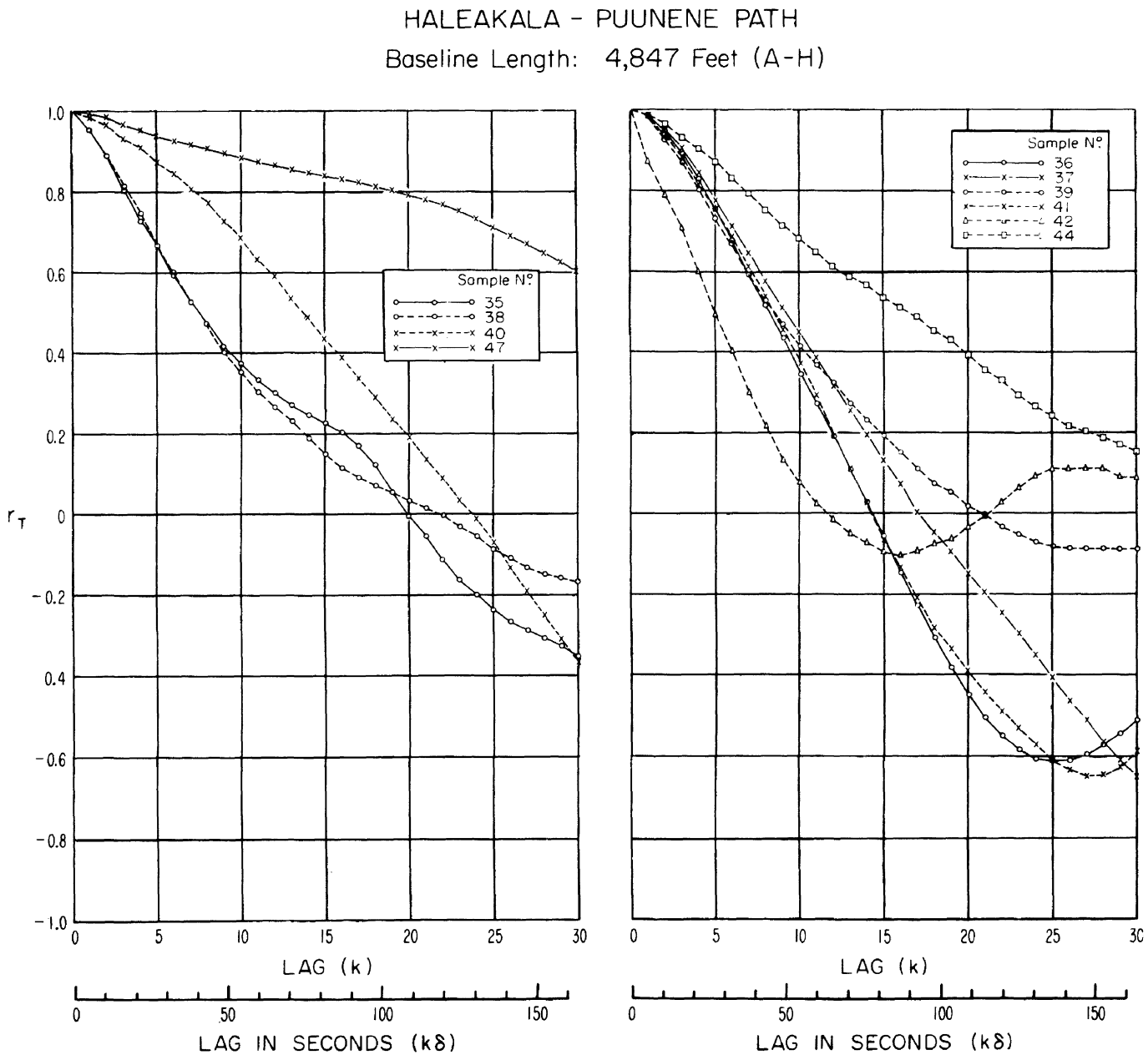

FIGURE 31. *Serial correlation functions of 9,414 Mc/s phase difference variations.*

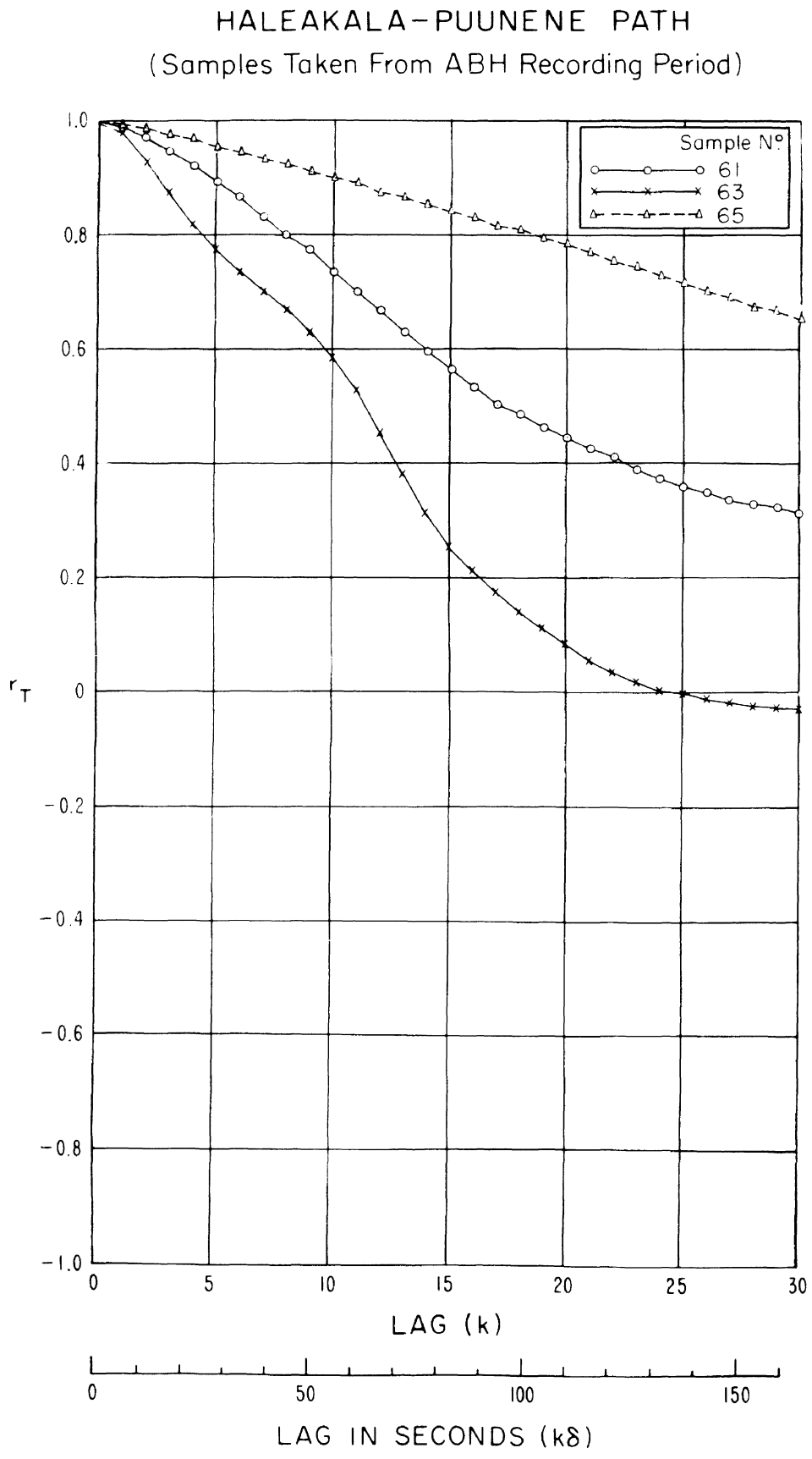

FIGURE 32. *Serial correlation functions of 9,414 Mc/s single-path phase variations.*

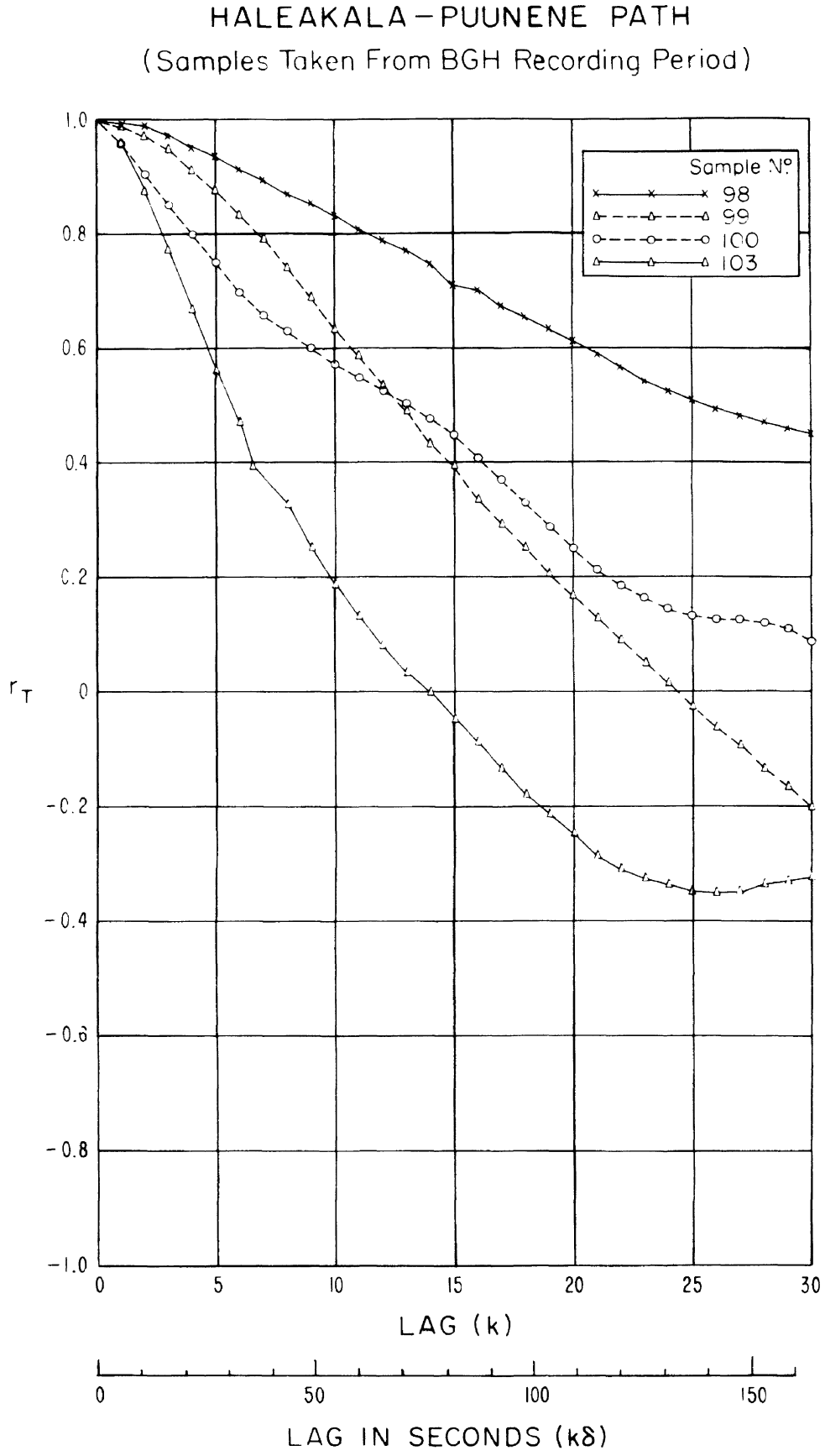

FIGURE 33. *Serial correlation functions of 9,414 Mc/s single-path phase variations.*

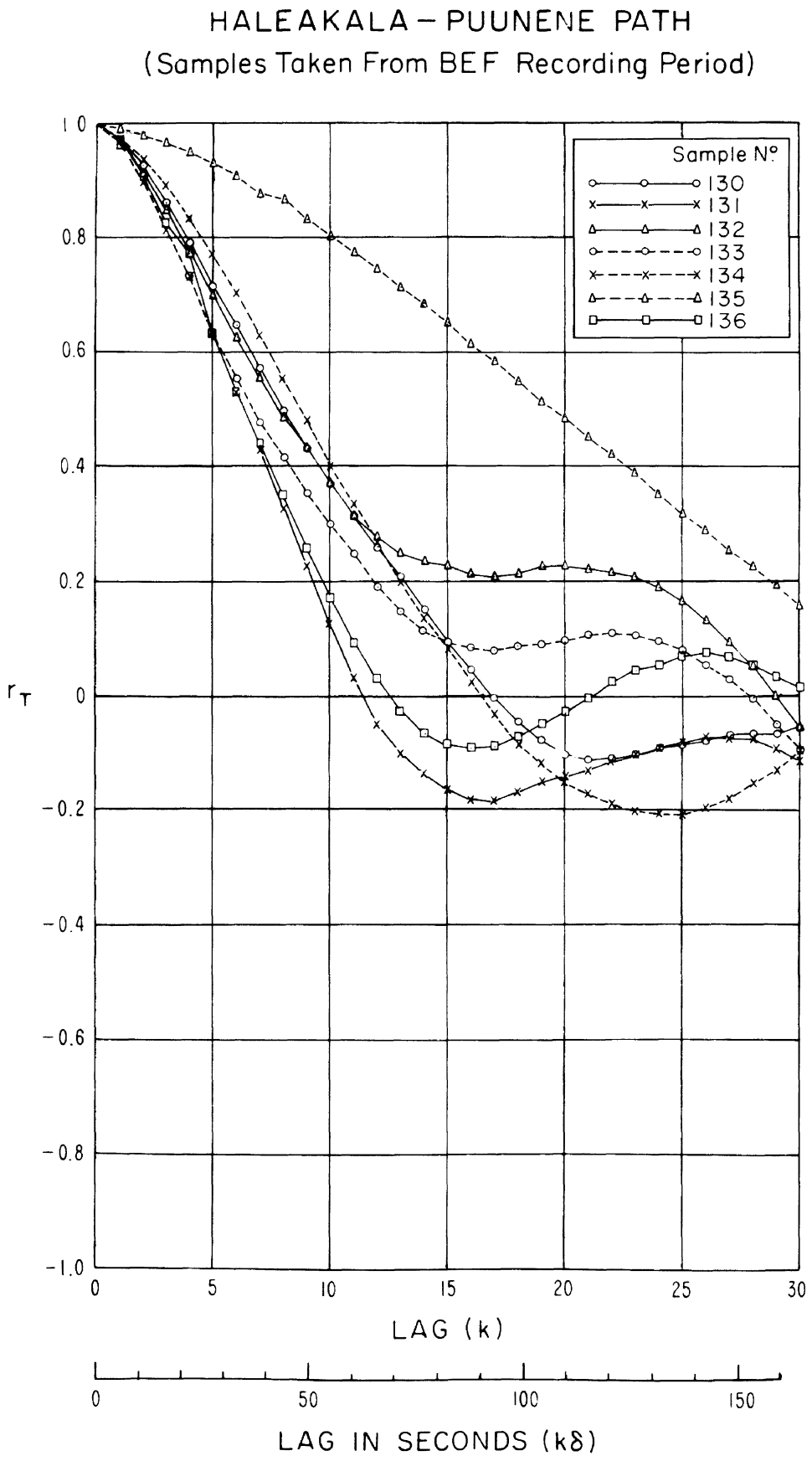

FIGURE 34. *Serial correlation functions of 9,414 Mc/s single-path phase variations.*

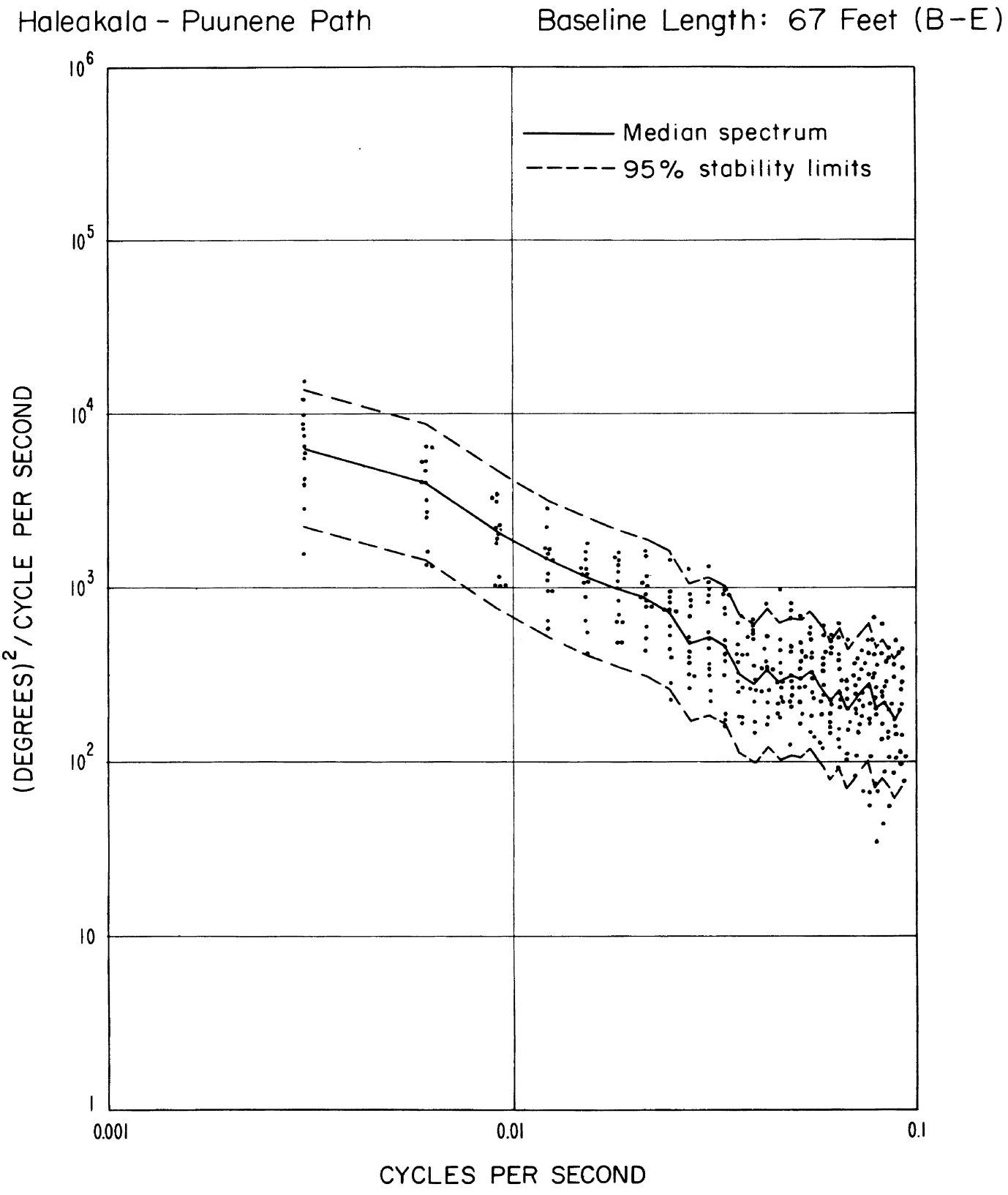

FIGURE 35. *Power spectra of 9,414 Mc/s phase difference variations.*

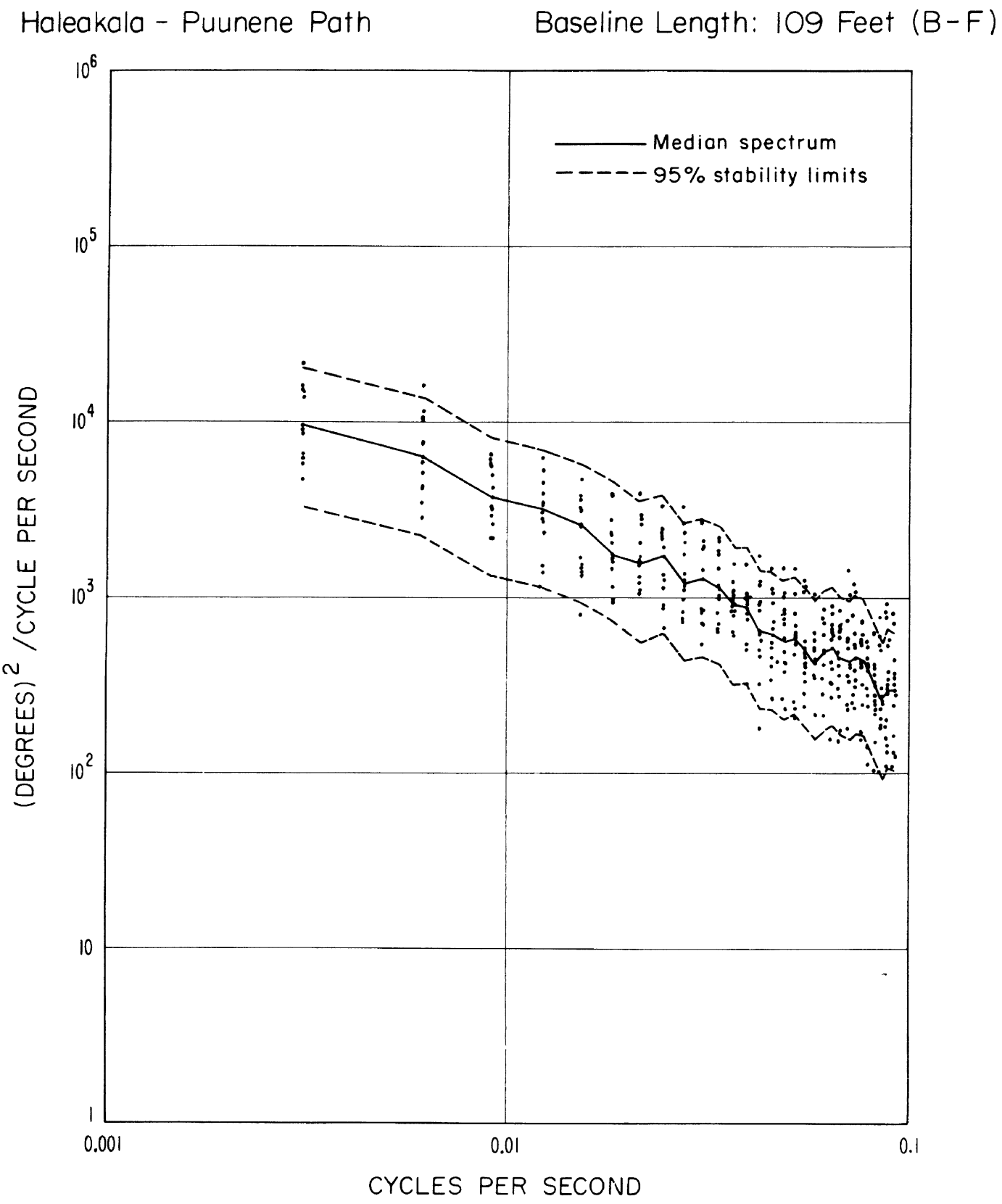

FIGURE 36. *Power spectra of 9,414 Mc/s phase difference variations.*
(Data samples 117 to 129, incl.)

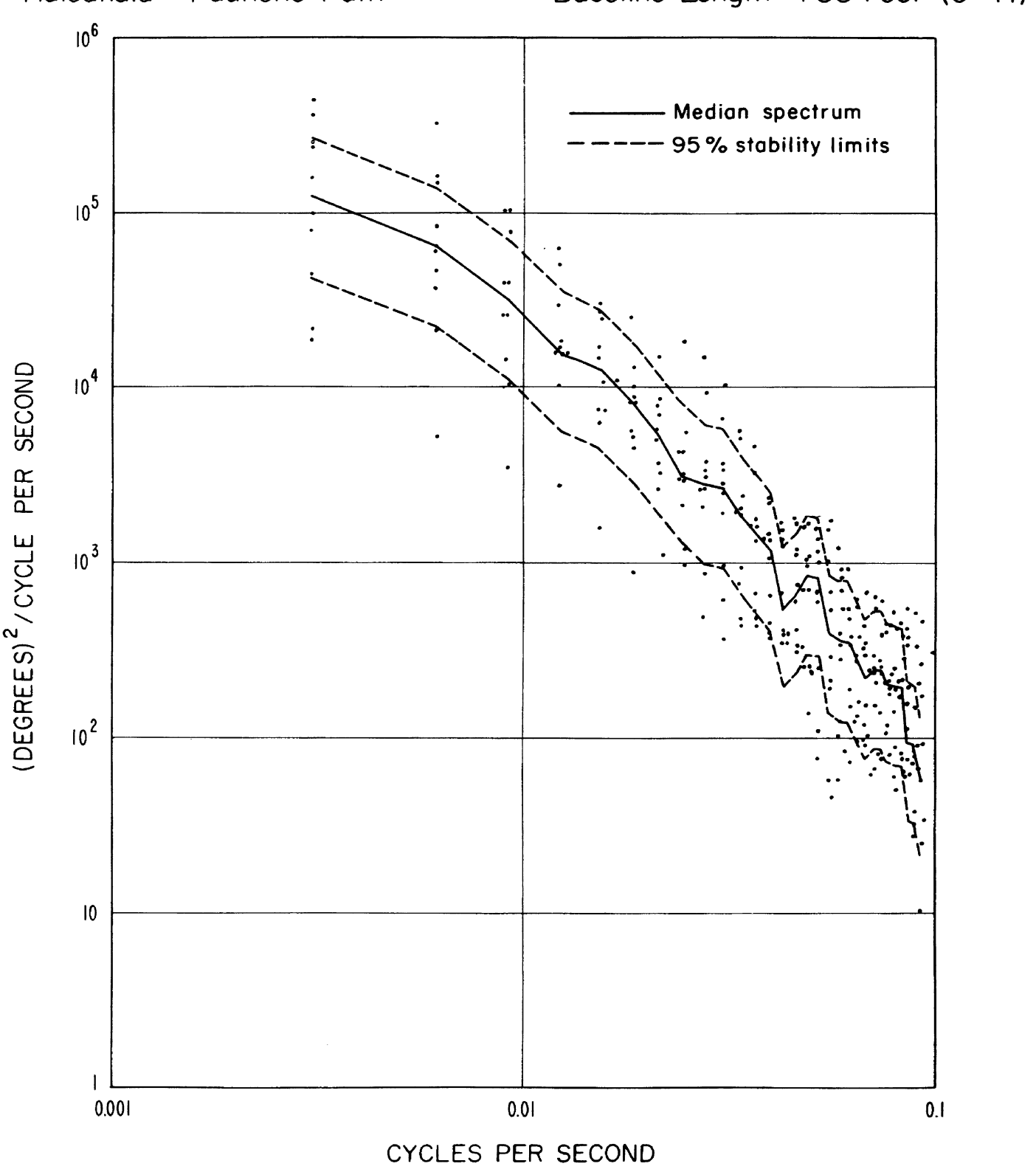

FIGURE 37. *Power spectra of 9,414 Mc/s phase difference variations.*
(Data samples 67 to 76, incl.)

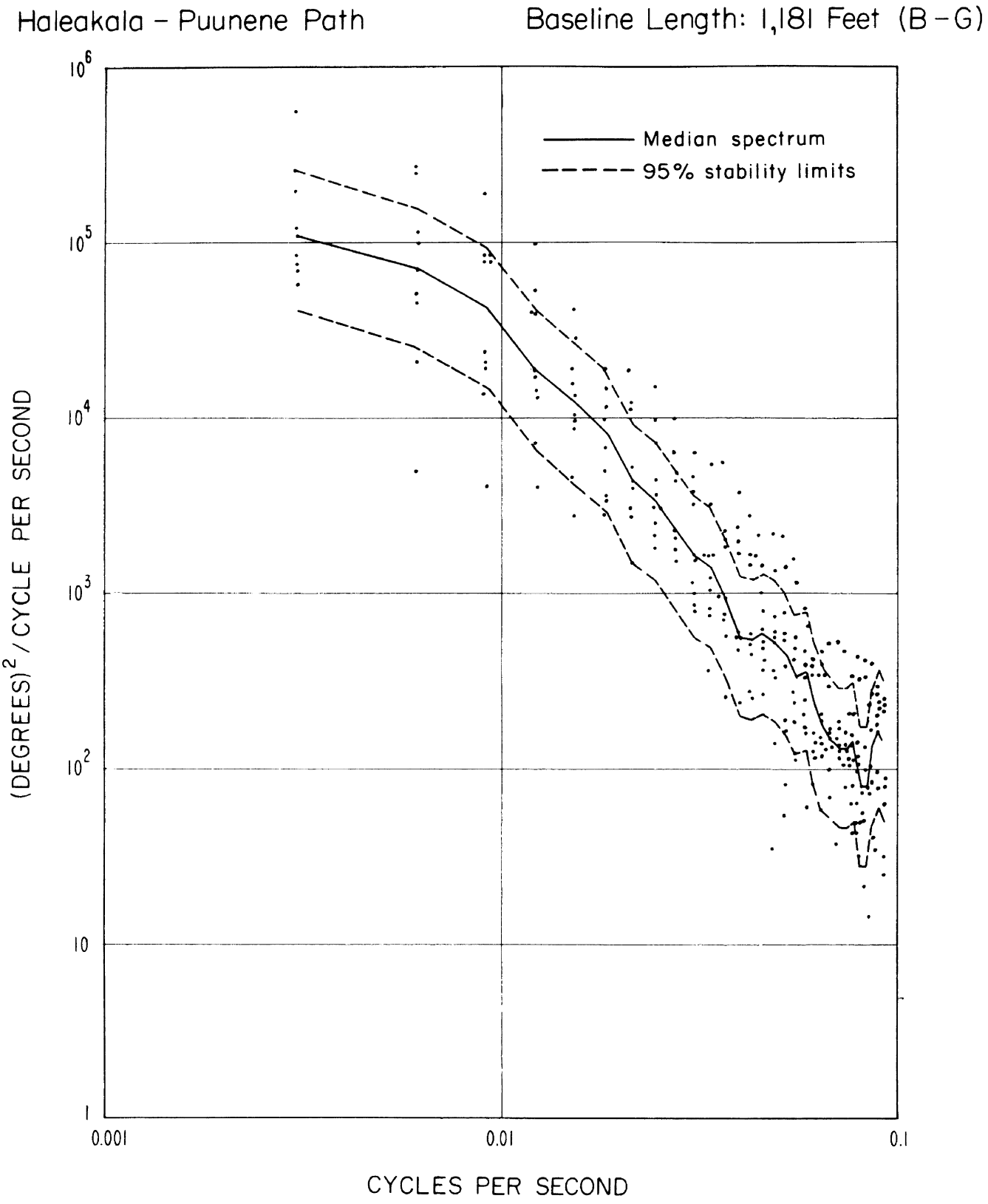

FIGURE 38. *Power spectra of 9,414 Mc/s phase difference variations.*
(Data samples 77 to 86, incl.)

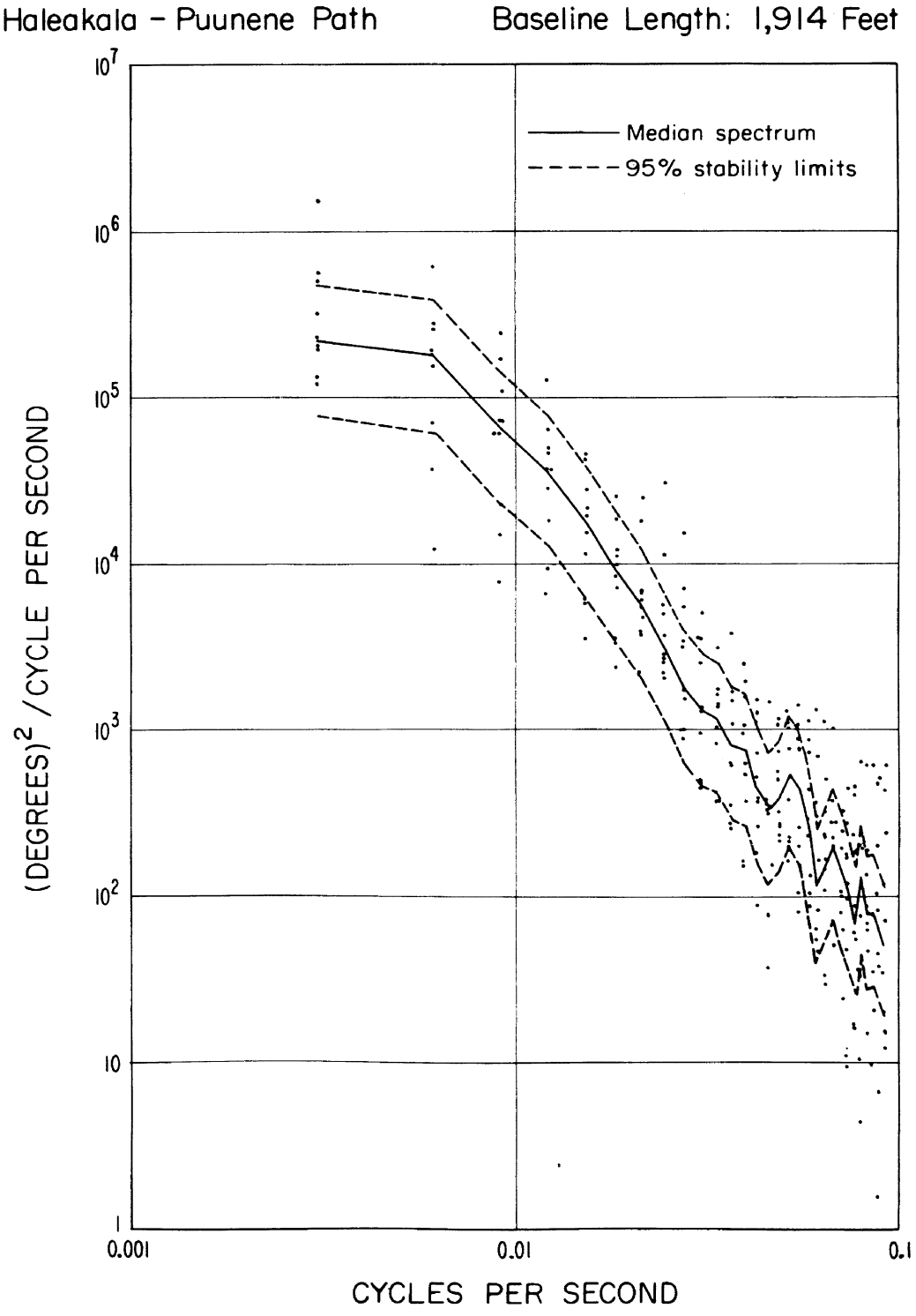

FIGURE 39. *Power spectra of 9,414 Mc/s phase difference variations.*
(Data samples 87 to 96, incl., from ABH recording period)

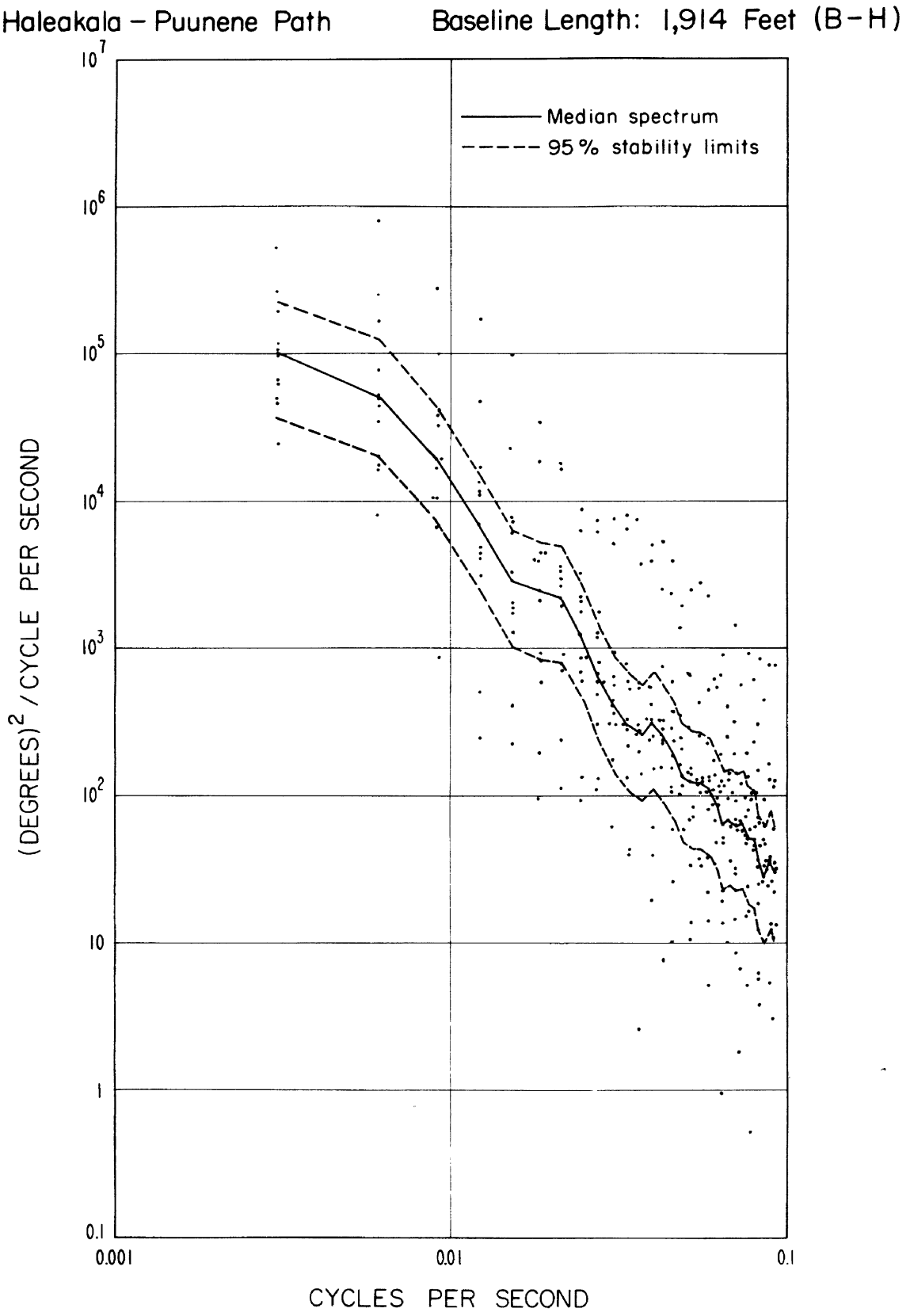

FIGURE 40. *Power spectra of 9,414 Mc/s phase difference variations.*
(Data samples 48 to 60, incl., from ABH recording period)

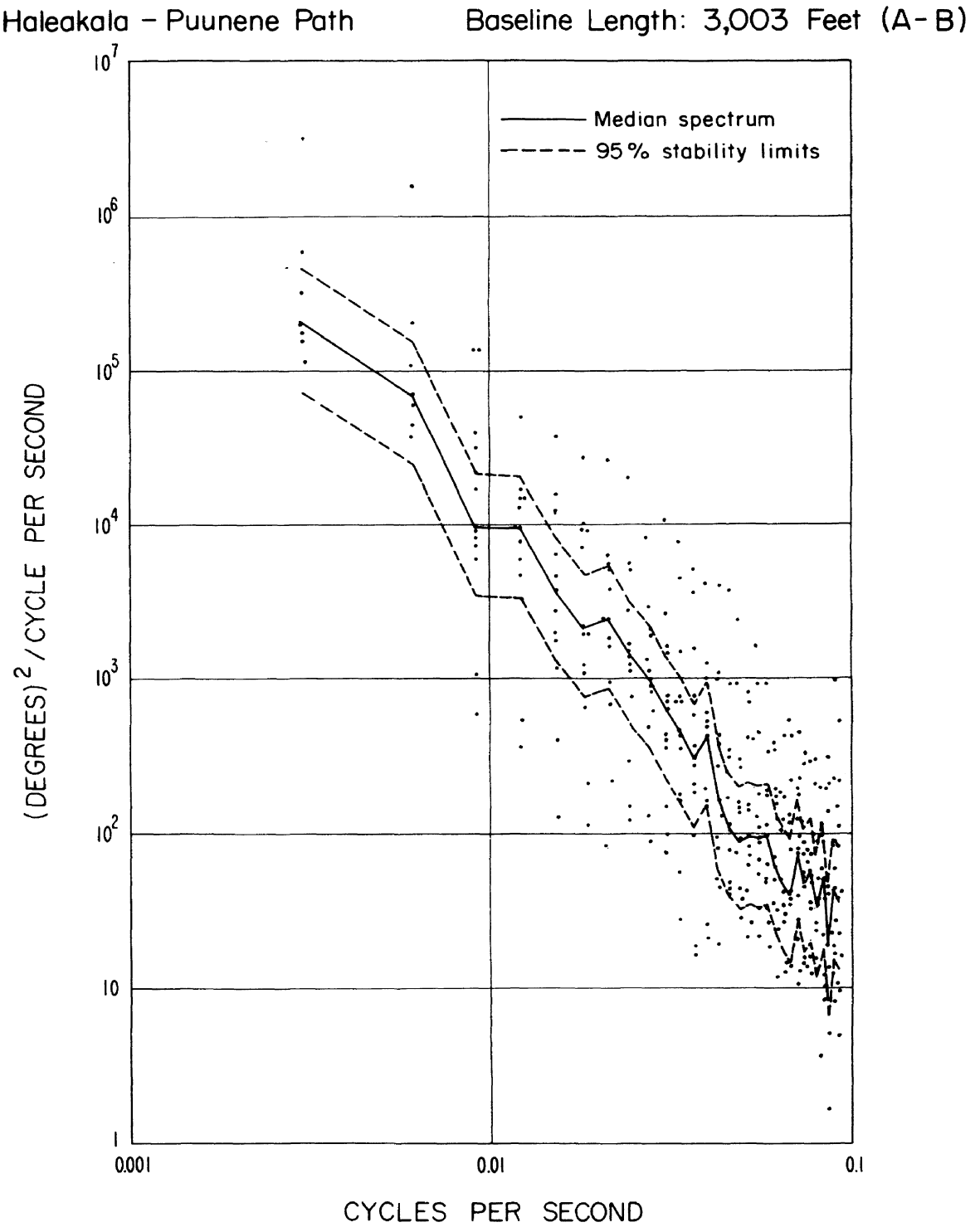

FIGURE 41. *Power spectra of 9,414 Mc/s phase difference variations.*
(Data samples 22 to 34, incl.)

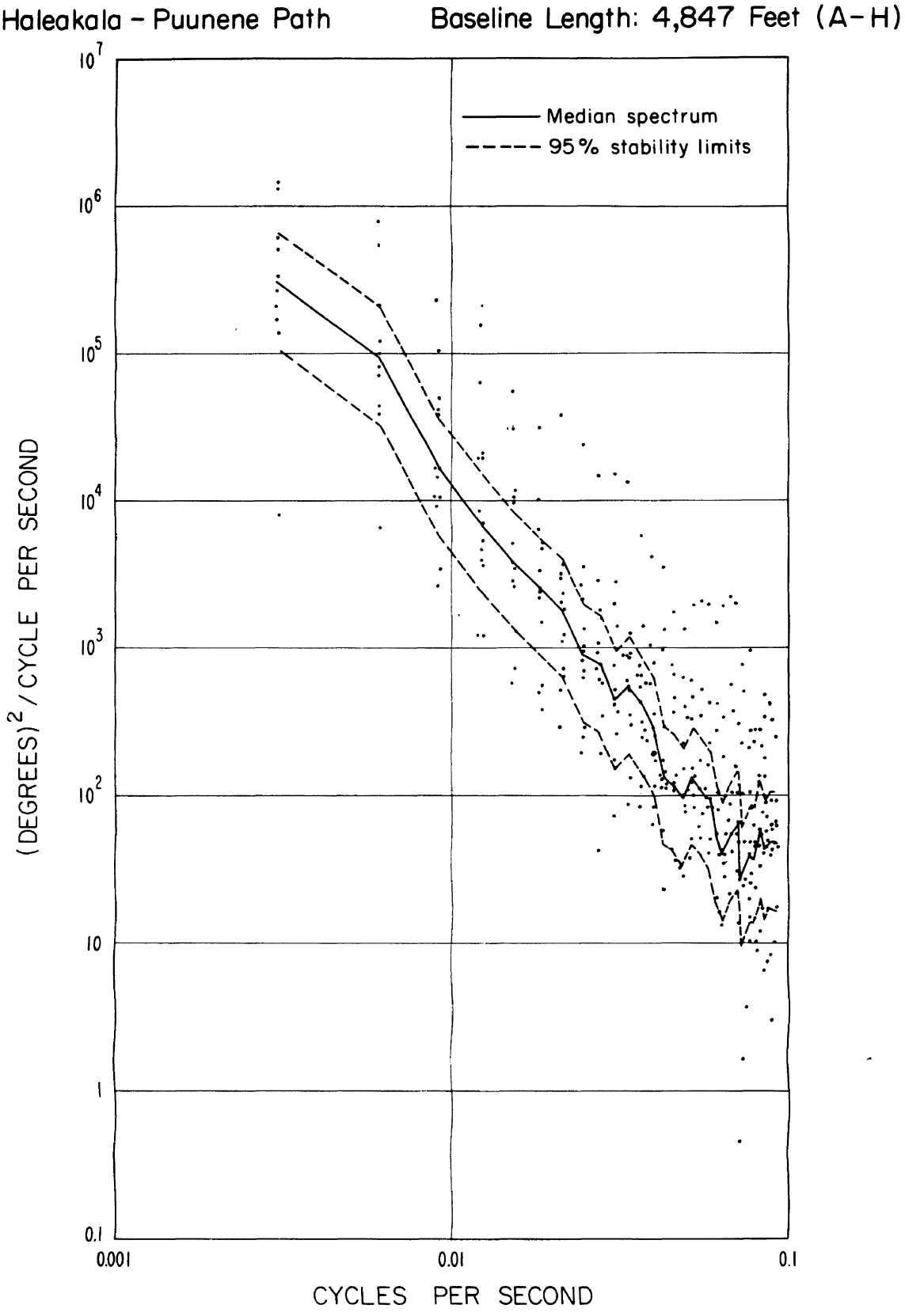

FIGURE 42. *Power spectra of 9,414 Mc/s phase difference variations.*
(Data samples 35 to 47, incl.)

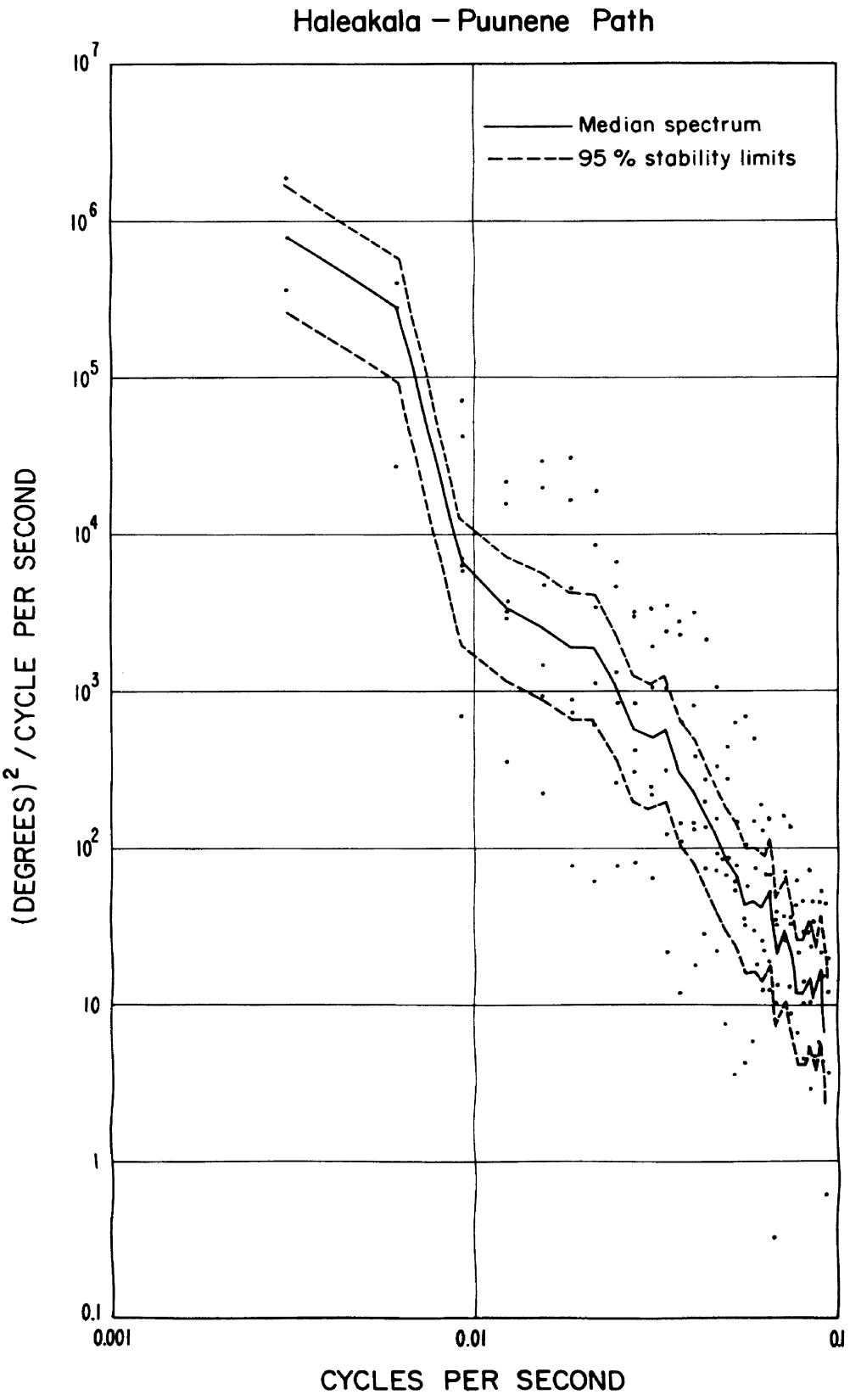

FIGURE 43. *Power spectra of 9,414 Mc/s single-path phase variations.*
(Data samples 61 to 66 incl., from ABH recording period)

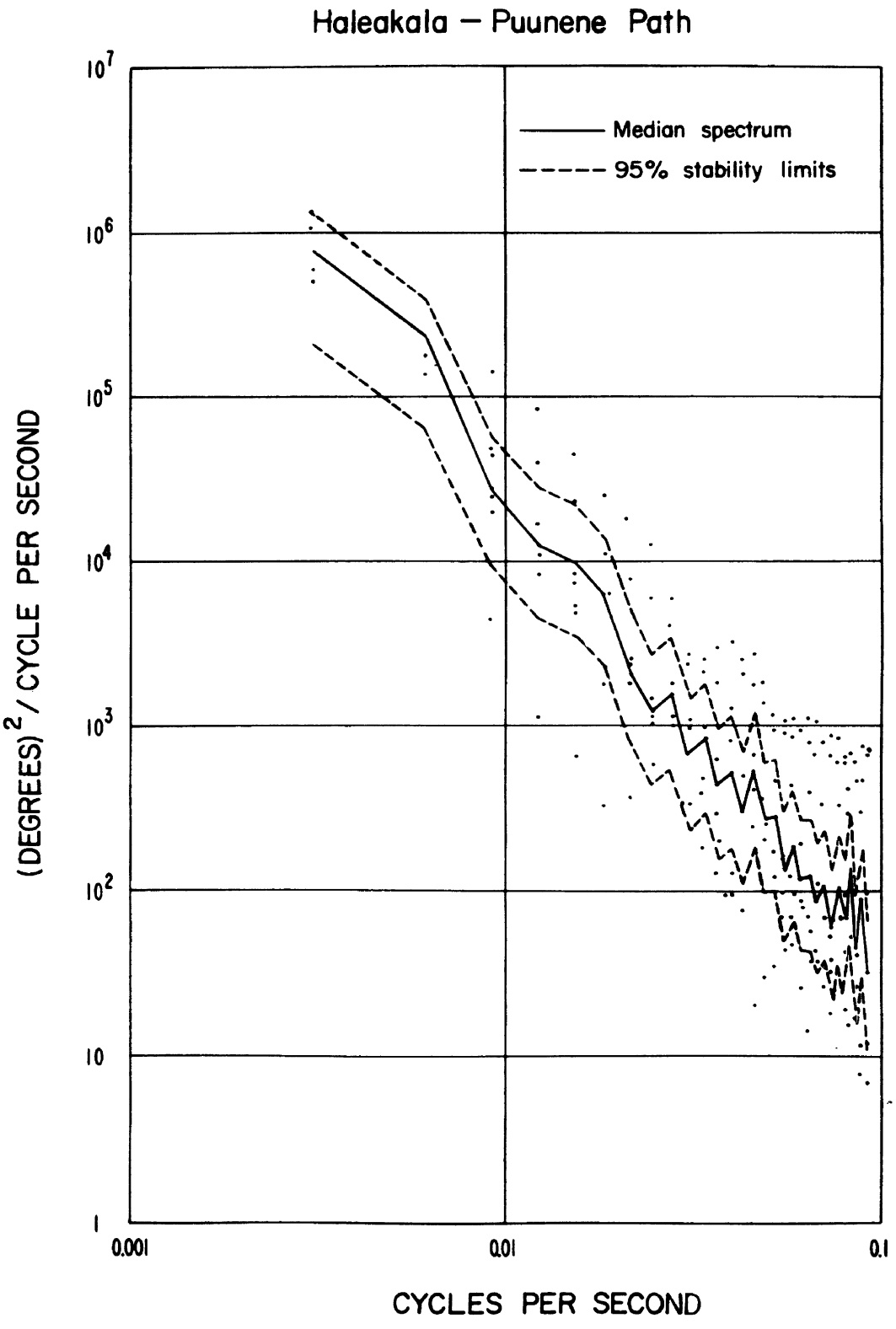

FIGURE 44. *Power spectra of 9,414 Mc/s single-path phase variations.*
(Data samples 97 to 103 incl., from BGH recording period)

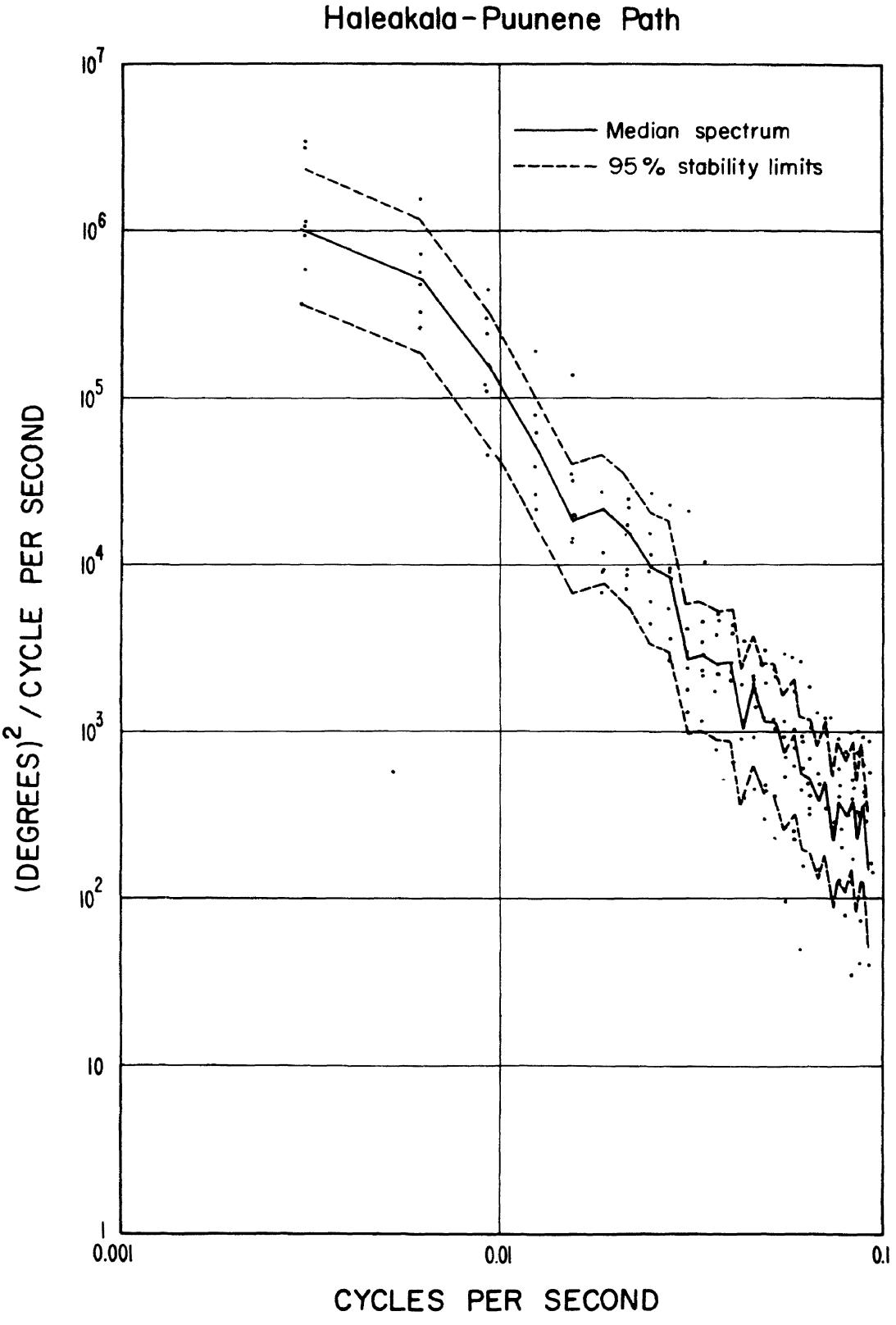

FIGURE 45. *Power spectra of 9,414 Mc/s single-path phase variations.*
(Data samples 130 to 136 incl., from BEF recording period)

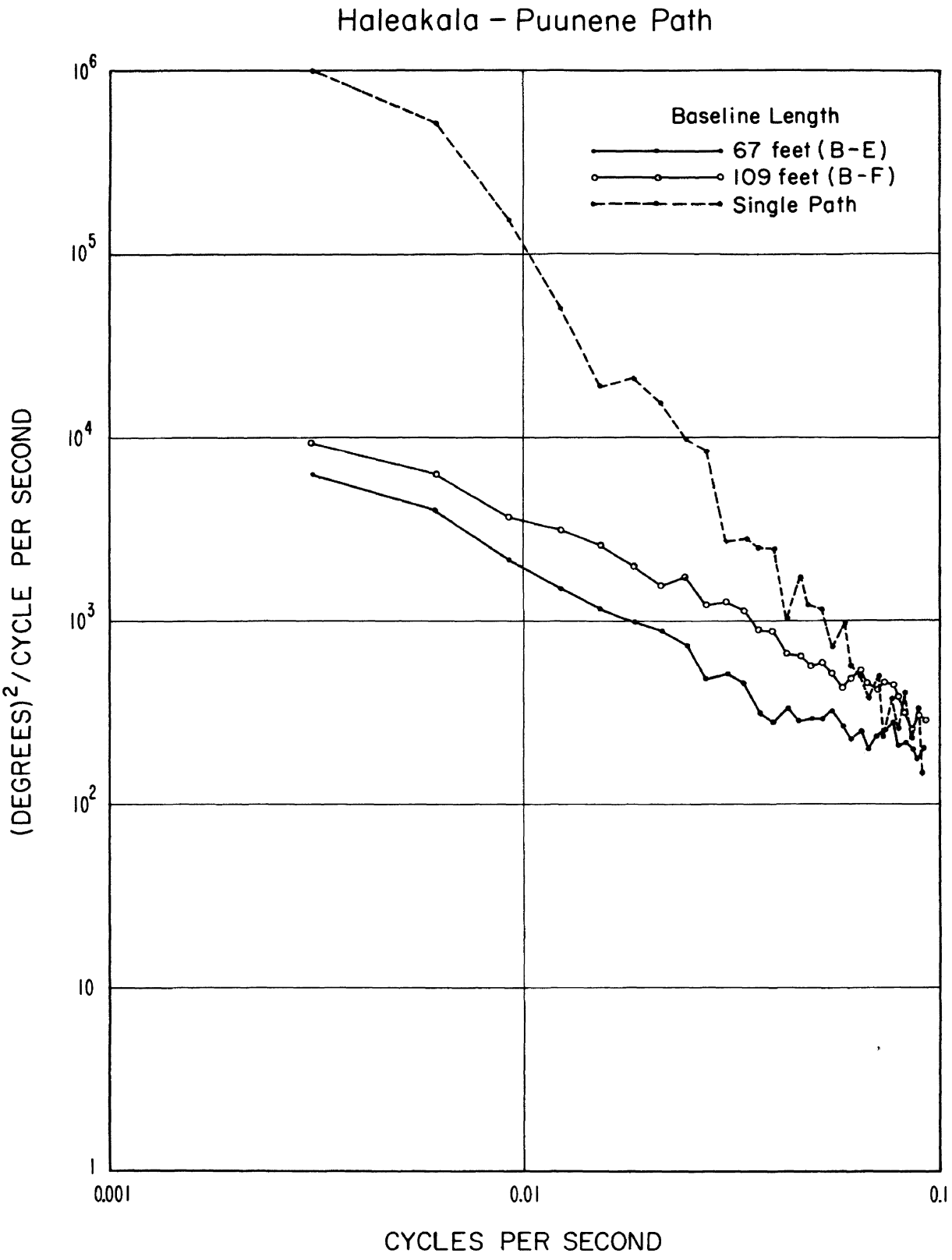

FIGURE 46. *Median phase variation spectra from BEF recording period.*

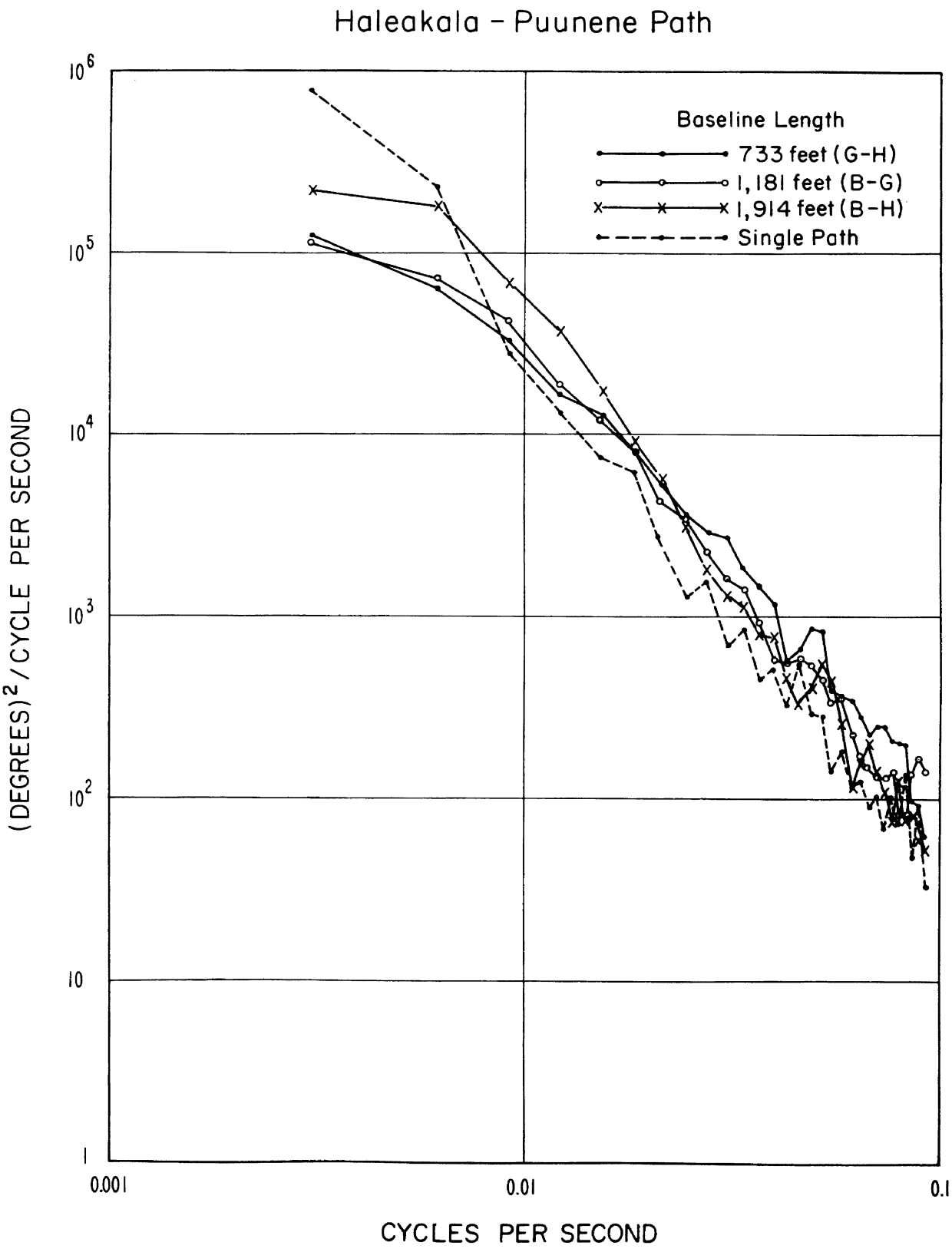

FIGURE 47. *Median phase variation spectra from BGH recording period.*

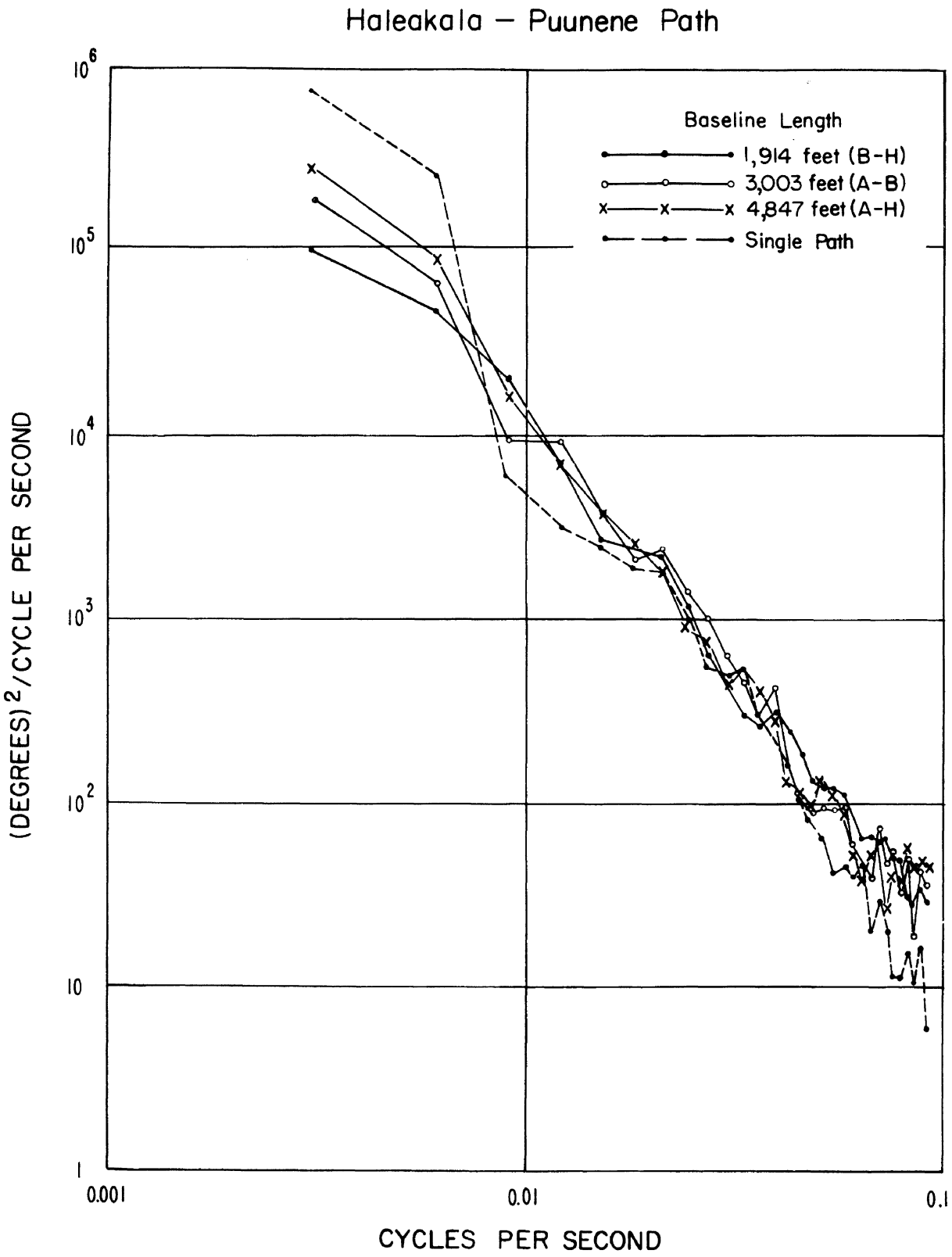

FIGURE 48. *Median phase variation spectra from ABH recording period.*

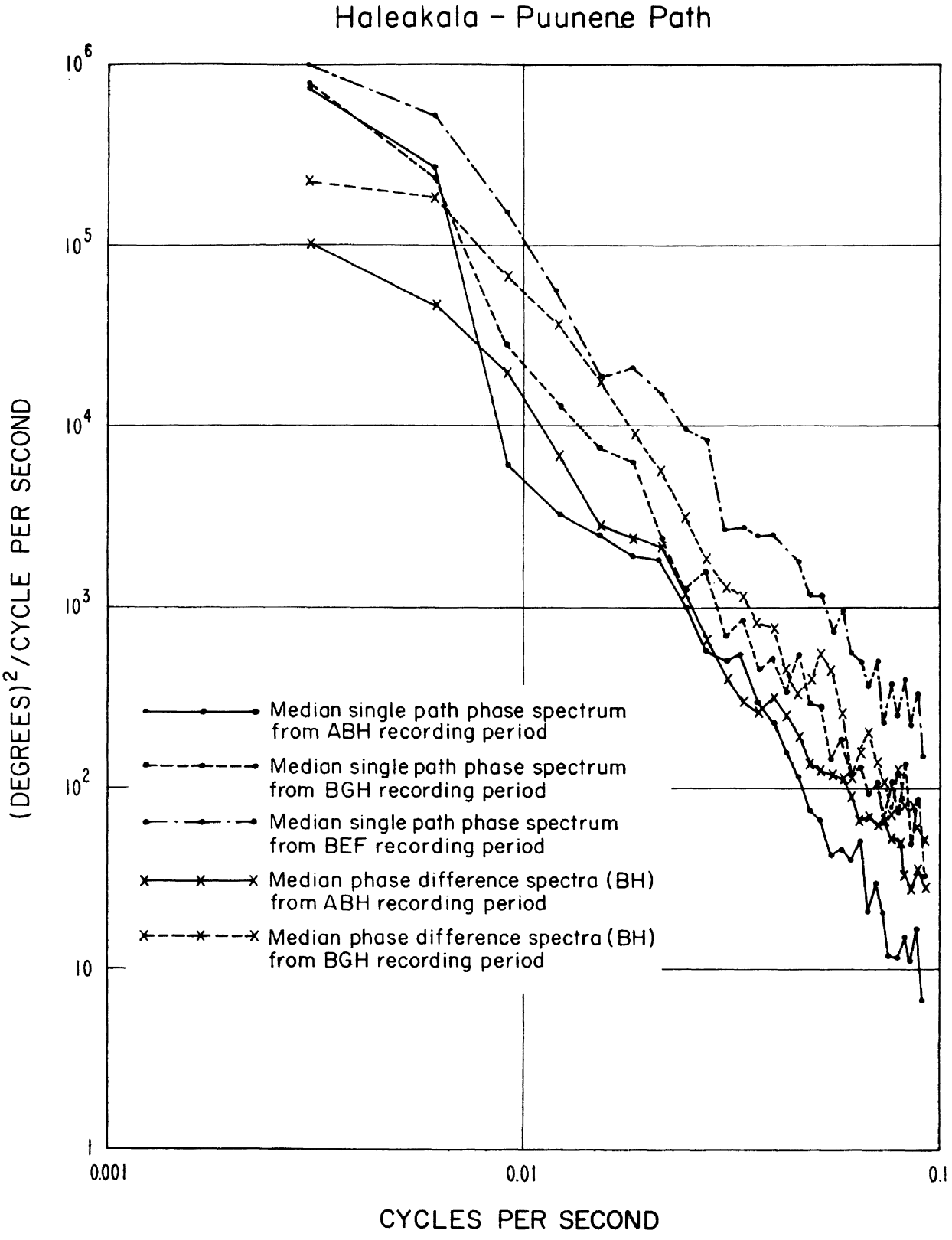

FIGURE 49. *Comparison of median spectra obtained from different recording periods.*

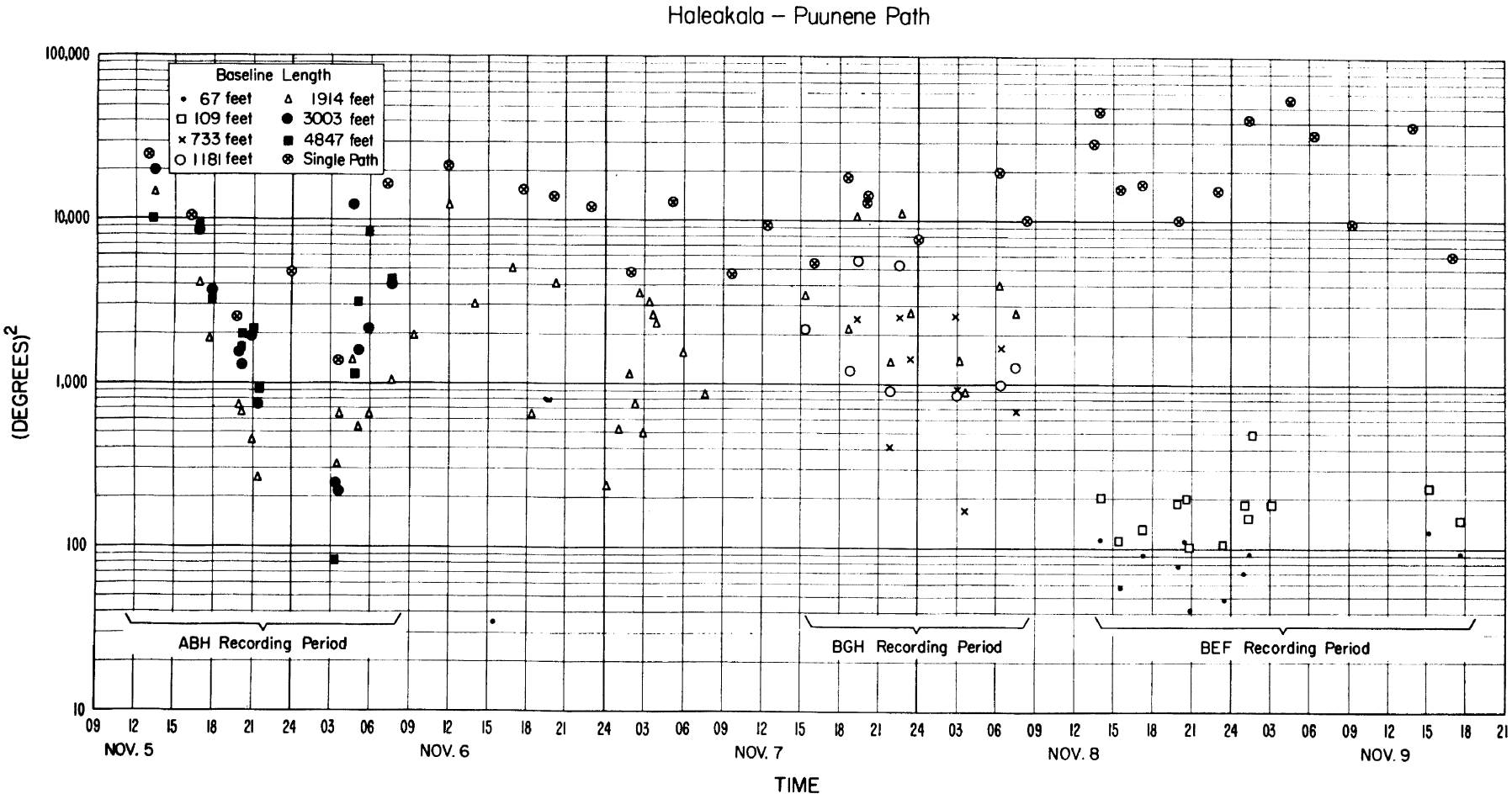

FIGURE 50. *Variance of phase difference and single-path phase versus time of day.*

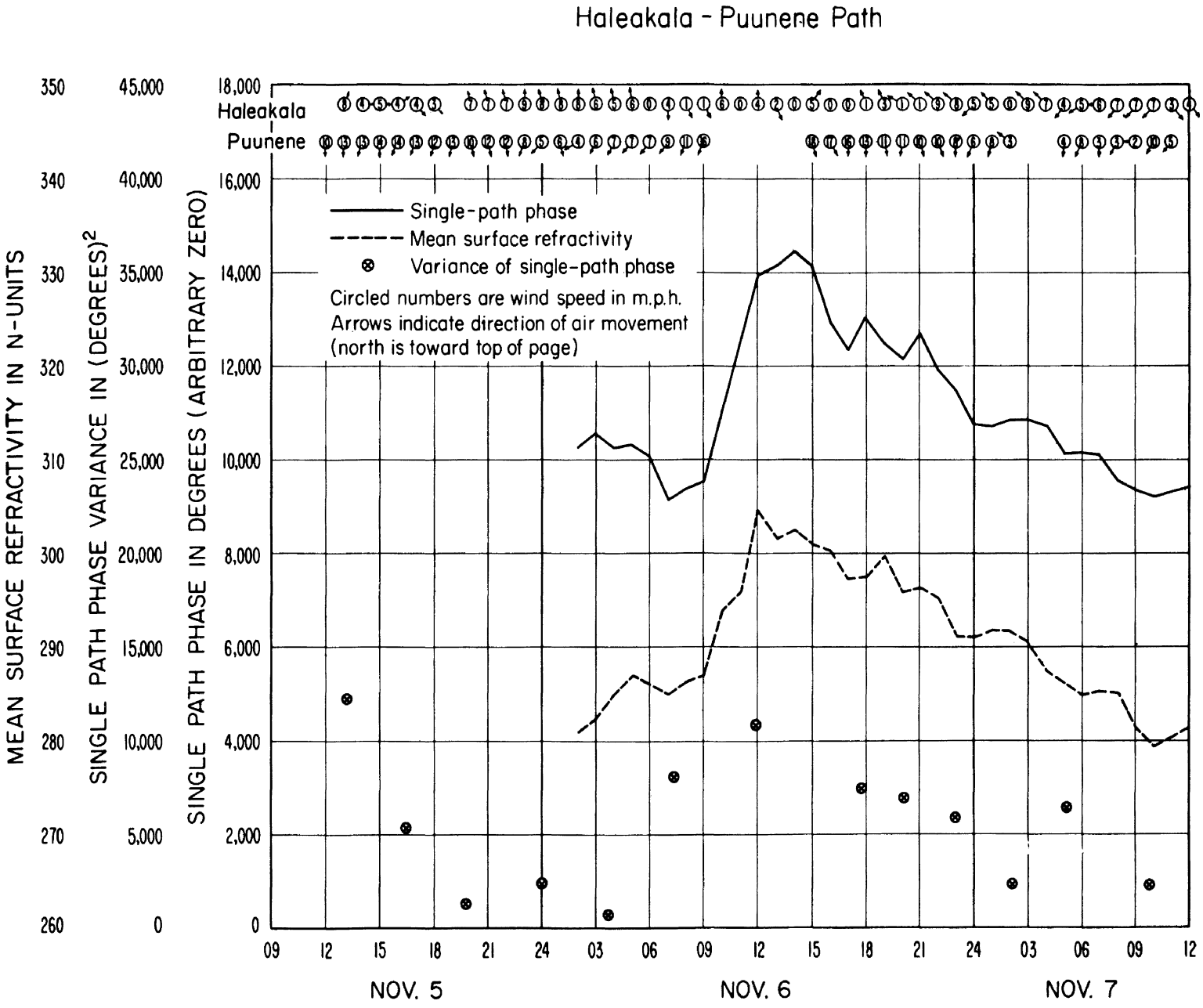

FIGURE 51. *Variation of single-path phase, surface refractivity wind velocity with time of day.*

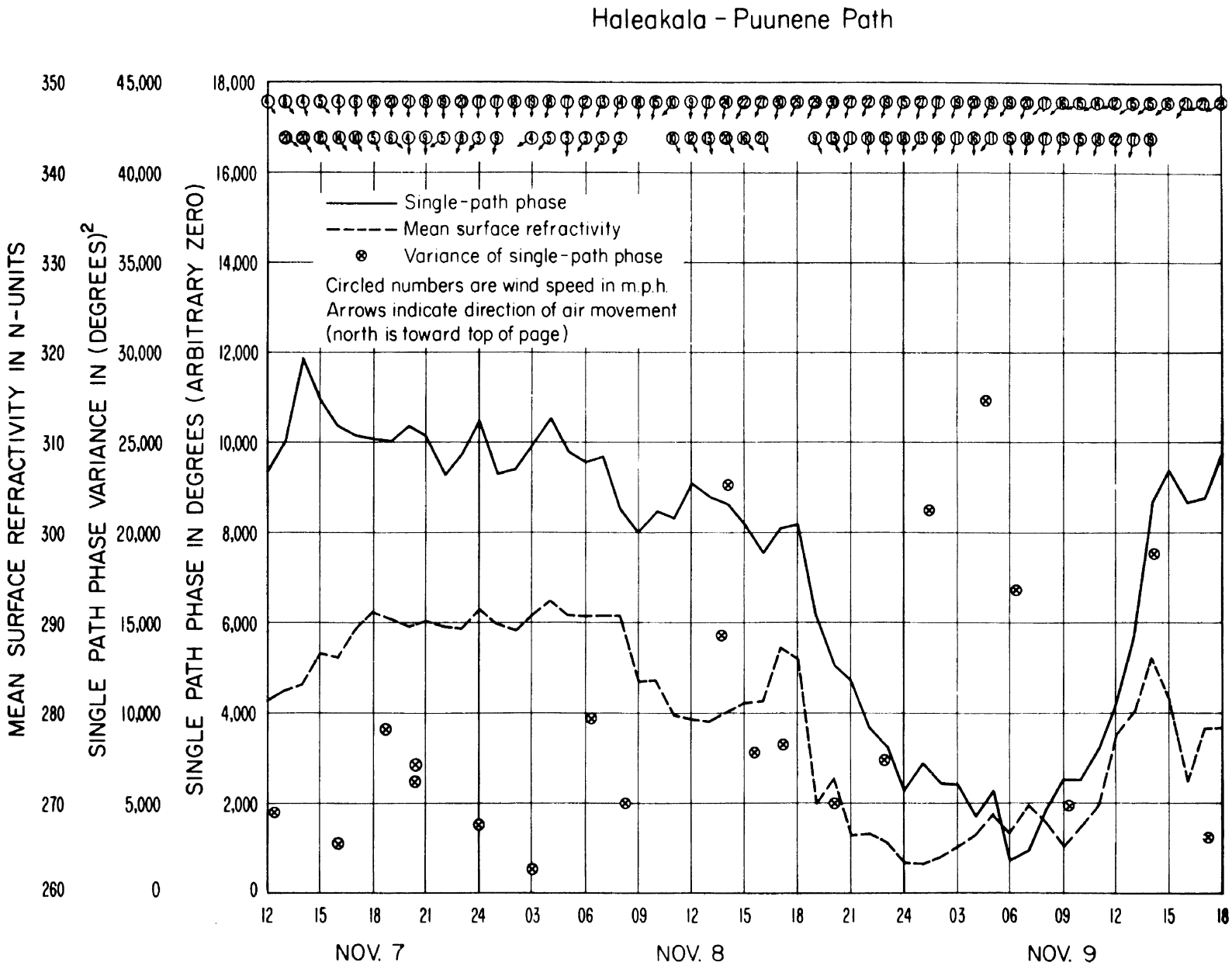

FIGURE 52. *Variation of single-path phase, surface refractivity and wind velocity with time of day.*

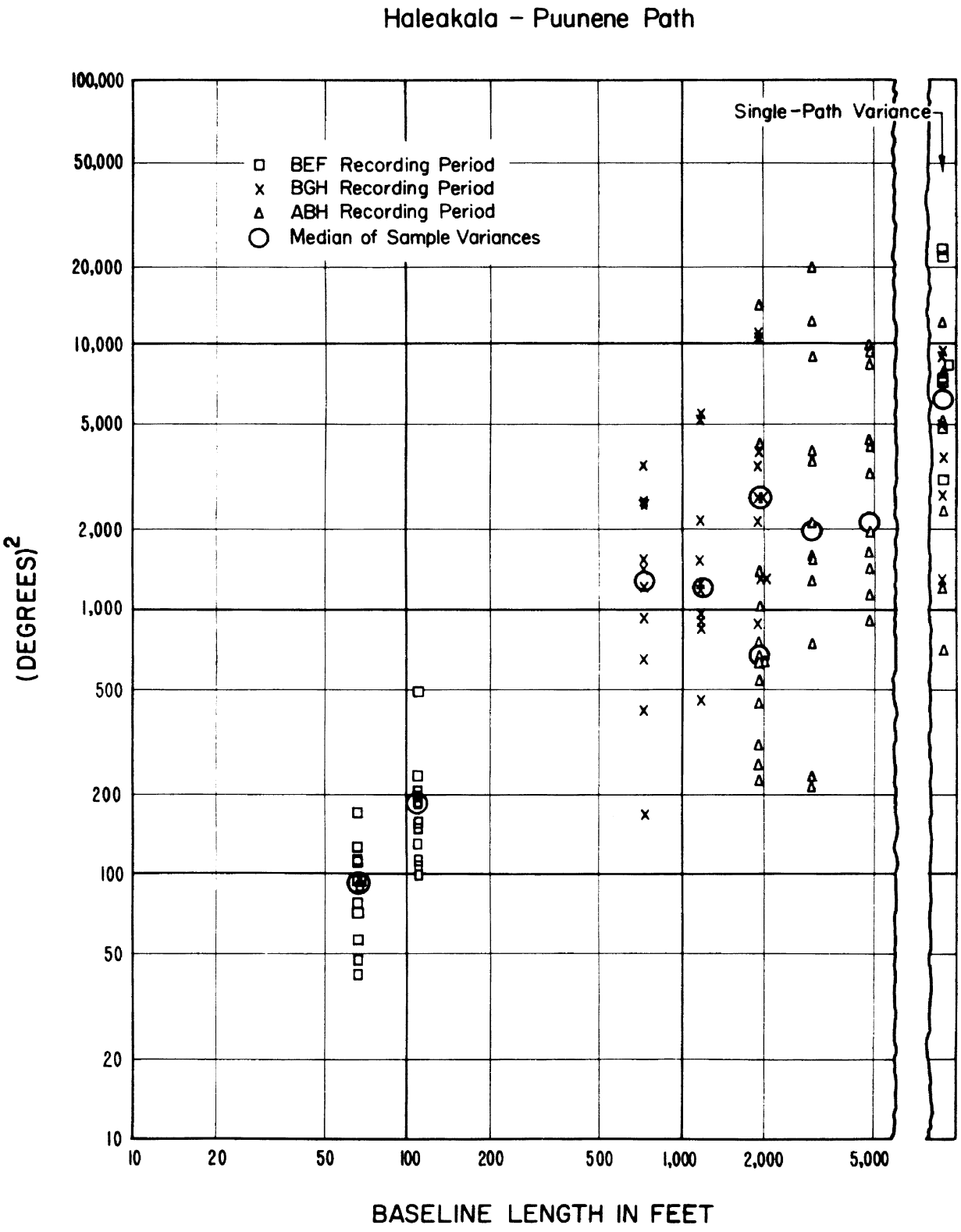

FIGURE 53. *Variance of phase difference versus baseline length.*

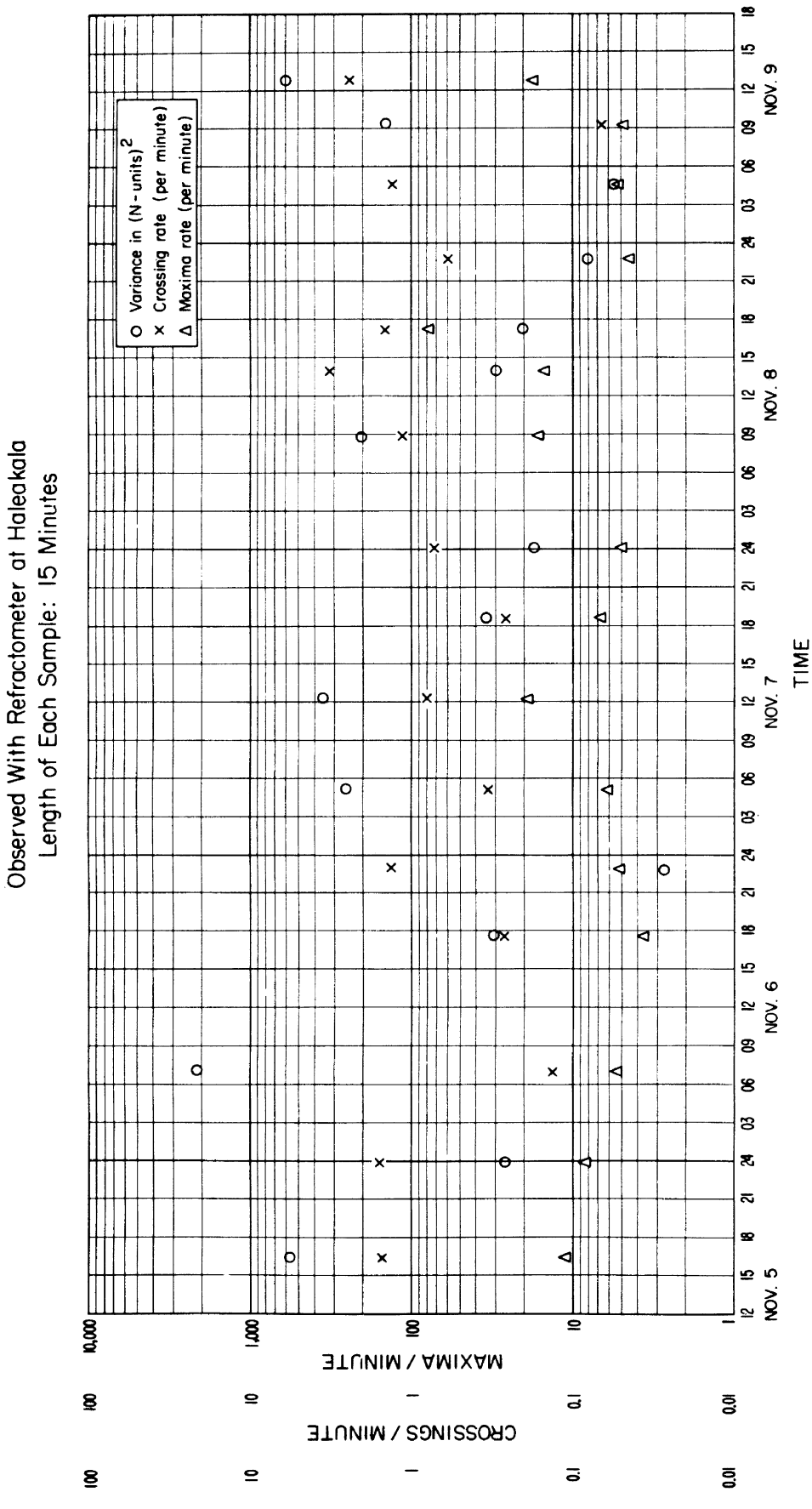

FIGURE 54. *Variance, crossing rate and maximum rate of surface refractivity variations.*

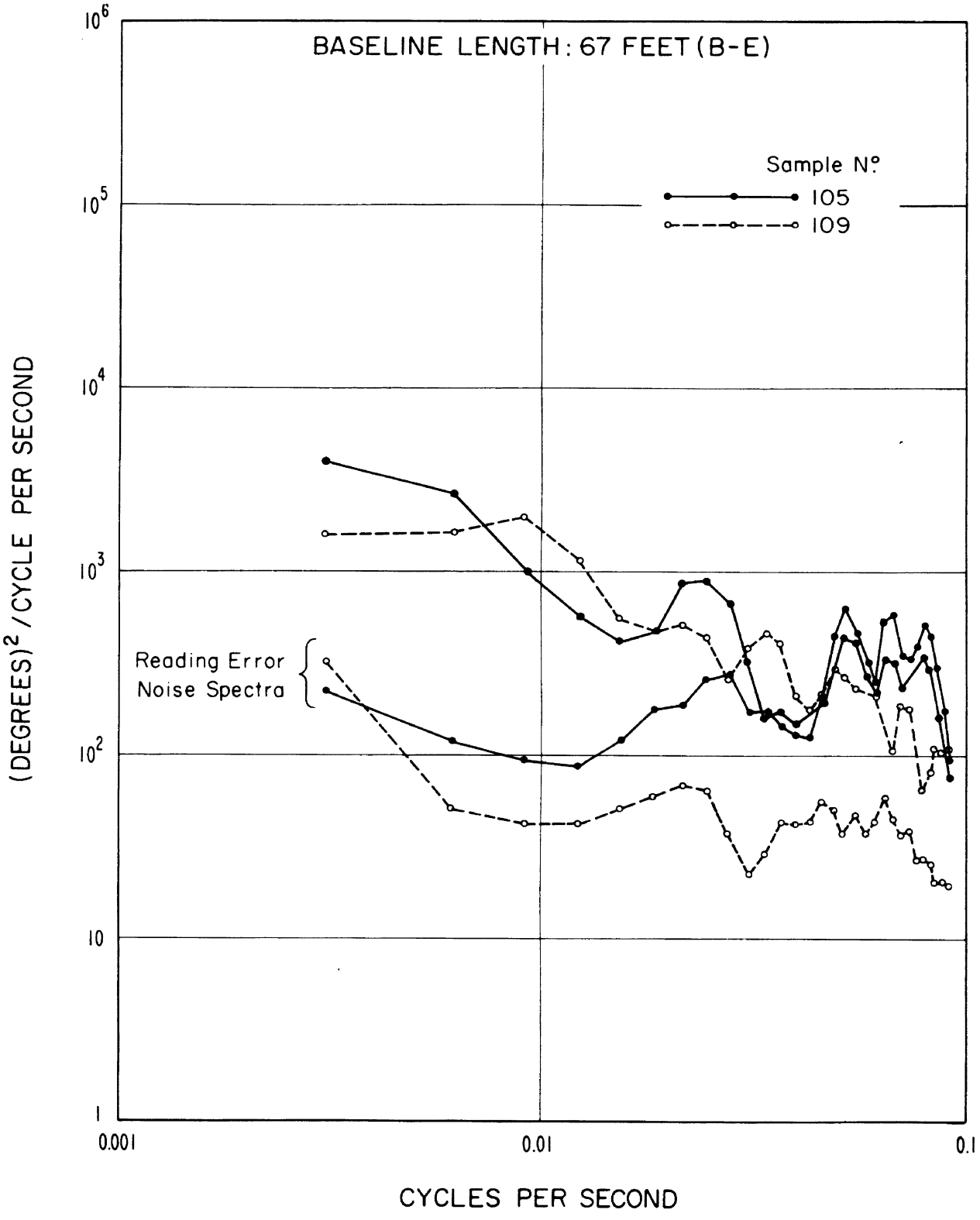

FIGURE 55. *Examples of reading error noise spectra compared to corresponding phase difference spectra.*

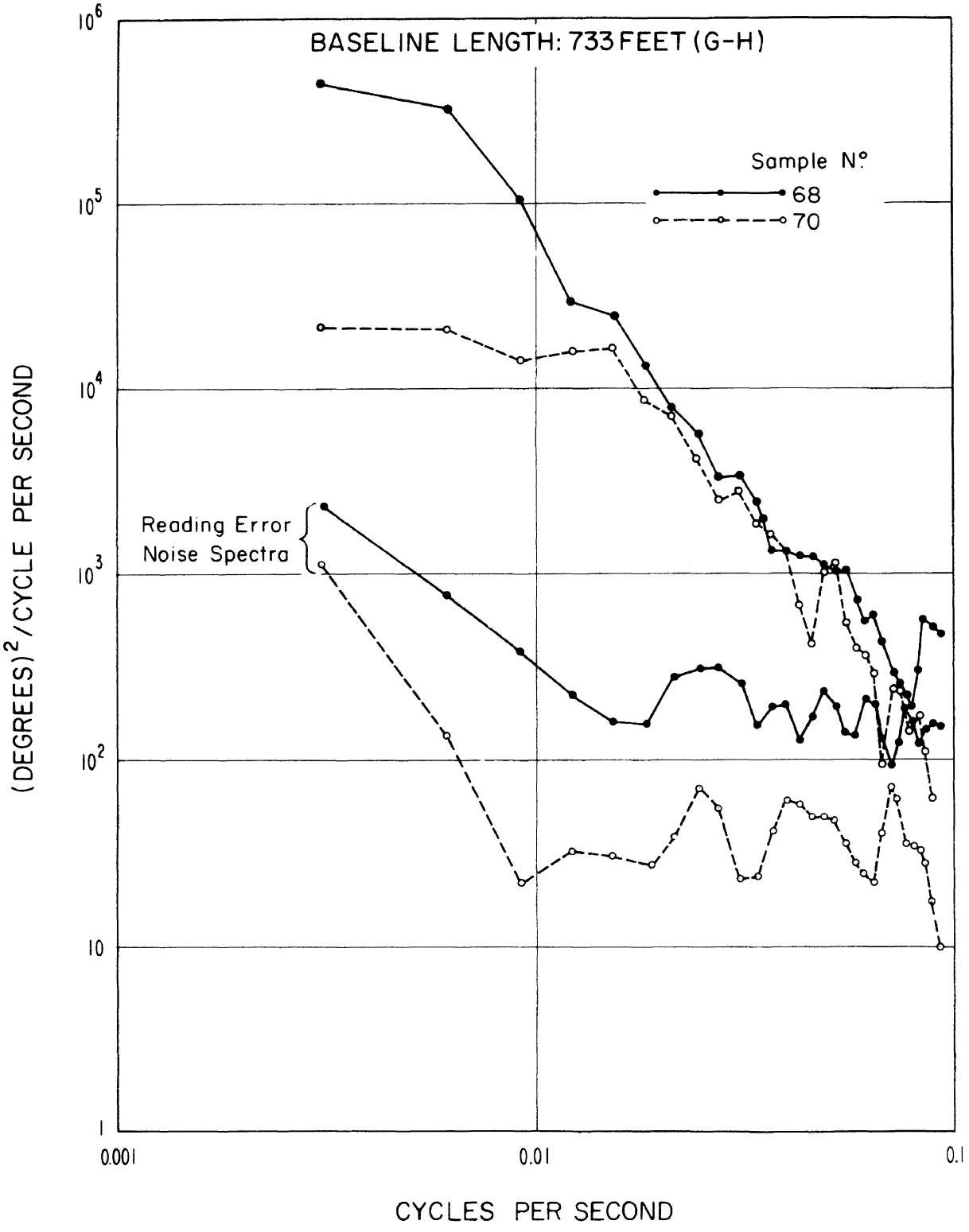

FIGURE 56. *Examples of reading error noise spectra compared to corresponding phase difference spectra.*

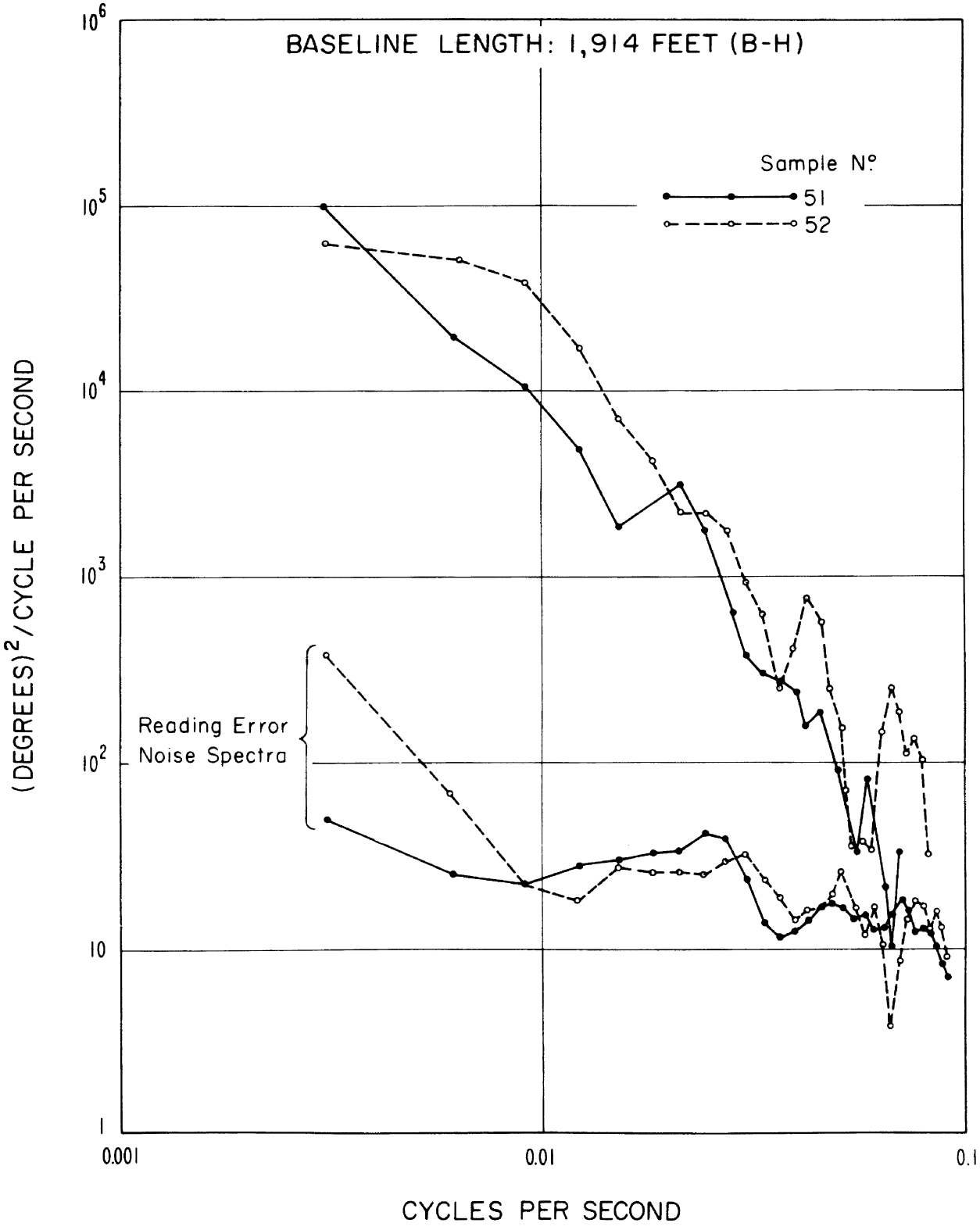

FIGURE 57. *Examples of reading error noise spectra compared to corresponding phase difference spectra.*

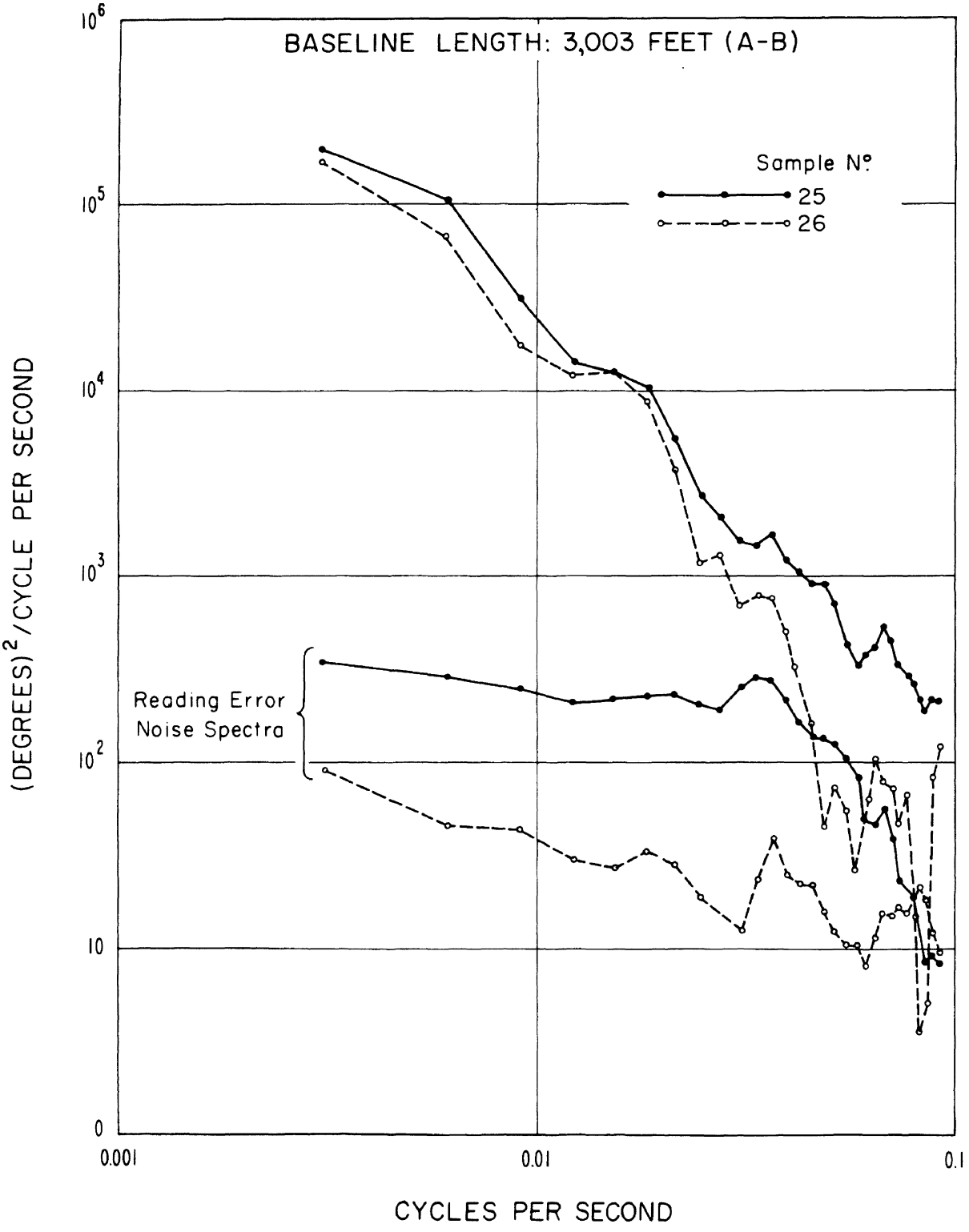

FIGURE 58. *Examples of reading error noise spectra compared to corresponding phase difference spectra.*

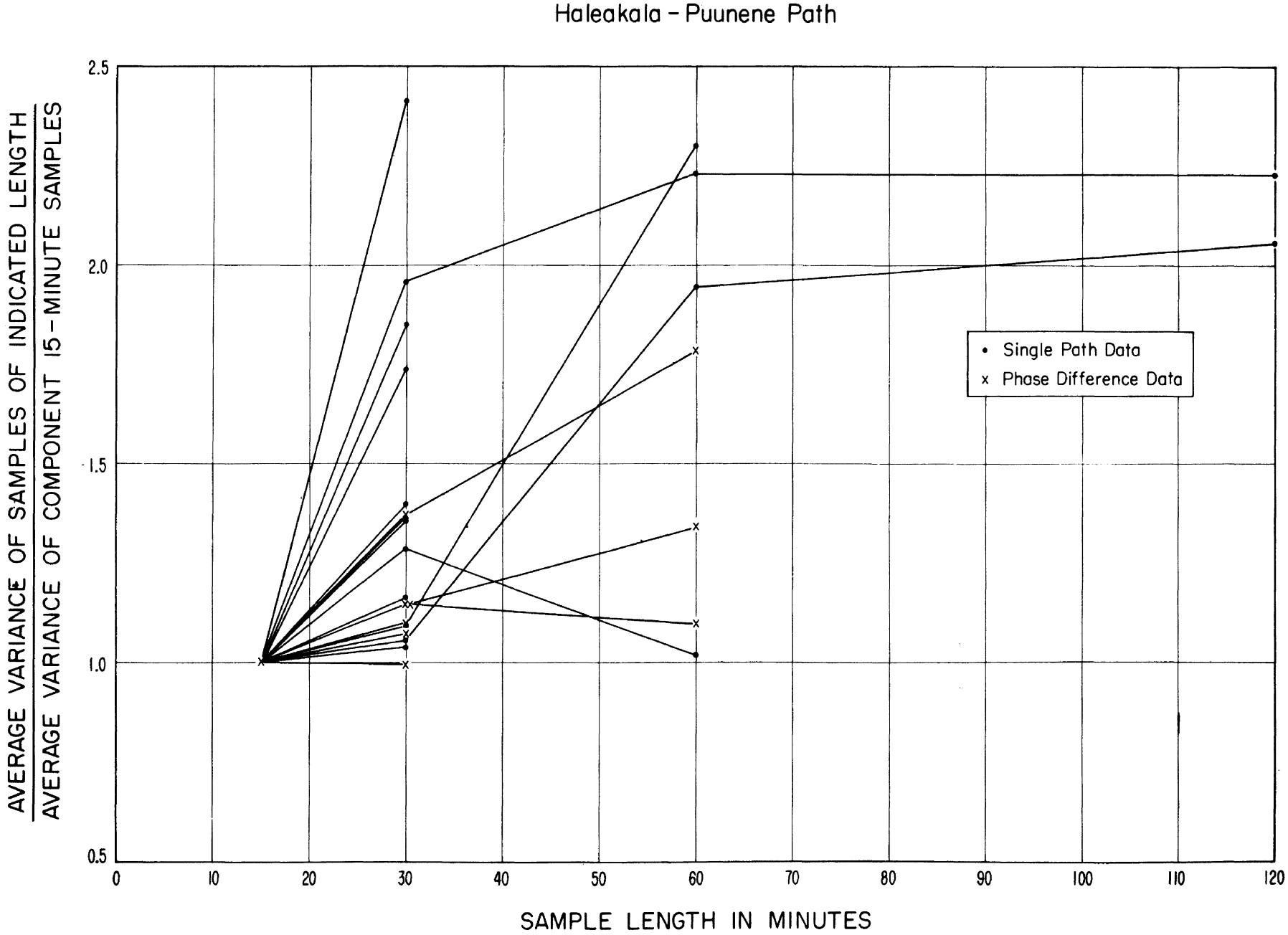

FIGURE 59. *Total variance of phase variations versus sample length.*

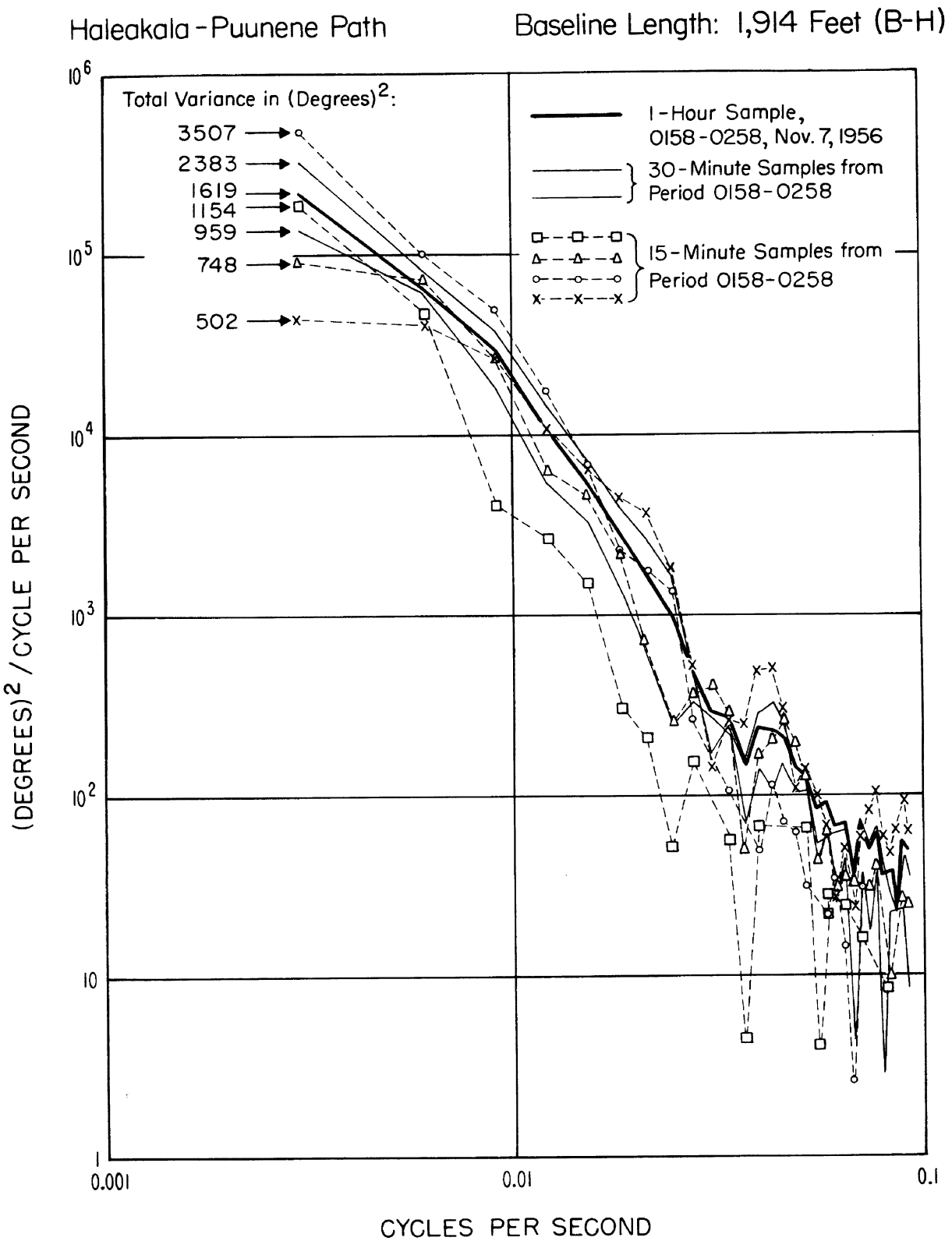

FIGURE 60. *Power spectra of phase difference variations with sample length as a parameter 9,414 Mc/s.*

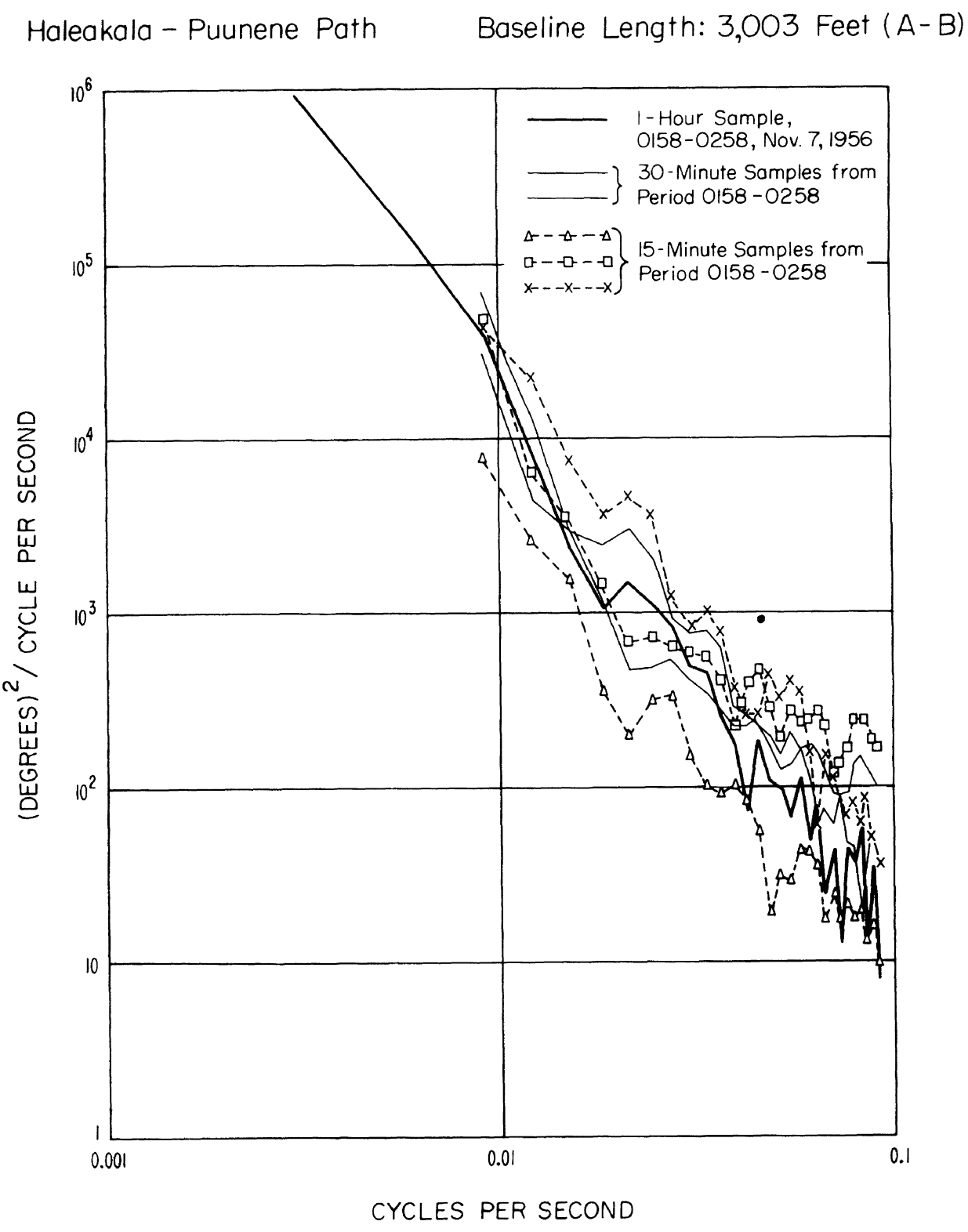

FIGURE 61. *Power spectra of phase difference variations with sample length as a parameter 9,414 Mc/s.*

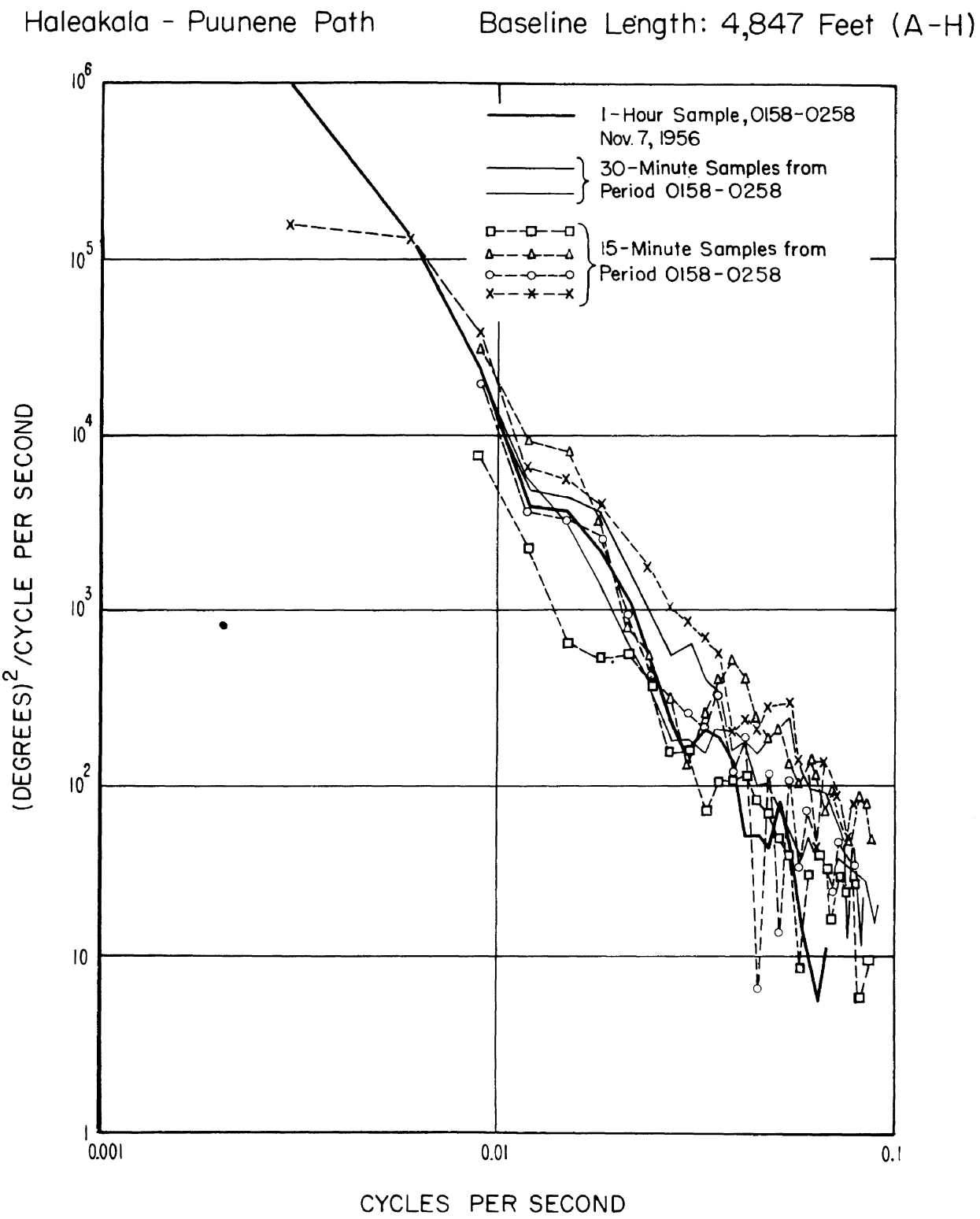

FIGURE 62. *Power spectra of phase difference variations with sample length as a parameter 9,414 Mc/s.*

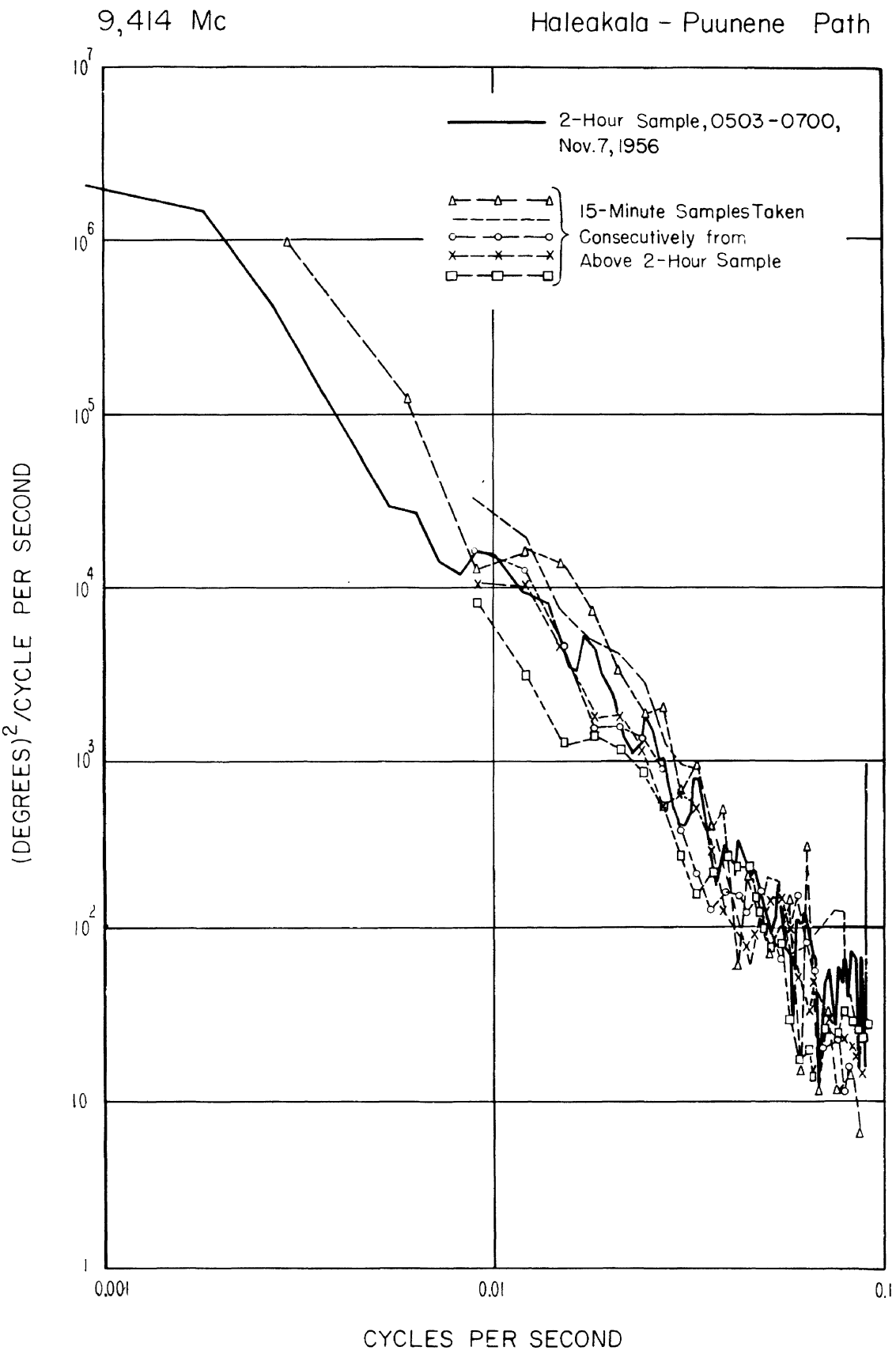

FIGURE 63. *Power spectra of single-path phase variations with sample length as a parameter.*

FROM PUUNENE

FROM HALEAKALA

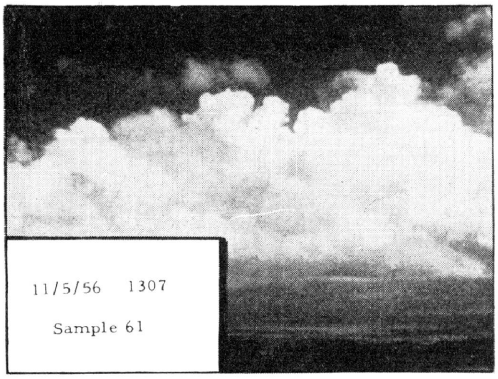

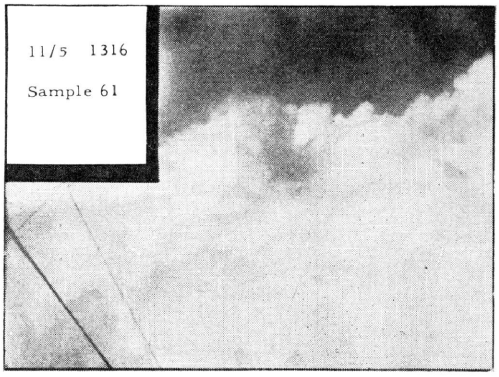

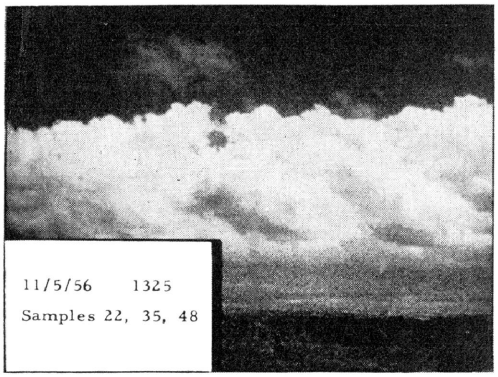

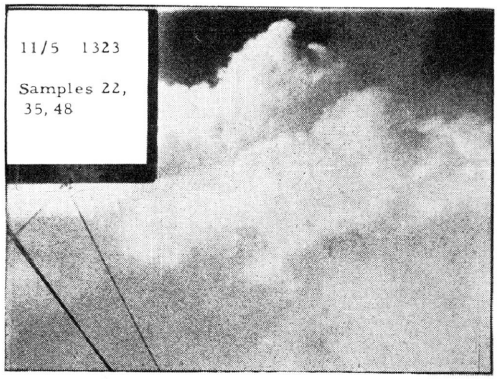

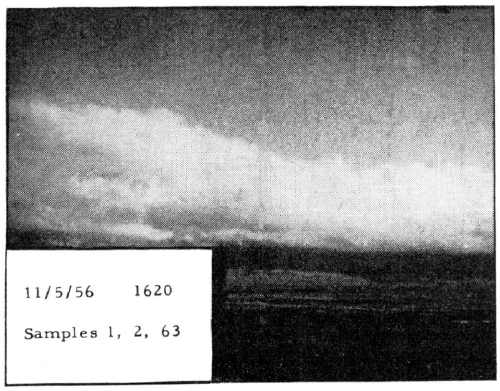

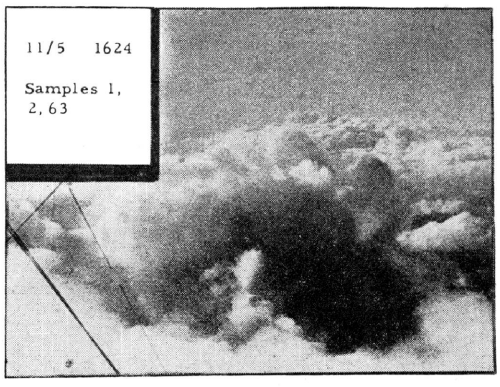

FIGURE 64. *Photographs of Haleakala-Puunene path corresponding in time to data samples indicated.*

FROM PUUNENE

FROM HALEAKALA

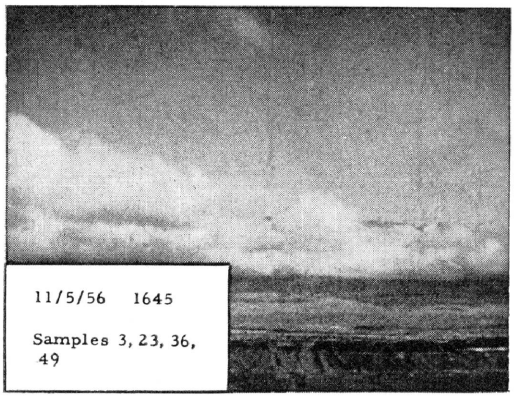

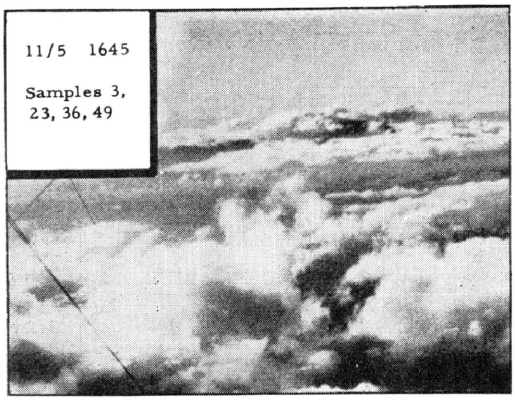

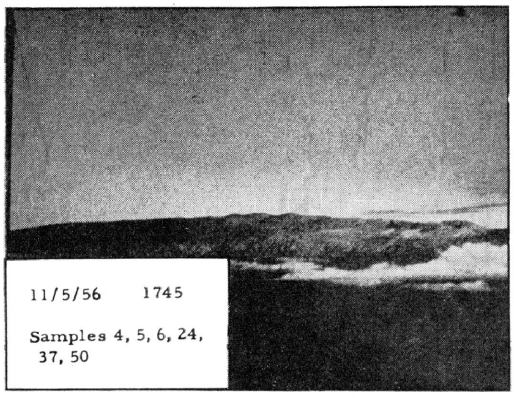

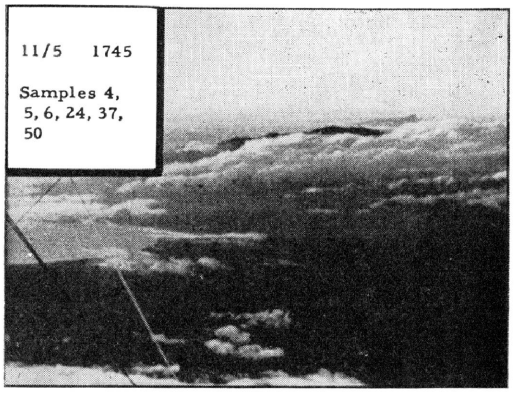

FIGURE 65. *Photographs of Haleakala-Puunene path corresponding in time to data samples indicated.*

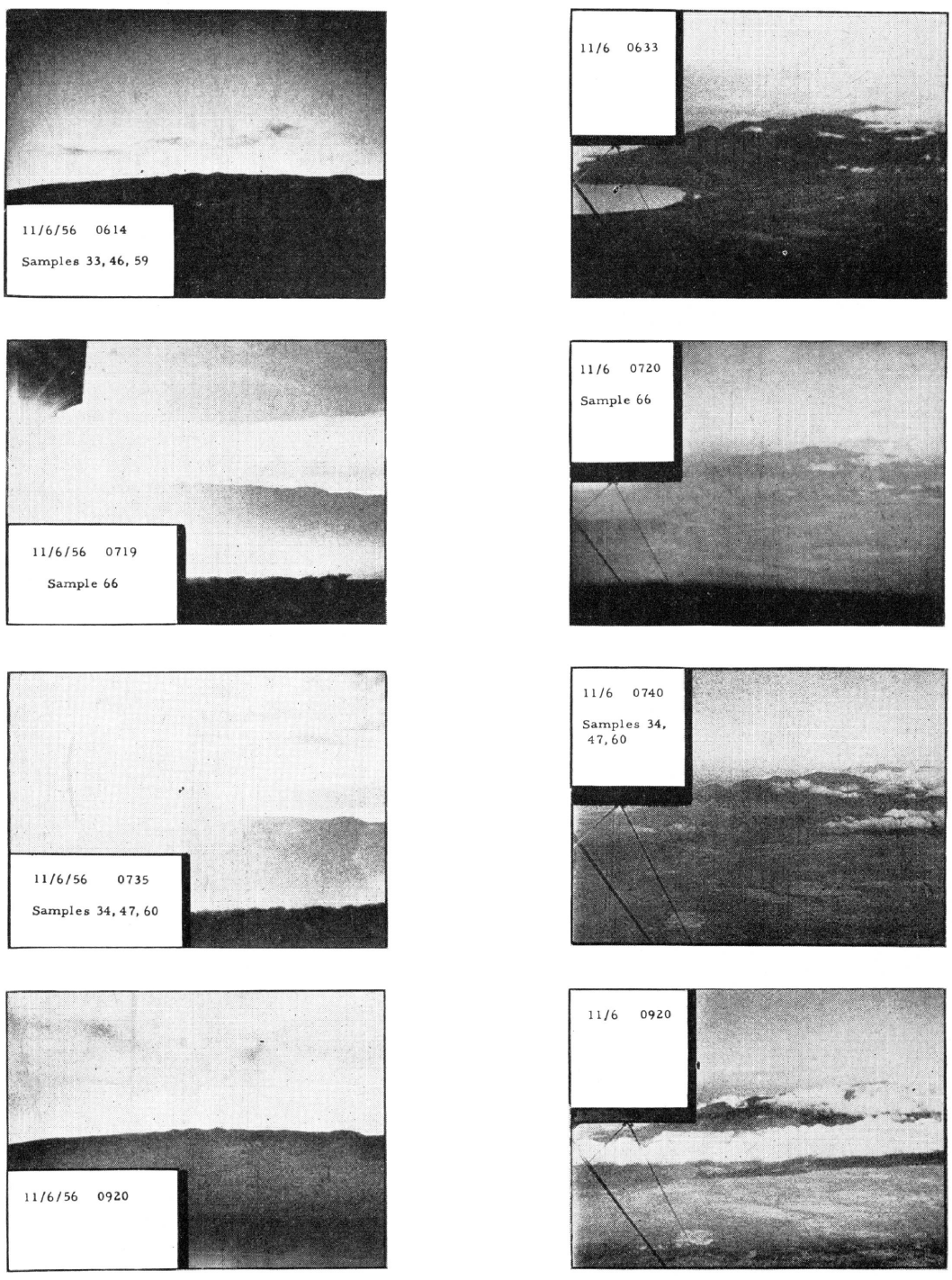

FIGURE 66. *Photographs of Haleakala-Puunene path corresponding in time to data samples indicated.*

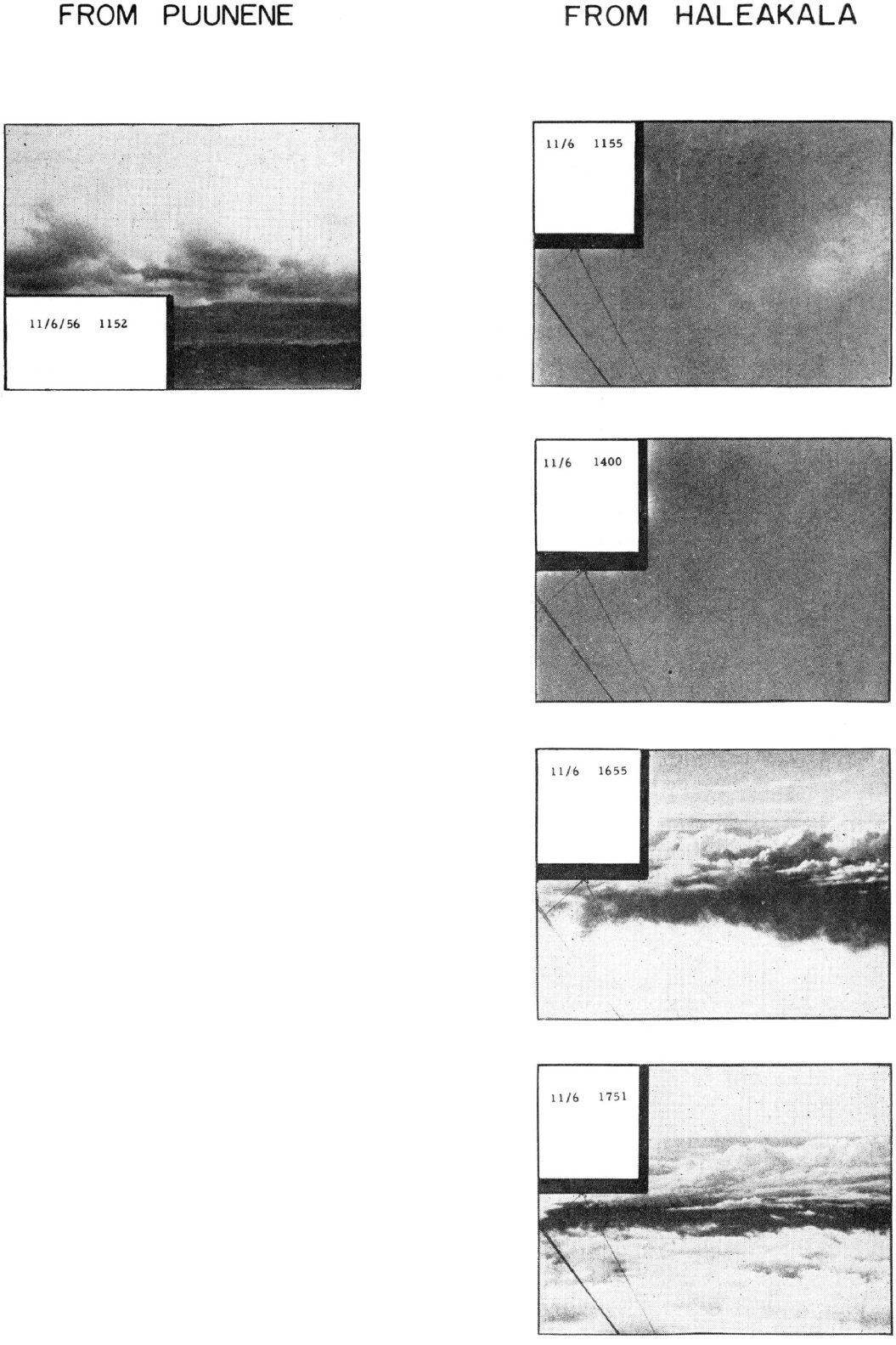

FIGURE 67. *Photographs of Haleakala-Puunene path corresponding in time to data samples indicated.*

FROM PUUNENE

FROM HALEAKALA

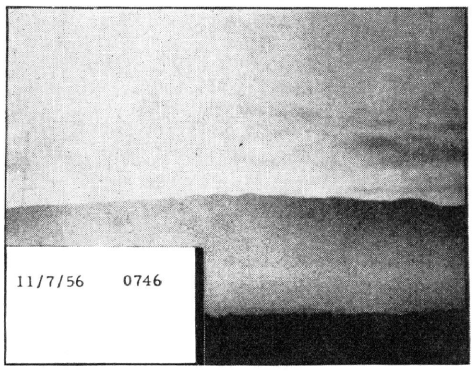

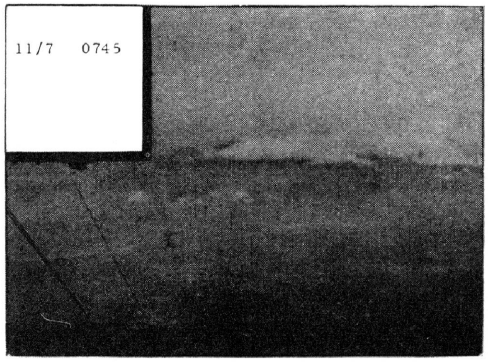

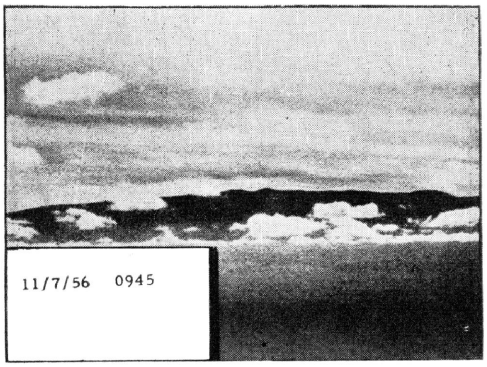

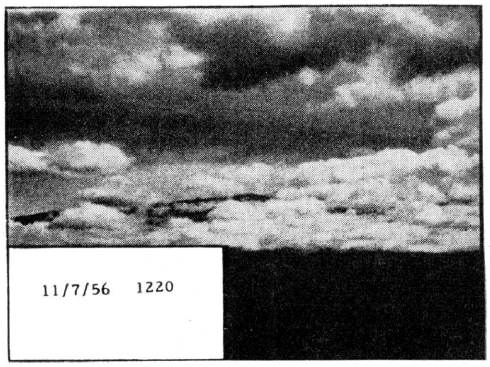

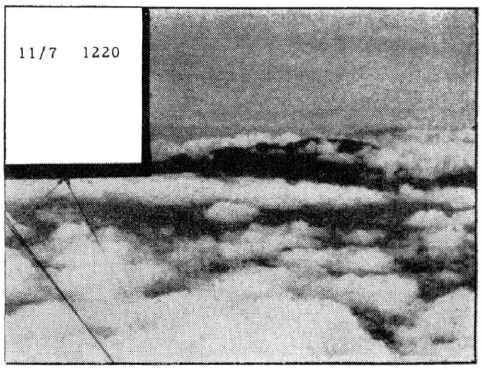

FIGURE 68. *Photographs of Haleakala-Puunene path corresponding in time to data samples indicated.*

FROM PUUNENE

FROM HALEAKALA

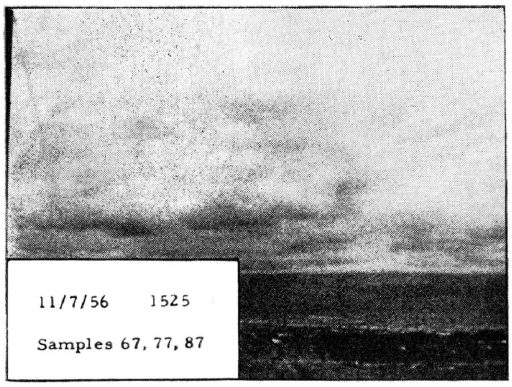

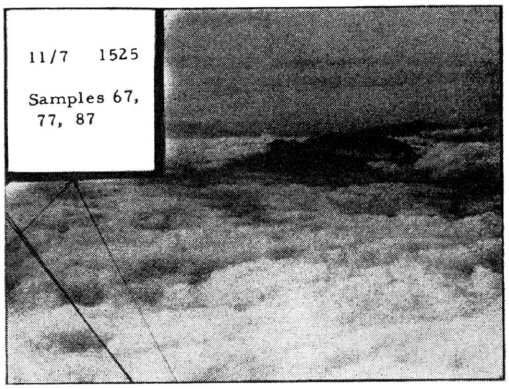

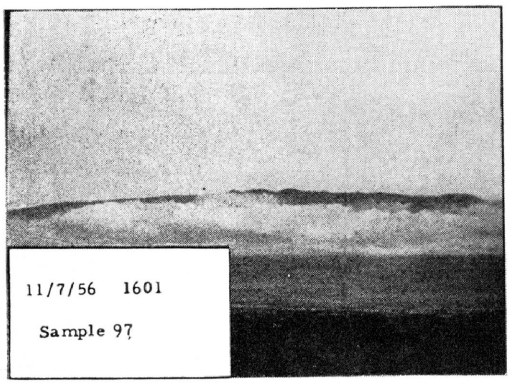

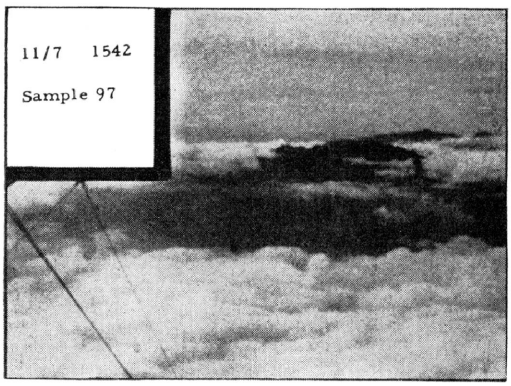

FIGURE 69. *Photographs of Haleakala-Puunene path corresponding in time to data samples indicated.*

FROM PUUNENE

FROM HALEAKALA

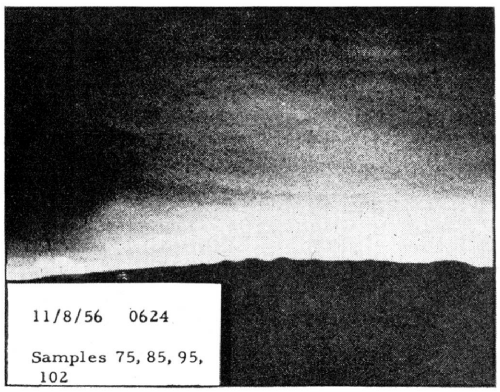

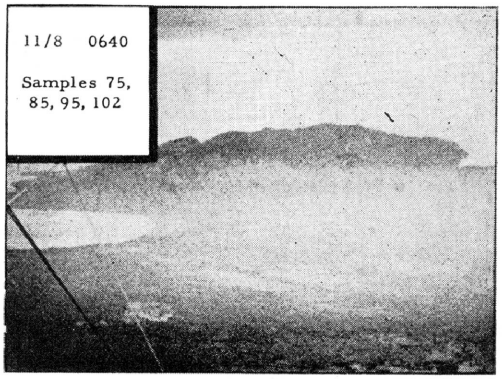

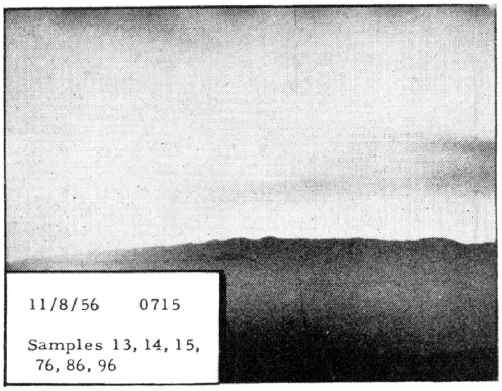

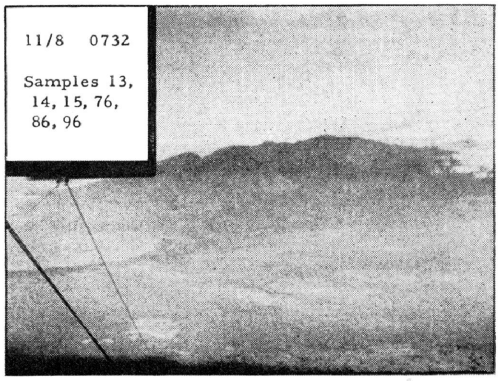

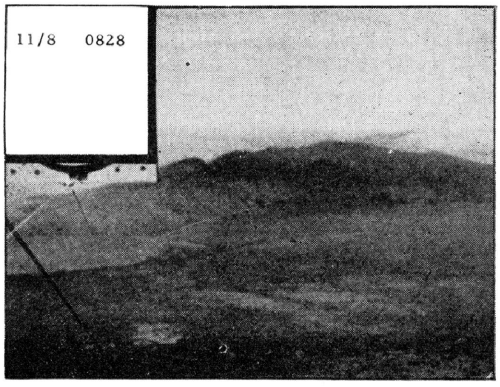

FIGURE 70. *Photographs of Haleakala-Puunene path corresponding in time to data samples indicated.*

FROM PUUNENE

FROM HALEAKALA

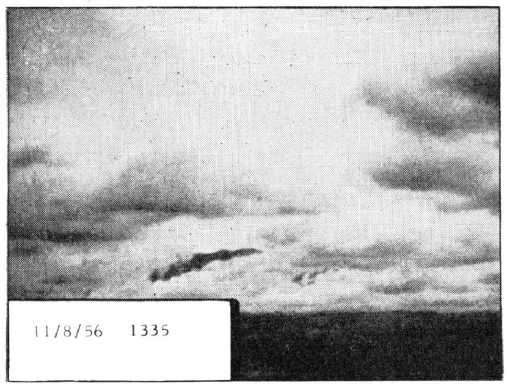

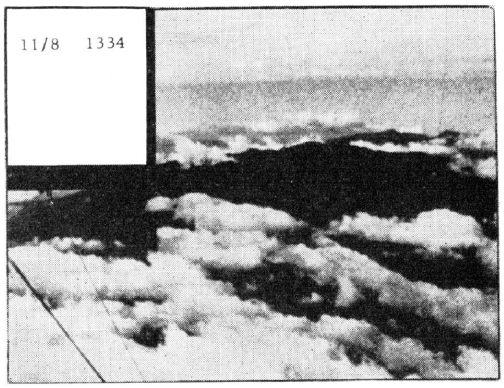

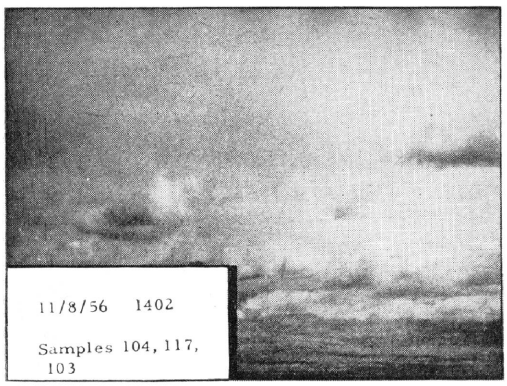

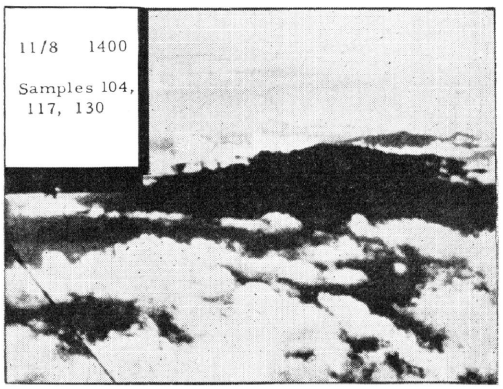

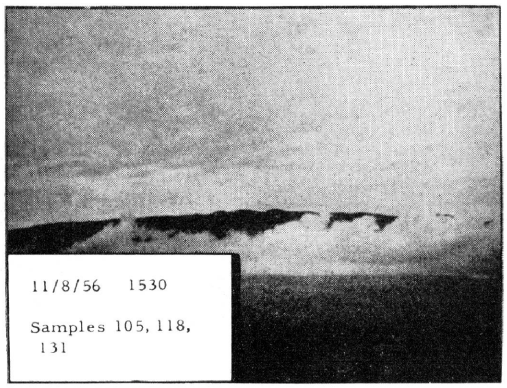

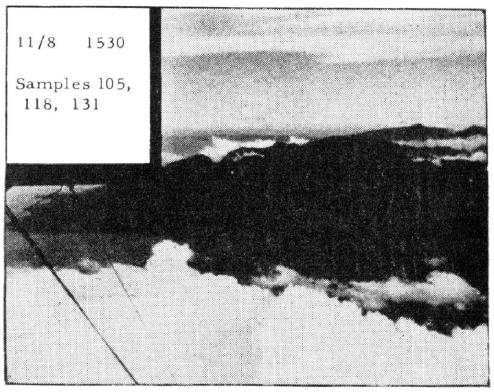

FIGURE 71. *Photographs of Haleakala-Puunene path corresponding in time to data samples indicated.*

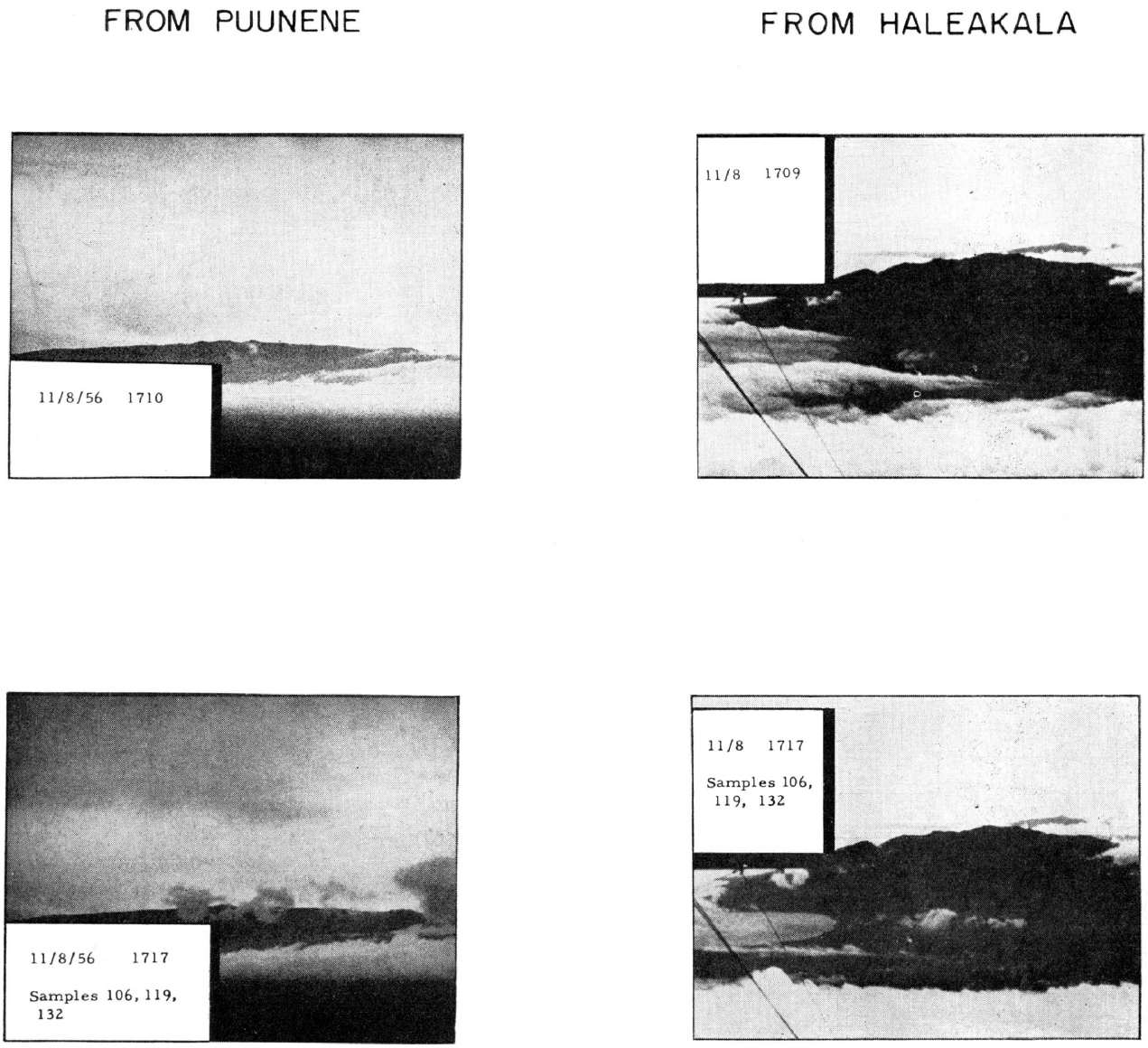

FIGURE 72. *Photographs of Haleakala-Puunene path corresponding in time to data samples indicated.*

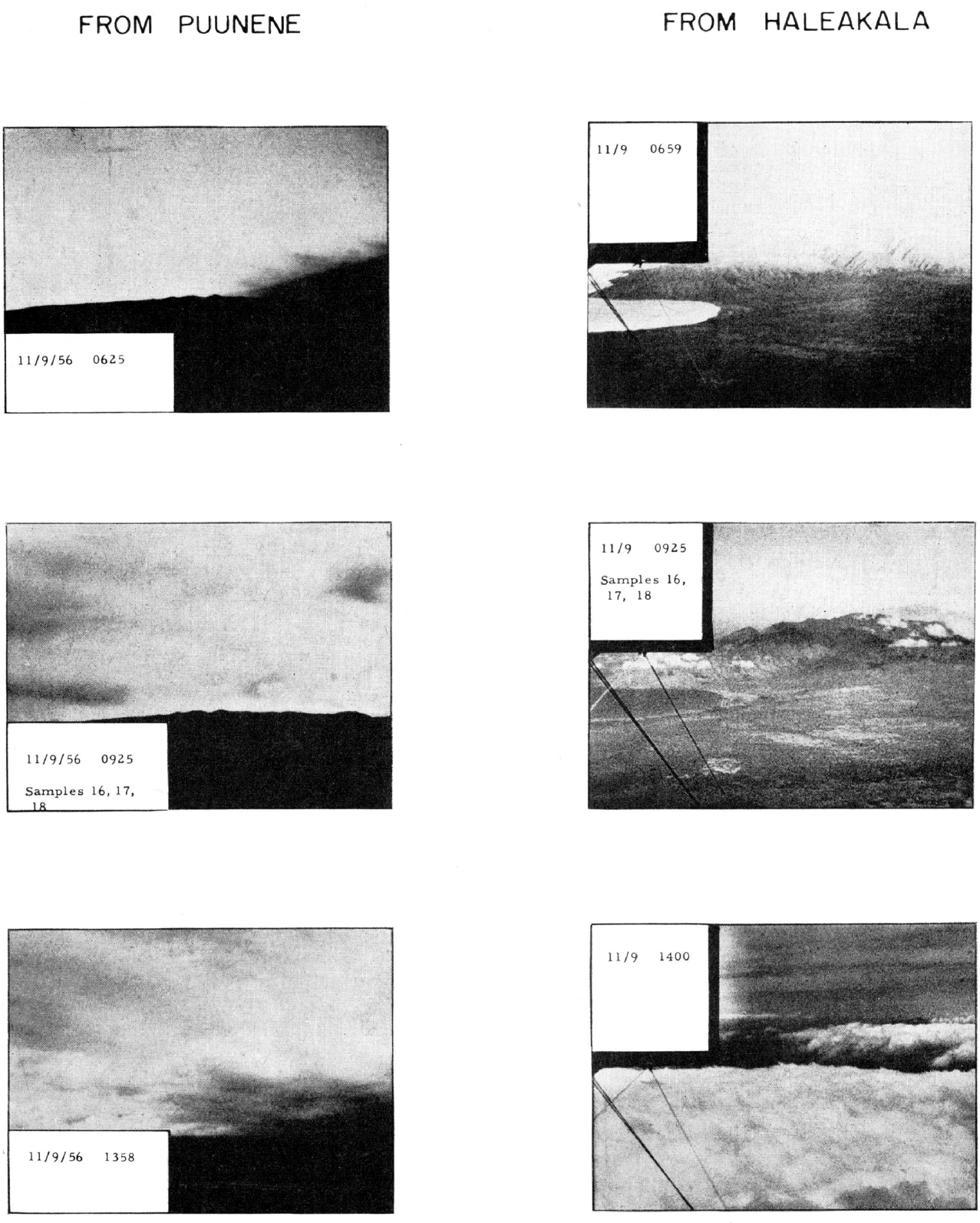

FIGURE 73. *Photographs of Haleakala-Puunene path corresponding in time to data samples indicated.*

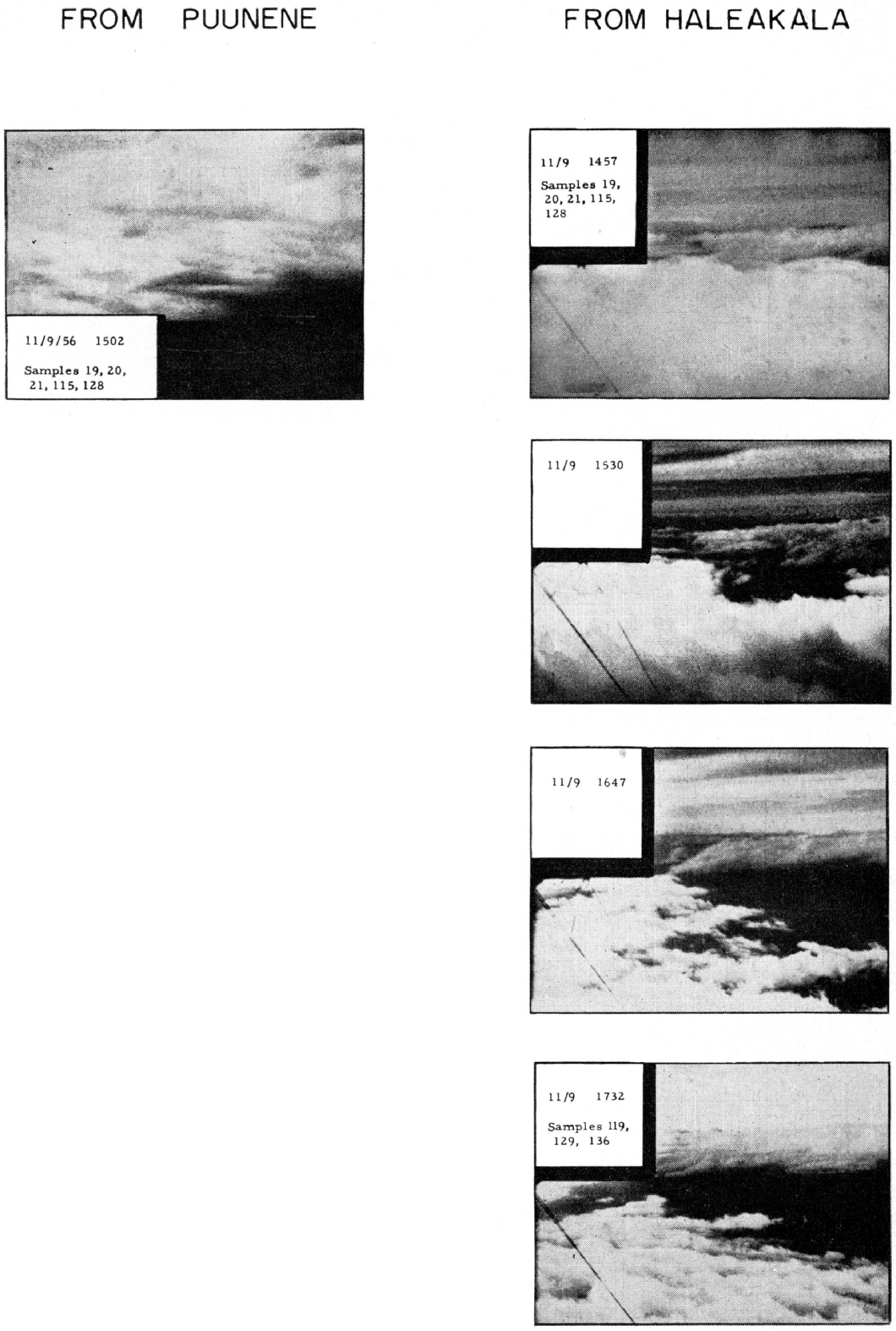

FIGURE 74. *Photographs of Haleakala-Puunene path corresponding in time to data samples indicated.*

BOULDER, COLO., February 10, 1961.

U. S. DEPARTMENT OF COMMERCE
Luther H. Hodges, *Secretary*

NATIONAL BUREAU OF STANDARDS
A. V. Astin, *Director*

THE NATIONAL BUREAU OF STANDARDS

The scope of activities of the National Bureau of Standards at its major laboratories in Washington, D.C., and Boulder, Colorado, is suggested in the following listing of the divisions and sections engaged in technical work. In general, each section carries out specialized research, development, and engineering in the field indicated by its title. A brief description of the activities, and of the resultant publications, appears on the inside of the front cover.

WASHINGTON, D.C.

Electricity. Resistance and Reactance. Electrochemistry. Electrical Instruments. Magnetic Measurements. Dielectrics.

Metrology. Photometry and Colorimetry. Refractometry. Photographic Research. Length. Engineering Metrology. Mass and Scale. Volumetry and Densimetry.

Heat. Temperature Physics. Heat Measurements. Cryogenic Physics. Equation of State. Statistical Physics.

Radiation Physics. X-Ray. Radioactivity. Radiation Theory. High Energy Radiation. Radiological Equipment. Nucleonic Instrumentation. Neutron Physics.

Analytical and Inorganic Chemistry. Pure Substances. Spectrochemistry. Solution Chemistry. Standards Reference Materials. Applied Analytical Research.

Mechanics. Sound. Pressure and Vacuum. Fluid Mechanics. Engineering Mechanics. Rheology. Combustion Controls.

Organic and Fibrous Materials. Rubber. Textiles. Paper. Leather. Testing and Specifications. Polymer Structure. Plastics. Dental Research.

Metallurgy. Thermal Metallurgy. Chemical Metallurgy. Mechanical Metallurgy. Corrosion. Metal Physics. Electrodeposition.

Mineral Products. Engineering Ceramics. Glass. Refractories. Enameled Metals. Crystal Growth. Physical Properties. Constitution and Microstructure.

Building Research. Structural Engineering. Fire Research. Mechanical Systems. Organic Building Materials. Codes and Safety Standards. Heat Transfer. Inorganic Building Materials.

Applied Mathematics. Numerical Analysis. Computation. Statistical Engineering. Mathematical Physics.

Data Processing Systems. Components and Techniques. Digital Circuitry. Digital Systems. Analog Systems. Applications Engineering.

Atomic Physics. Spectroscopy. Infrared Spectroscopy. Solid State Physics. Electron Physics. Atomic Physics.

Instrumentation. Engineering Electronics. Electron Devices. Electronic Instrumentation. Mechanical Instruments. Basic Instrumentation.

Physical Chemistry. Thermochemistry. Surface Chemistry. Organic Chemistry. Molecular Spectroscopy. Molecular Kinetics. Mass Spectrometry. Molecular Structure and Radiation Chemistry.

• Office of Weights and Measures.

BOULDER, COLO.

Cryogenic Engineering. Cryogenic Equipment. Cryogenic Processes. Properties of Materials. Gas Liquefaction.

Ionosphere Research and Propagation. Low Frequency and Very Low Frequency Research. Ionosphere Research. Prediction Services. Sun-Earth Relationships. Field Engineering. Radio Warning Service.

Radio Propagation Engineering. Data Reduction Instrumentation. Radio Noise. Tropospheric Measurements. Tropospheric Analysis. Propagation-Terrain Effects. Radio-Meteorology. Lower Atmosphere Physics.

Radio Standards. High Frequency Electrical Standards. Radio Broadcast Service. Radio and Microwave Materials. Atomic Frequency and Time Interval Standards. Electronic Calibration Center. Millimeter-Wave Research. Microwave Circuit Standards.

Radio Systems. High Frequency and Very High Frequency Research. Modulation Research. Antenna Research. Navigation Systems. Space Telecommunications.

Upper Atmosphere and Space Physics. Upper Atmosphere and Plasma Physics. Ionosphere and Exosphere Scatter. Airglow and Aurora. Ionospheric Radio Astronomy.

☆ U.S. GOVERNMENT PRINTING OFFICE: 1961—597154